

**Calvet et al. (2015), [www.soil-discuss.net/2/737/2015/](http://www.soil-discuss.net/2/737/2015/)**

*Impact of gravels and organic matter on the thermal properties of grassland soils in southern France*

13 January 2016.

Dear Prof. Nunzio Romano,

Please find enclosed a point by point response to the reviewers' comments, together with changes in the revised version of our work. In response to the reviewers' comments, we implemented a new data analysis procedure able to sort out flawed soil thermal conductivity estimates. This greatly improved our results and we are confident in the new retrieved values of volumetric fraction of quartz. We used the data published by Lu et al. (2007) to validate and discuss our results. For the sake of consistency, the empirical Lu et al. (2007) model was used. We have endeavoured to characterize the impact of uncertainties in data and models. We extensively revised the text, added new Figures, Tables, and Supplements. The Title and Abstract were rewritten.

Moreover, we made the soil profile data available on the web and the Supplements provide all the information needed to reproduce our calculations.

Sincerely,

Jean-Christophe Calvet and co-authors

Calvet et al. (2015), [www.soil-discuss.net/2/737/2015/](http://www.soil-discuss.net/2/737/2015/)

*Impact of gravels and organic matter on the thermal properties of grassland soils in southern France*

## **Response to Reviewer #1 and changes in the revised version of the paper**

(X. Xiao, [xinhua.xiao@aamu.edu](mailto:xinhua.xiao@aamu.edu); [xiaoxinhua2009@gmail.com](mailto:xiaoxinhua2009@gmail.com))

The authors thank Dr. Xinhua Xiao (NC State University Soil Physics) for her review of the manuscript and for the fruitful comments.

1.1 [Accuracy of predicative  $\lambda$  models highly depends on accurate estimation of  $\lambda_{\text{sat}}$  and  $q$ , which has been oversimplified as sand fraction. It is interesting and important to predict  $q$  and  $\lambda_{\text{sat}}$  in  $\lambda$  models using data of soil texture and gravel and SOM and to further examine their impacts on  $\lambda$  models. The methodology in this work to address the research question is appropriate. Discussion of model applicability is covered. The new pedotransfer functions for  $\lambda_{\text{sat}}$  and  $q$  derived from their original data will add good contribution to the literature. I however have major concerns about the presentation/organization of this paper that I feel in some sections focus is lacking and/or reorganization needed. Better justification of adopting some key empirical models and more relevant discussion are also desired.]

### **RESPONSE 1.1**

Many thanks for these positive comments. We will do our best to account for your remarks in a revised version of the manuscript.

#### **Additional comments**

**In response to the reviewers' comments, we have revised our approach. The  $\lambda$  retrievals influenced by heterogeneities in soil properties are now sorted out. As a result, we now obtain realistic  $\lambda_{\text{sat}}$  values for 14 soils. We improved the assessment of uncertainties on the pedotransfer function for quartz volumetric fraction:**

- a variety of pedotransfer functions is now proposed, not only one
- a confidence interval for the coefficients of pedotransfer functions is given
- the impact of errors on the volumetric heat capacity of soil minerals is assessed
- the data from Lu et al. (2007) are used as an independent benchmark to verify the obtained pedotransfer functions.

In order to clarify the definition of symbols, the volumetric fraction of quartz is now written as " $f_q$ " (instead of " $q$ ").

Finally, the Kersten number model of Lu et al. (2007) is now used instead of the Yang et al. (2005) model.

1.2 [On obtaining site/station specific  $\lambda_{\text{sat}}$  and  $q$  values. Equations 7-11 are the core functions for authors to enable retrieval of the site/station-specific  $\lambda_{\text{sat}}$  (and  $q$  value accordingly) by parameter fitting via reverse modeling. I think these equations/models (specifically Lu et al 2007 and Yang et al 2005) should to some extent be justified why they were chosen as opposed to other alternative equations in the literatures.]

## RESPONSE 1.2

Yes, two key equations are used for  $\lambda_{\text{dry}}$  and for  $K_e$  (Eqs. (7) and (9), respectively).

For  $\lambda_{\text{dry}}$  we used the Lu et al. (2007) parameterization. Figure R1.1 shows that this parameterization produces larger  $\lambda_{\text{dry}}$  values than the  $\lambda_{\text{dry}}$  estimates derived from Côté and Konrad (2005) for mineral soils. We checked that using Côté and Konrad (2005) instead of Lu et al. (2007) has a very limited impact on  $\lambda_{\text{sat}}$  and  $q$  retrievals ( $\leq 0.005 \text{ W m}^{-1} \text{ K}^{-1}$  and  $\leq 0.01 \text{ m}^{-3} \text{ m}^{-3}$ , respectively).

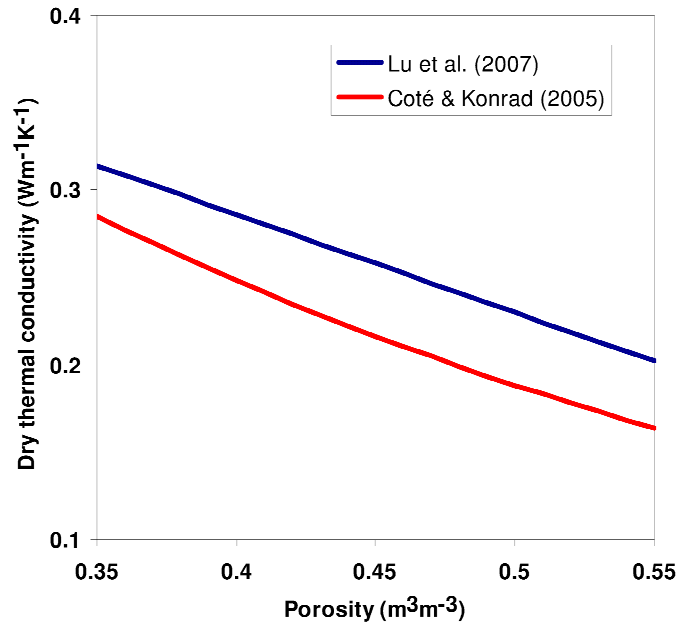


**Figure R1.1** - Modelled  $\lambda_{\text{dry}}$  for the range of porosity values encountered in this study, using Lu et al. (2007) and Côté and Konrad (2005).

In the first version of this work, we used the Kersten number calculation used by Yang et al. (2005). Figure R1.2 shows the resulting  $K_e$  value, together the  $K_e$  value obtained using the Lu et al. (2007) model for fine and coarse soils. It can be seen that most differences between these models occur for  $S_d$  values  $< 0.4$ . Since we only use  $\lambda$  retrievals for  $S_d$  values  $> 0.4$ , the impact of the uncertainties in the determination of  $K_e$  is limited. However, using Lu et al. (2007) instead of Yang et al. (2005) tends to produce smaller values of  $\lambda_{\text{sat}}$  and  $f_q$  retrievals, as shown by Figs. R1.3 and R1.4. The impact of the Kersten number calculation will be discussed in the final version of this work.

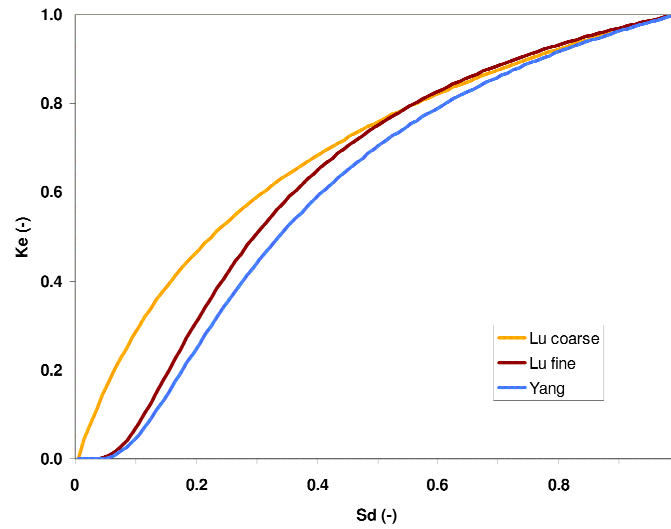


**Figure R1.2** - Kersten number vs. degree of saturation as modelled by Lu et al. (2007) for coarse and fine soils, and as modelled by Yang et al. (2005).

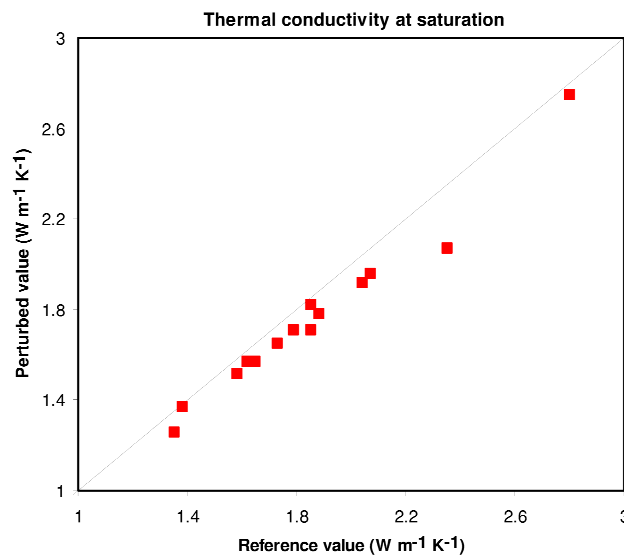


**Figure R1.3** -  $\lambda_{\text{sat}}$  retrievals using the Kersten number as modelled by Lu et al. (2007) vs. those using the Kersten number as modelled by Yang et al. (2005).

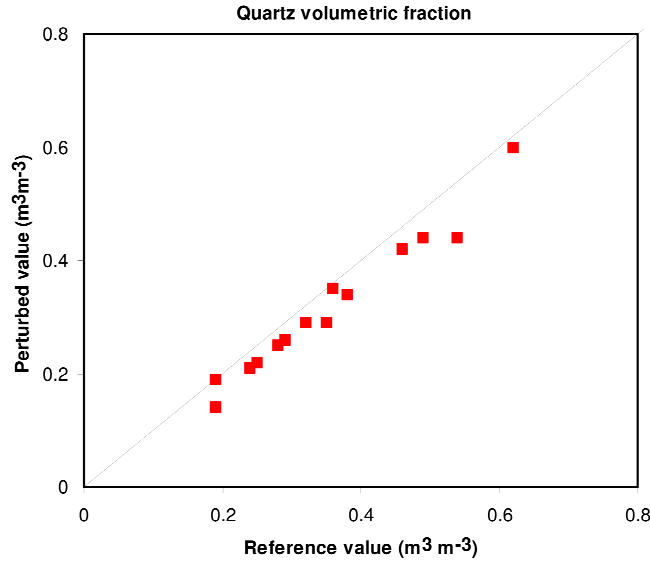


**Figure R1.4** - As in Fig. R1.3, except for  $f_q$  retrievals.

**CHANGES 1.2 (Sect. 2.5)**

In this study, the formula recommended by Lu et al. (2007) is used:

$$K_e = \exp\left\{\alpha\left(1 - S_d^{(\alpha-1.33)}\right)\right\},$$

with  $\alpha = 0.96$  for  $Mn_{\text{sand}} \geq 0.4 \text{ kg kg}^{-1}$ ,  $\alpha = 0.27$  for  $Mn_{\text{sand}} < 0.4 \text{ kg kg}^{-1}$ , and

$$S_d = \theta/\theta_{\text{sat}} \tag{9}.$$

$Mn_{\text{sand}}$  represents the sand mass fraction of fine earth minerals (values are given in Supplement 1).

Following Peters-Lidard et al. (1998),  $\lambda_{\text{other}}$  is taken as  $2.0 \text{ Wm}^{-1}\text{K}^{-1}$  for soils with  $Mn_{\text{sand}} > 0.2 \text{ kg kg}^{-1}$ , and  $3.0 \text{ Wm}^{-1}\text{K}^{-1}$  otherwise. In this study,  $Mn_{\text{sand}} > 0.2 \text{ kg kg}^{-1}$  for all soils except for URG, PRG, and CDM.

1.3 [On discussion. First, the pedotransfer function for  $q$  (and thus  $\lambda_{\text{sat}}$ ) was evaluated with 11 stations/sites in this study but not tested. One alternative to be discussed is to

**divide the 11 stations that some are used for model development and others for testing its predictive/generalization power.]**

### **RESPONSE 1.3**

Yes, this is a very good point. In order to address this issue, we have used a simple bootstrapping resampling technique consisting in calculating a new estimate of  $f_q$  for each soil using the pedotransfer function obtained without using this specific soil. Gathering these new  $f_q$  estimates, one can calculate new scores with respect to the retrieved  $f_q$  values. Also, this method provides a range of possible values of the coefficients of the pedotransfer function and permits assessing the influence of a given  $f_q$  retrieval on the final result.

These additional scores will be published in the final version of this work.

### **CHANGES 1.3**

**New Tables were added in order to list the potential pedotransfer functions and the associated scores (see below). The bootstrapping is described in Sect. 2.7.**

**Table 3** – Coefficients of four pedotransfer functions of  $f_q$  for 14 soils of this study, together with indicators of the coefficient uncertainty derived by bootstrapping and by perturbing the volumetric heat capacity of soil minerals ( $C_{hmin}$ ).

Predictor of $f_q$	Coefficients for 14 soils		Confidence interval from bootstrapping		Impact of a change of $\pm 0.08 \text{ MJ m}^{-3} \text{ K}^{-1}$ in $C_{hmin}$	
	$a_0$	$a_1$	$a_0$	$a_1$	$a_0$	$a_1$
$m_{sand} / m_{SOM}$	0.12	0.0134	[0.10,0.14]	[0.012,0.014]	[0.11,0.13]	[0.013,0.013]
$m_{sand}^*$	0.08	0.944	[0.00,0.11]	[0.85,1.40]	[0.07,0.09]	[0.919,0.966]
$m_{sand}$	0.15	0.572	[0.08,0.17]	[0.54,0.94]	[0.14,0.17]	[0.55,0.56]
$1 - \theta_{sat} - f_{sand}$	0.73	-1.020	[0.71,0.89]	[-1.38,-0.99]	[0.70,0.73]	[-1.00,-0.99]

(\* ) only  $m_{sand}$  values smaller than  $0.6 \text{ kg kg}^{-1}$  are used in the regression



**Table 4** – Scores of four pedotransfer functions of  $f_q$  for 14 soils of this study, together with the scores obtained by bootstrapping, without the sandy SBR soil. The MAE score of these pedotransfer functions for three Chinese soils of Lu et al. (2007), for which  $m_{\text{sand}}/m_{\text{SOM}} < 40$  is given.

Predictor of $f_q$	Regression scores			Bootstrap scores			Scores without SBR (and MAE for 3 Lu soils)		
	$r^2$	RMSD ( $\text{m}^3\text{m}^{-3}$ )	MAE ( $\text{m}^3\text{m}^{-3}$ )	$r^2$	RMSD ( $\text{m}^3\text{m}^{-3}$ )	MAE ( $\text{m}^3\text{m}^{-3}$ )	$r^2$	RMSD ( $\text{m}^3\text{m}^{-3}$ )	MAE ( $\text{m}^3\text{m}^{-3}$ )
$m_{\text{sand}} / m_{\text{SOM}}$	<b>0.77</b>	<b>0.067</b>	0.053	<b>0.72</b>	<b>0.074</b>	<b>0.059</b>	<b>0.62</b>	<b>0.070</b>	0.057 (0.135)
$m_{\text{sand}}^*$	0.74	0.072	<b>0.052</b>	0.67	0.126	0.100	0.56	0.075	<b>0.056</b> (0.071)
$m_{\text{sand}}$	0.67	0.081	0.060	0.56	0.121	0.084	0.56	0.075	<b>0.056</b> (0.086)
$1 - \theta_{\text{sat}} - f_{\text{sand}}$	0.65	0.084	0.064	0.56	0.102	0.079	0.45	0.084	0.061 (0.158)

(\*) only  $m_{\text{sand}}$  values smaller than  $0.6 \text{ kg kg}^{-1}$  are used in the regression

1.4 [Second, the impact of  $q$  on  $\lambda$  prediction actually has been studied in Tarnawski et al 2009, in which  $q$  was shown mostly linearly dependent on coarse fraction including sand and gravel. Authors recognized that work in this paper yet need to perform enough comparisons with that work and/or other related previous work in the literatures.]

#### RESPONSE 1.4

Yes. It is interesting to test the statistical relationships we get between  $f_q$  retrievals and soil characteristics using the independent data from Lu et al. (2007) and Tarnawski et al. (2009). We checked that the pedotransfer function(s) we get from our observations produce  $\lambda_{\text{sat}}$  values close to those observed for the fine-textured Lu soils. For coarse-textured soils, our pedotransfer function(s) tend(s) to overestimate  $\lambda_{\text{sat}}$  values. Note that Lu et al. (2007) obtained a similar result with their model, which assumes that  $f_q = (1 - \theta_{\text{sat}}) \times m_{\text{SAND}}$ . It must be noted that most of these soils contain very little organic matter and consisted of reassembled sieved soil samples, while our data concern undisturbed soils.

#### REFERENCES :

Lu, S., Ren, T., Gong, Y., and Horton, R.: An improved model for predicting soil thermal conductivity from water content at room temperature, *Soil Sci. Soc. Am. J.*, 71, 8–14, doi:10.2136/sssaj2006.0041, 2007.

Tarnawski V. R., T. Momose , W. H. Leong, 2009: Assessing the impact of quartz content on the prediction of soil thermal conductivity. *Géotechnique* 59 (4), 331-338, doi:10.1680/geot.2009.59.4.331.

#### CHANGES 1.4 (Sect. 4.3)

The characteristics of ten Chinese soils used by Lu et al. (2007) to investigate soil thermal conductivity are given in Table S1 (Supplement). We used three soils from the Lu et al. (2007) data to validate our approach: Silty clay loam 8, Silt loam 6, Silt loam 5. These soils were used as they present  $m_{\text{sand}}/m_{\text{SOM}}$  values lower than 40, as the soils considered in this study. The other seven soils were used to propose alternative coefficient values for contrasting soil characteristics ( $m_{\text{sand}}/m_{\text{SOM}} > 40$ ).

We derived gravimetric and volumetric fraction of quartz ( $Q$  and  $f_q$ , respectively) from the  $\lambda_{\text{sat}}$  observations of Lu et al. (2007). Figure 10 shows that  $f_q$  correlates to  $m_{\text{sand}}$  better than  $Q$ . Similar results are found for other predictors. This is consistent with the results we obtained

for 14 French soils: pedotransfer functions for quartz present systematically better scores using  $f_q$  instead of  $Q$ , as shown by Fig. 5.

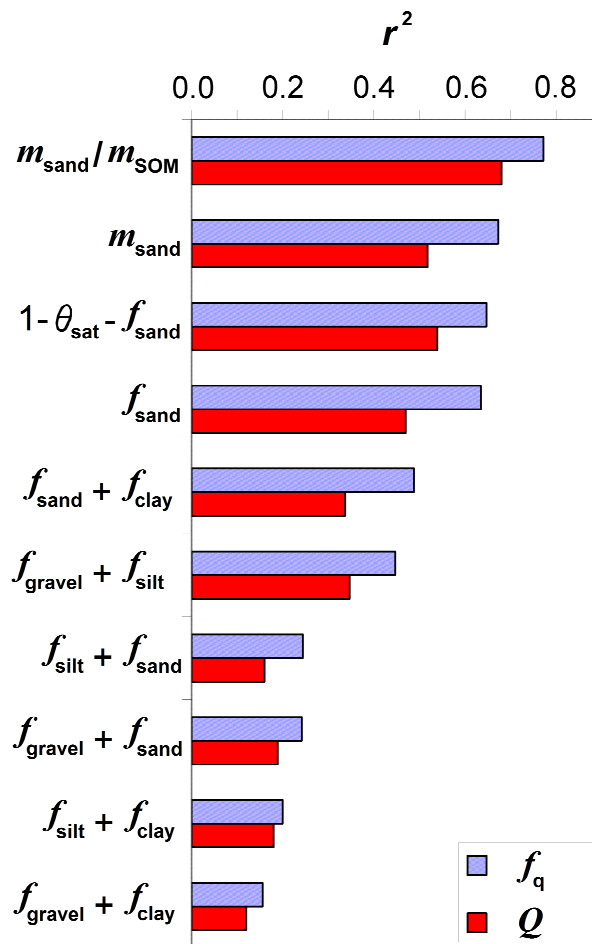


**Figure 5** - Fraction of variance ( $r^2$ ) of gravimetric and volumetric fraction of quartz ( $Q$  and  $f_q$ , red and blue bars, respectively) explained by various predictors.

**Table S3.1** – Soil characteristics of ten Chinese soils of Lu et al. (2007).  $\rho_d$ ,  $\theta_{sat}$ ,  $f$ , and  $m$ , stand for soil bulk density, porosity, volumetric fractions, and gravimetric fractions, respectively.  $\lambda_{sat}$  experimental values are derived from Table 3 in Tarnawski et al. (2009). Soil density is derived from porosity values inverting Eq. (1). The soils are sorted from the largest to the smallest ratio of  $m_{sand}$  to  $m_{SOM}$ . The ratio values smaller than 40 are in bold.

Lu et al. (2007) soils	$\lambda_{sat}$ observations ( $Wm^{-1}K^{-1}$ )	$\rho_d$ ( $kg\ m^{-3}$ )	$\theta_{sat}$ ( $m^3m^{-3}$ )	$f_{sand}$ ( $m^3m^{-3}$ )	$f_{clay}$ ( $m^3m^{-3}$ )	$f_{silt}$ ( $m^3m^{-3}$ )	$f_{SOM}$ ( $m^3m^{-3}$ )	$m_{sand}$ ( $kg\ kg^{-1}$ )	$m_{clay}$ ( $kg\ kg^{-1}$ )	$m_{silt}$ ( $kg\ kg^{-1}$ )	$m_{gravel}$ ( $kg\ kg^{-1}$ )	$m_{SOM}$ ( $kg\ kg^{-1}$ )	$\frac{m_{sand}}{m_{SOM}}$
Sand 2	1.87	1567	0.41	0.548	0.035	0.006	0.001	0.929	0.060	0.010	0	0.001	1327.6
Sand 1	2.19	1567	0.41	0.553	0.029	0.006	0.001	0.939	0.050	0.010	0	0.001	1043.5
Loam 11	1.62	1350	0.49	0.253	0.046	0.208	0.003	0.499	0.090	0.409	0	0.003	199.5
Clay loam 9	1.36	1270	0.52	0.152	0.143	0.181	0.003	0.319	0.299	0.379	0	0.003	118.2
Sandy loam 3	1.68	1333	0.49	0.333	0.060	0.104	0.009	0.664	0.119	0.208	0	0.009	77.2
Loam 4	1.40	1264	0.52	0.189	0.052	0.232	0.005	0.398	0.109	0.488	0	0.005	81.2
Silty clay loam 7	1.34	1267	0.52	0.090	0.128	0.256	0.004	0.189	0.269	0.538	0	0.004	48.5
Silt loam 5	1.38	1272	0.51	0.128	0.104	0.241	0.012	0.267	0.217	0.504	0	0.012	<b>22.4</b>
Silt loam 6	1.47	1255	0.52	0.051	0.089	0.328	0.008	0.109	0.188	0.694	0	0.008	<b>13.0</b>
Silty clay loam 8	1.31	1202	0.52	0.035	0.140	0.263	0.028	0.078	0.310	0.582	0	0.030	<b>2.6</b>

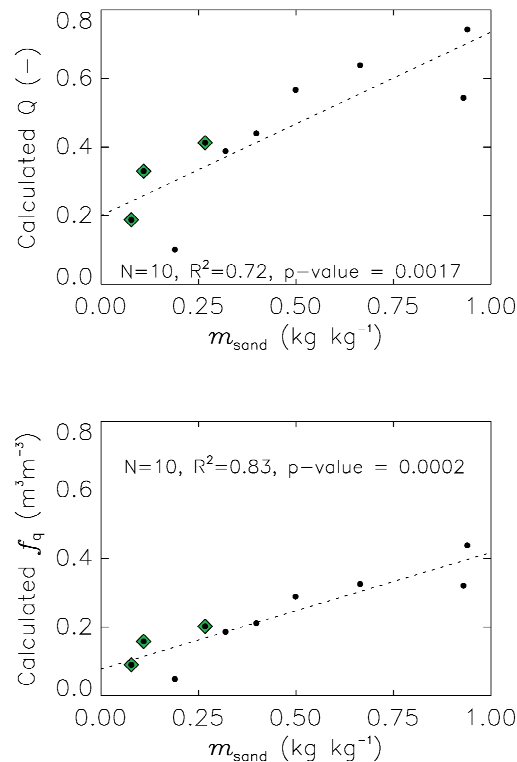


**Figure 10** - Gravimetric and volumetric fraction of quartz (top and bottom, respectively) derived from the  $\lambda_{sat}$  observations of Lu et al. (2007) for 10 Chinese soils given by Tarnawski et al. (2009), vs. the gravimetric fraction of sand  $m_{sand}$ . The three soils for which  $m_{sand}/m_{SOM} < 40$  are indicated by green diamonds.

**Table 6** – Pedotransfer functions of  $f_q$  for 7 soils of Lu et al. (2007) with  $m_{\text{sand}}/m_{\text{SOM}} > 40$ .

Predictor of $f_q$	Regression scores for 7 Lu soils with $m_{\text{sand}}/m_{\text{SOM}} > 40$			Coefficients	
	$r^2$ ( <i>p</i> -value)	RMSD ( $\text{m}^3\text{m}^{-3}$ )	MAE ( $\text{m}^3\text{m}^{-3}$ )	$a_0$	$a_1$
$m_{\text{sand}} / m_{\text{SOM}}$	0.40 (0.13)	0.089	0.075	0.20	0.000148
$m_{\text{sand}}^*$	0.82 (0.005)	0.073	0.054	0.07	0.425
$m_{\text{sand}}$	<b>0.82</b> ( <b>0.005</b> )	<b>0.048</b>	<b>0.042</b>	0.04	0.386
$1 - \theta_{\text{sat}} - f_{\text{sand}}$	0.81 (0.006)	0.050	0.043	0.44	-0.814

(\* ) only  $m_{\text{sand}}$  values smaller than  $0.6 \text{ kg kg}^{-1}$  are used in the regression

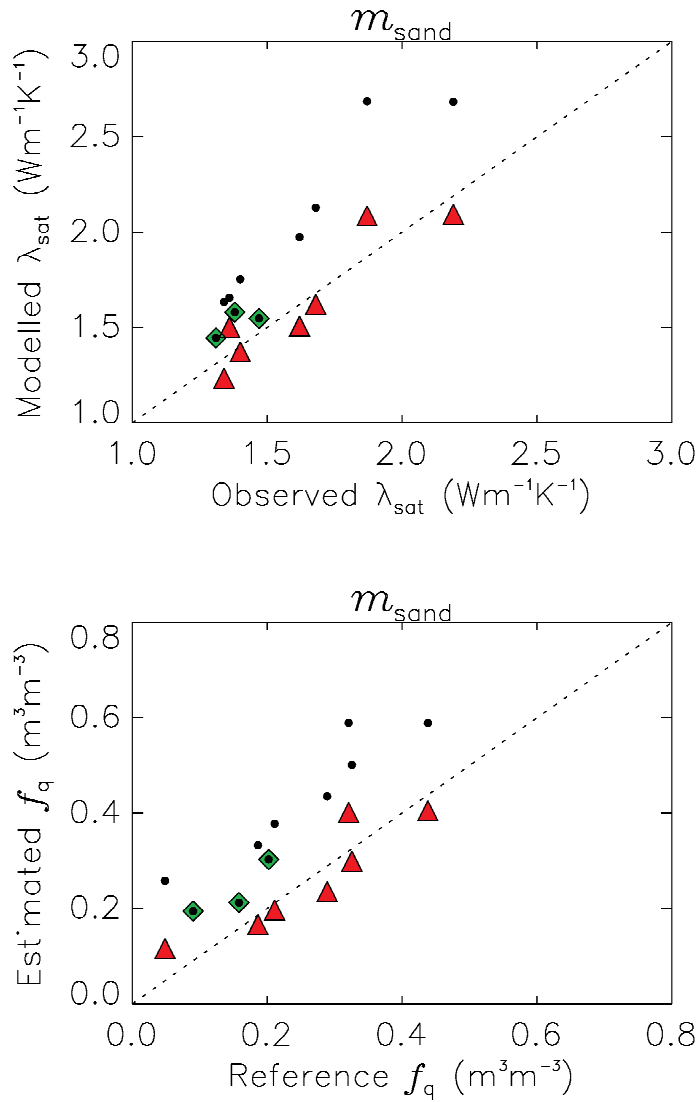


**Figure 11** - Estimated  $\lambda_{\text{sat}}$  and volumetric fraction of quartz  $f_q$  (top and bottom, respectively) vs. values derived from the  $\lambda_{\text{sat}}$  observations of Lu et al. (2007) given by Tarnawski et al. (2009) for 10 Chinese soils, using the gravimetric fraction of sand  $m_{\text{sand}}$  as a predictor of  $f_q$ . Dark dots correspond to the estimations obtained using the  $m_{\text{sand}}$  pedotransfer function for southern France and the three soils for which  $m_{\text{sand}}/m_{\text{SOM}} < 40$  are indicated by green diamonds. Red triangles correspond to the estimations obtained using the  $m_{\text{sand}}$  pedotransfer function for the seven soils for which  $m_{\text{sand}}/m_{\text{SOM}} > 40$ .

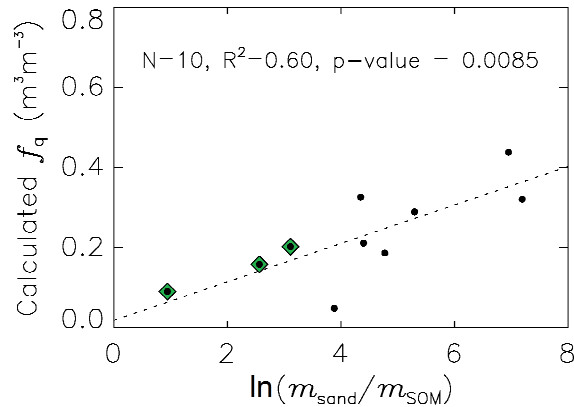


**Figure 12** - Volumetric fraction of quartz derived from the  $\lambda_{\text{sat}}$  observations of Lu et al. (2007) given by Tarnawski et al. (2009), vs. the logarithm of the  $m_{\text{sand}}/m_{\text{SOM}}$  ratio. The three soils for which  $m_{\text{sand}}/m_{\text{SOM}} < 40$  are indicated by green diamonds.

1.5 [Focus. I believe the pedotransfer function and its evaluation constitute the main contribution of this work. The derivation of soil thermal properties from soil temperature profile, the soil temperature resolution (0.1 C) and its impact on the model applicability can be concise. To me Figure 3 seems dispensable. The Conclusion section also needs revision with a concise description concerning these.]

#### RESPONSE 1.5

Yes. In the revised version of this work, we will use a slightly more sophisticated  $q$  retrieval technique able to cope with soil heterogeneities (see the response to Reviewer 2). The details will be described in a supplement, making the main text more concise.

#### CHANGES 1.5

Part of the technical developments were moved to Supplements. The evaluation of potential pedotransfer functions is the main focus of the revised version of the paper. A new Section 4.4 addresses the issue of using a single predictor across soil types. It is shown that the gravimetric fraction of sand within soil solids, including gravels and SOM, is a good predictor of the volumetric fraction of quartz when a large variety of soil types is considered.

1.6 [Organization. Section 4.1 is about evaluating impact of gravel and SOM with sensitivity analysis. I suggest it be included/appended following the pedotransfer

functions in the Results section. Indeed authors intended doing so (in Page 740 Line 6 “in Sect 3 a sensitivity analysis of  $\lambda_{sat}$  to SOM and gravel fractions”).]

#### **RESPONSE 1.6**

We agree. Sect 4.1 will be moved to Sect. 3.

#### **CHANGES 1.6**

**Sect 4.1 was moved to Sect. 3.3.**

1.7 [On Abstract. Authors should do better job in these sections. In Abstract the last three sentences are key results and conclusions of this work and need a great expansion with details; conversely the remaining should be more concise. Please rewrite it and include question, significance, methodology, results, conclusion and this work’s impact.]

#### **RESPONSE 1.7**

We agree. The Abstract will be rewritten.

#### **CHANGES 1.7**

**New abstract:**

**"The information on quartz fraction in soils is usually unavailable but has a major effect on the accuracy of soil thermal conductivity models and on their application in land surface models. This paper investigates the influence of quartz fraction, soil organic matter (SOM) and gravels on soil thermal conductivity. Field observations of soil temperature and water content from 21 weather stations in southern France, along with the information on soil texture and bulk density, are used to estimate soil thermal diffusivity and heat capacity, and then thermal conductivity. The quartz fraction is inversely estimated using an empirical thermal conductivity model. Several pedotransfer functions for estimating quartz content from soil texture information are analysed. It is found that the soil volumetric fraction of quartz ( $f_q$ ) is systematically better correlated to soil characteristics than the gravimetric fraction of quartz. More than 60 % of the variance of  $f_q$  can be explained using indicators based on the sand fraction. It is shown that SOM and (or) gravels may have a marked impact on thermal conductivity values depending on which predictor of  $f_q$  is used. For the grassland soils examined in this study, the ratio of sand to SOM fractions is the best predictor of  $f_q$ . An error propagation analysis and a comparison with independent data from Lu et al. (2007) show that the gravimetric fraction of sand is the most robust predictor of  $f_q$  when a larger variety of soil types is considered."**

1.8 [Page 738 Line 11. “there is no map of q”? Reword to clarify.]



## **RESPONSE 1.8**

We mean that today,  $q$  estimates are not given in global digital soil maps. Therefore, land surface modellers need to use a pedotransfer function for  $q$ .

### **1.9 [Page 745 Line 9. How/why is 0.4 chosen/set as cutoff of saturation degree?]**

## **RESPONSE 1.9**

In dry conditions, conduction is not the only mechanism for heat exchange in soils, as the convective water vapour flux may become significant (Schelde et al., 1998, Parlange et al. 1998). Also, the  $K_e$  functions found in the literature display more variability in dry conditions (see Fig. R1.2). Therefore, this threshold value of  $S_d = 0.4$  results from a compromise between the need of limiting the influence of convection, of the shape of the  $K_e$  function on the retrieved values of  $\lambda_{sat}$ , and of using as many observations as possible in the retrieval process. For example, if we had taken a threshold of 0.6, we would not have been able to retrieve  $\lambda_{sat}$  for SBR, SVN, LZC, PRD, LGC, BRN, and CBR.

## **REFERENCES :**

Schelde, K., A. Thomsen, T. Heidmann, P. Schjonning and P.-E. Jansson: Diurnal fluctuations of water and heat flows in a bare soil, *Water Resour. Res.*, 34, 11, 2919-2929, 1998.

Parlange, M.B., A.T. Cahill, D.R. Nielsen, J.W. Hopmans, O. Wendroth: Review of heat and water movement in field soils, *Soil & Tillage Research*, 47, 5-10, 1998.

## **CHANGES 1.9**

**Sect. 2.6: "The threshold value of  $S_d = 0.4$  results from a compromise between the need of limiting the influence of convection, of the shape of the  $K_e$  function on the retrieved values of  $\lambda_{sat}$ , and of using as many observations as possible in the retrieval process."**

1.10 [Page 745 Lines 15-17. I suggest an explicit specifying that the three “contrasting retrieved values of  $\lambda_{sat}$ ” are for high, medium and low levels of  $\lambda_{sat}$  values respectively.]

#### **RESPONSE 1.10**

Agreed.

#### **CHANGES 1.10**

**Start of Sect. 3.1: "Figure 3 shows retrieved and modelled  $\lambda$  values vs. the observed degree of saturation of the soil, at a depth of 0.10 m, for contrasting retrieved values of  $\lambda_{sat}$ , from high to low  $\lambda_{sat}$  values (2.80, 1.96, 1.52, and 1.26 Wm-1K-1) at the SBR, MNT, MTM, and PRD stations, respectively."**

1.11 [Page 746 Eq 13. I suggest relating this  $\theta_{satMOD}$  equation to Eq. 12 for quartz pedotransfer function and further to  $\lambda_{sat}$ .]

#### **RESPONSE 1.11**

Yes, the use of Eq. (13) in determining a pedotransfer function will be discussed.

#### **CHANGES 1.11**

**Sect. 3.3: "These results are illustrated in Fig. 8 in the case of the  $m_{sand}^*$  pedotransfer function. Figure 8 also shows that using the  $\theta_{sat}$  observations instead of  $\theta_{satMOD}$  (Eq. (13)) has little impact on  $\lambda_{satMOD}$  (Sect. 3.2)."**

1.12 [Page 747 Lines 1-4 about Eq 14. I do not see how dMOD is related to  $\lambda_{sat}$  here. I do not see dMOD is mentioned elsewhere. This dMOD is distracting/interruptive to the  $\theta_{satMOD}$  and can be deleted.]

#### **RESPONSE 1.12**

Eq. (14) is equivalent to Eq. (1). The impact of using Eqs. (13)-(14) in the sensitivity study (current Sect. 4.1) will be shown and discussed.

#### **CHANGES 1.12**

**Sect. 3.3:** "These results are illustrated in Fig. 8 in the case of the  $m_{\text{sand}}^*$  pedotransfer function. Figure 8 also shows that using the  $\theta_{\text{sat}}$  observations instead of  $\theta_{\text{satMOD}}$  (Eq. (13)) has little impact on  $\lambda_{\text{satMOD}}$  (Sect. 3.2)."

1.13 [Page 756 Table 2. The 6 stations with no eligible observations ( $n = 0$ ), filtered by saturation degree of 0.4, can be simply omitted since they are not informative.]

### RESPONSE 1.13

Agreed.

### CHANGES 1.13

New Table 2 is as follows:

**Table 2** – Thermal properties of 14 grassland soils in southern France:  $\lambda_{\text{sat}}$ ,  $f_q$  and  $Q$  retrievals using the  $\lambda$  model (Eqs. (7)-(9) and Eq. (10), respectively) for degree of saturation values higher than 0.4, together with the minimized RMSD between the simulated and observed  $\lambda$  values, and the number of used  $\lambda$  observations ( $n$ ). The soils are sorted from the largest to the smallest ratio of  $m_{\text{sand}}$  to  $m_{\text{SOM}}$ .

Station	Station full name	$\lambda_{\text{sat}}$ ( $\text{Wm}^{-1}\text{K}^{-1}$ )	RMSD ( $\text{Wm}^{-1}\text{K}^{-1}$ )	$n$	$f_q$ ( $\text{m}^3\text{m}^{-3}$ )	$Q$ (-)	$\frac{m_{\text{sand}}}{m_{\text{SOM}}}$
SBR	SABRES	2.80	0.255	6	0.62	0.96	37.2
LGC	LA-GRAND-COMBE	2.07	0.311	20	0.44	0.77	26.6
CBR	CABRIERES-D'AVIGNON	1.92	0.156	20	0.44	0.88	18.4
LZC	LEZIGNAN-CORBIERES	1.71	0.107	20	0.29	0.51	17.3
SVN	SAVENES	1.78	0.163	20	0.34	0.61	15.4
MNT	MONTAUT	1.96	0.058	20	0.42	0.76	13.8
BRN	BARNAS	1.71	0.131	20	0.25	0.40	13.5
SFL	SAINT-FELIX-DE-LAURAGAIS	1.57	0.134	20	0.22	0.37	12.5
MTM	MOUTHOMET	1.52	0.095	20	0.21	0.35	7.0
URG	URGONS	1.37	0.066	20	0.05	0.10	6.2
LHS	LAHAS	1.57	0.136	20	0.26	0.45	5.3
CDM	CONDOM	1.82	0.086	20	0.26	0.44	5.0
PRG	PEYRUSSE-GRANDE	1.65	0.086	20	0.18	0.32	3.7
PRD	PRADES-LE-LEZ	1.26	0.176	20	0.14	0.28	3.7

1.14 [Page 762 Figure 4 legend. These three stations were chosen as examples to illustrate contrasting levels of  $\lambda_{\text{sat}}$  values. I suggest specifying this in legend.]

**RESPONSE 1.14**

Agreed.

**CHANGES 1.14**

**Start of Sect. 3.1: "Figure 3 shows retrieved and modelled  $I$  values vs. the observed degree of saturation of the soil, at a depth of 0.10 m, for contrasting retrieved values of  $\lambda_{\text{sat}}$ , from high to low  $\lambda_{\text{sat}}$  values (2.80, 1.96, 1.52, and 1.26 Wm<sup>-1</sup>K<sup>-1</sup>) at the SBR, MNT, MTM, and PRD stations, respectively."**

1.15 [Page 764 Figure 6. I may have missed, but I do not see the top and middle plots mentioned in the text.]

**RESPONSE 1.15**

Yes. The Figure is insufficiently discussed in the text. More emphasis will be put on the use of pedotranfer function(s) for quartz in the revised version of this paper.

1.16 [Page 739 Line 15-16. "hydrom-eteorology" should be properly hyphenated as "hydro-meteorology".]

**RESPONSE 1.16**

Yes. This typo will be corrected.

1.17 [Page 751 Line 16. To be more accurate, change "proposed for quartz" to "proposed for volumetric fraction of quartz".]

**RESPONSE 1.17**

Agreed.

1.18 [Page 760 and page 761. Figure 2 and Figure 3 are misplaced and with wrong legend; the figures should be swapped if they are to be included.]

**RESPONSE 1.18**

Agreed.

=====END=====

**Calvet et al. (2015), [www.soil-discuss.net/2/737/2015/](http://www.soil-discuss.net/2/737/2015/)**

*Impact of gravels and organic matter on the thermal properties of grassland soils in southern France*

**Response to Reviewer #2 and changes in the revised version of the paper**

**(T. Ren, [tsren@cau.edu.cn](mailto:tsren@cau.edu.cn))**

The authors thank Dr. Tusheng Ren (China Agricultural University, Beijing) for his review of the manuscript and for the fruitful comments.

2.1 [This paper investigates the influences of quartz fraction, soil organic matter (SOM) and gravel component on soil thermal conductivity. Field observations of soil temperature and water content from 21 weather stations in southern France, along with the information of soil texture and bulk density, were used to estimate soil thermal diffusivity and heat capacity, and then thermal conductivity. The quartz fraction was inversely estimated with an empirical thermal conductivity model. A pedotransfer function was further proposed for estimating quartz content from soil texture information. The effects of SOM and gravels on thermal conductivity values were also discussed. The information of quartz fraction in a soil is usually unavailable but has a major effect on the accuracy of many thermal conductivity models and their applications in other comprehensive models (e.g., the land-surface models). Therefore, the topic is interesting and has general applications in soil sciences and related areas. However, I have some concerns about the current approach for estimating soil thermal properties and quartz content, the presentation of the results, and the conclusions.]

#### **RESPONSE 2.1**

Many thanks for these encouraging comments. We will do our best to account for your remarks in a revised version of the manuscript.

**[Additional comments](#)**

**In response to the reviewers' comments, we have revised our approach. The  $\lambda$  retrievals influenced by heterogeneities in soil properties are now sorted out. As a result, we now obtain realistic  $\lambda_{\text{sat}}$  values for 14 soils. We improved the assessment of uncertainties on the pedotranfer function for quartz volumetric content:**

- a variety of pedotransfer functions is now proposed, not only one**
- a confidence interval for the coefficients of pedotransfer functions is given**
- the impact of errors on the volumetric heat capacity of soil minerals is assessed**
- the data from Lu et al. (2007) are used as an independent benchmark to verify the obtained pedotransfer functions.**

**In order to clarify the definition of symbols, the volumetric fraction of quartz is now written as " $f_q$ " (instead of " $q$ ").**

**Finally, the Kersten number model of Lu et al. (2005) is now used instead of the Yang et al. (2005) model.**

2.2 [First, the method presented in the paper is based mainly on the 1D heat transfer equation and the de Vries (1963) mixed model for soil heat capacity. The authors estimated the apparent soil thermal diffusivity at 10-cm depth from temperature measurements at 5, 10, and 20 cm depths, and calculated soil heat capacity from the information of soil texture, bulk density, and water content at 10 cm. To apply the 1D Fourier heat transfer equation, they assumed that the soil physical properties were uniform and isothermal in the 5-20 cm layer, which was not the case. They stated that “soil properties are relatively homogeneous”, but it is difficult to accept this because 1) at least 14 soils had a gravel fraction over 10% (as high as 70% in some soils); 2) there were strong soil moisture and temperature gradients in the 0-20 cm layer; and 3) the existence and spatial distribution of grass roots were ignored. The authors are required to convince the readers that the 0-20 cm soil layer was uniform, and soil temperature and water content measurements at each depth were representative values of the depth.

Otherwise, the soil thermal diffusivity estimates are flawed, and further analysis is invalid.]

## RESPONSE 2.2

Yes, we agree. This is a very good point.

We acknowledge that the impact of vertical heterogeneities in  $\lambda$  values has to be properly accounted for in the  $\lambda$  retrieval technique we used. In order to address this issue, we revised our data analysis procedure in order to limit this effect as much as possible. In particular, we used only the soil temperature data presenting a relatively low vertical gradient close to the soil surface, where most differences with deeper layers are found. This refined data sorting increased the  $\lambda_{\text{sat}}$  retrieved value for all the stations. A very interesting side effect of the improved procedure was that LHS, SVN, and PRD now present non-zero values of  $q$ . On the other hand, the NBN observations are now filtered out as NBN presents very large differences in soil density from one soil depth to another. The new procedure is described below.

The 1D Fourier equation in heterogeneous soil conditions can be written as:

$$C_h \frac{\partial T}{\partial t} = \frac{\partial}{\partial z} \left( \lambda \frac{\partial T}{\partial z} \right) \quad (\text{R1})$$

and discretized as:

$$\frac{T_i^n - T_i^{n-1}}{\Delta t} = \frac{1}{C_{hi}} \left[ \frac{1}{2} \left( \frac{\lambda_{i+1/2} \gamma_{i+1}^n - \lambda_{i-1/2} \gamma_i^n}{\Delta z_m} \right) + \frac{1}{2} \left( \frac{\lambda_{i+1/2} \gamma_{i+1}^{n-1} - \lambda_{i-1/2} \gamma_i^{n-1}}{\Delta z_m} \right) \right] \quad (\text{R2})$$

In this study, we assume that the retrieved  $\lambda$  values, at a depth of  $-0.10\text{m}$ , are representative of a bulk soil layer including the three soil temperature probes used to retrieve the thermal diffusivity, and do not differ much from the interfacial  $\lambda$  values along the bottom and top edges of the considered soil layer ( $\lambda_{i+1/2}$  and  $\lambda_{i-1/2}$ , respectively):

$$\lambda \approx \lambda_{i+1/2} \approx \lambda_{i-1/2} \quad (\text{R3})$$

and, at a given time  $n$ ,

$$\lambda \gamma_{i+1}^n - \lambda \gamma_i^n \approx \lambda_{i+1/2} \gamma_{i+1}^n - \lambda_{i-1/2} \gamma_i^n \quad (\text{R4}).$$

In reality, differences may occur:



$$\Delta\lambda = \lambda_{i+1/2} - \lambda_{i-1/2} \quad (\text{R5}).$$

Considering the temperature gradient ratio  $R_{TG}$  at a given time  $n$ :

$$R_{TG} = \frac{\gamma_i^n}{\gamma_i^n - \gamma_{i+1}^n} \quad (\text{R6})$$

and combining Eqs. (R4), (R5) and (R6), the retrieved  $\lambda$  can be written as:

$$\lambda \approx \lambda_{i+1/2} - R_{TG} \Delta\lambda \quad (\text{R7}).$$

Since soil temperature gradients were more pronounced close to the soil surface and since soil density presented smaller values close to the soil surface, the  $\Delta\lambda$ ,  $R_{TG}$ , and  $R_{TG}\Delta\lambda$  values were  $\geq 0$ . Since in the soils considered in this study, differences in soil density were much less pronounced at depth than between the  $-0.05\text{m}$  and  $-0.10\text{m}$  soil layers, we considered that  $\lambda_{i+1/2}$  was closer to the final value to be retrieved,  $\lambda^*$ , than the initial  $\lambda$  retrieval:

$$\lambda^* \approx \lambda + R_{TG} \Delta\lambda \quad (\text{R8}).$$

Eq. (R8) shows that the target  $\lambda^*$  value is larger than the initial  $\lambda$  retrieval. The relative error on  $\lambda^*$  can be written as  $R_{TG}\Delta\lambda/\lambda^*$  (dimensionless). We used  $R_{TG}\Delta\lambda/\lambda^*$  as an indicator of the quality of the  $\lambda$  retrieval, with large values of  $R_{TG}\Delta\lambda/\lambda^*$  corresponding to erroneous estimates. In the revised data analysis procedure, a subset of 20  $\lambda$  retrievals per station was used, at most, corresponding to the lowest  $R_{TG}\Delta\lambda/\lambda^*$  values, with the condition  $R_{TG}\Delta\lambda/\lambda^* < 10\%$ . Since the NBN station presented  $R_{TG}\Delta\lambda/\lambda^*$  values systematically higher than 10%, the NBN data were excluded from the analysis.

The impact of the refined data selection is illustrated in Fig. R2.1 for the MNT station. For the LHS soil, which presented the highest  $\lambda$  RMSD together with  $q=0$ , the new procedure permits obtaining a non-zero value of  $q$  (Fig. R2.2).

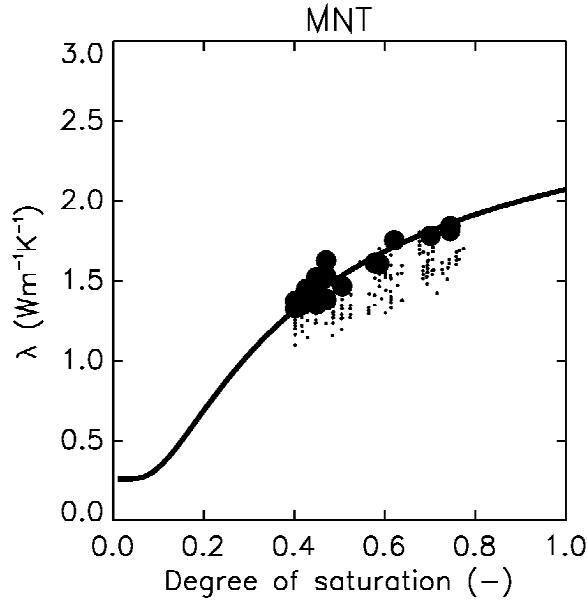


**Figure R2.1** - Retrieved and modelled  $\lambda$  values (dots and solid line, respectively) vs. the observed degree of saturation of the soil, at a depth of 0.10 m for the MNT station. The 20  $\lambda$  retrievals used to fit  $\lambda_{\text{sat}}$  are represented by large dots.

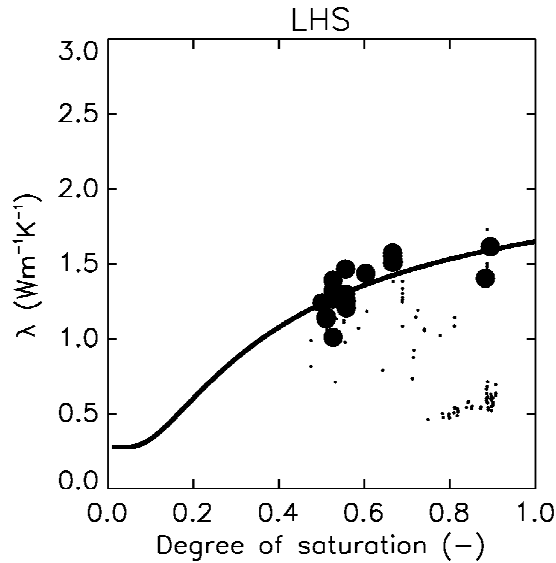


**Figure R2.2** - As in Fig. R2.1, except for LHS station.

In practise, the  $\Delta\lambda$  term was estimated using top-soil and deep dry density observations (at  $-0.05\text{m}$  and  $-0.10\text{m}$ , respectively) and the sensitivity of  $\lambda$  to changes in dry density,  $\Delta\lambda/\Delta\rho_d$ . The latter was derived numerically using the Eqs. (10)-(13) model, in soil wetness conditions ranging from  $S_d = 0.4$  to  $S_d = 1$ . Since the derivation of  $\Delta\lambda/\Delta\rho_d$  depends on the obtained  $q$  pedotransfer function (Eq. (12)),  $\Delta\lambda/\Delta\rho_d$  values were recalculated with the new pedotransfer function, and a few iterations permitted refining these estimates.

At saturation ( $S_d = 1$ )  $\Delta\lambda/\Delta\rho_d$  ranged between  $0.64 \times 10^{-3} \text{ Wm}^2\text{K}^{-1}\text{kg}^{-1}$  for PRD to  $1.24 \times 10^{-3} \text{ Wm}^2\text{K}^{-1}\text{kg}^{-1}$  for SBR. At  $S_d = 0.4$ ,  $\Delta\lambda/\Delta\rho_d$  ranged between  $0.46 \times 10^{-3} \text{ Wm}^2\text{K}^{-1}\text{kg}^{-1}$  for PRD to  $0.81 \times 10^{-3} \text{ Wm}^2\text{K}^{-1}\text{kg}^{-1}$  for SBR.

The  $\Delta\rho_d$  term ranged from  $10 \text{ kg m}^{-3}$  for CBR to  $284 \text{ kg m}^{-3}$  for NBN.  $R_{TG}$  ranged between 0.5 and 2.4, with a median value of 1.3.

## **CHANGES 2.2**

**The data selection method described above was included in a Supplement, together with Fig. S2.1. It is mentioned that the NBN, PZN, BRZ, and MJN observations are completely filtered out using the condition  $R_{TG}\Delta\lambda/\lambda^* < 10\%$ .**

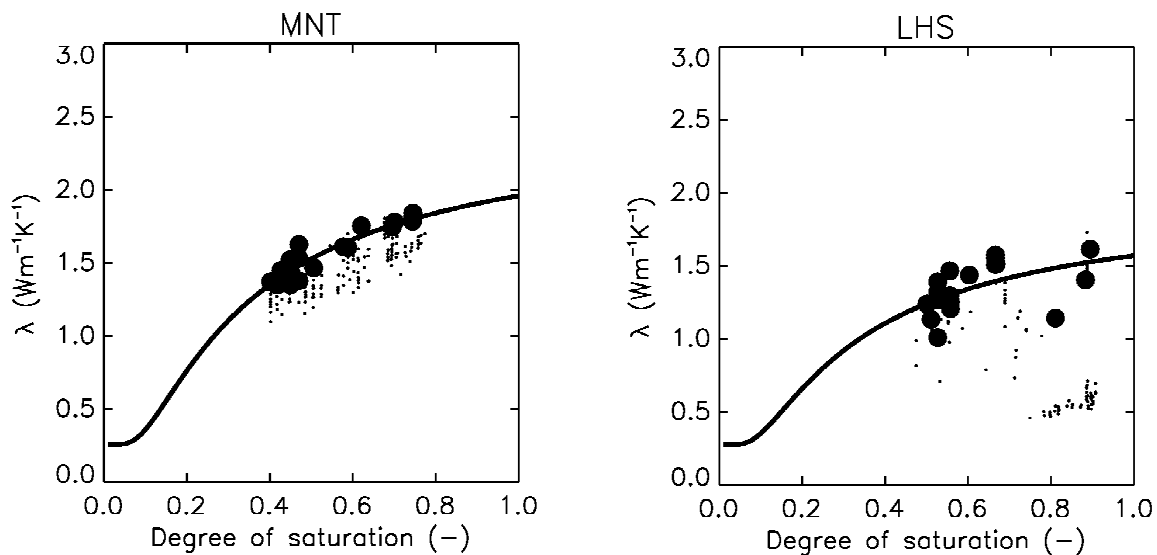


**Figure S2.1** - Retrieved and modelled  $\lambda$  values (dots and solid line, respectively) vs. the observed degree of saturation of the soil, at a depth of 0.10 m for the MNT and LHS stations.

The 20  $\lambda$  retrievals used to fit  $\lambda_{\text{sat}}$  are represented by large dots.

2.3 [Second, the de Vries (1963) mixing model was applied to estimate soil volumetric heat capacity. To do so, a fixed value of  $2.0 \text{ MJ m}^{-3} \text{ K}^{-1}$  was used for soil solids. The authors should give justification to use a constant value for the 21 soils with different

textures. Tarara and Ham (1997) used a value of 1.92 MJ m<sup>-3</sup> K<sup>-1</sup>. A soil-specific value may be better for estimating the volumetric heat capacity of soil solids.]

### RESPONSE 2.3

Yes, soil-specific values for the volumetric heat capacity of soil minerals ( $C_{hmin}$ ) may be more appropriate than using a constant standard value. However, we were not able to find such values in the literature and we did not measure this quantity.

We investigated the sensitivity of our results to these uncertainties, considering the following minimum and maximum  $C_{hmin}$  values:  $C_{hmin} = 1.8 \text{ J m}^{-3} \text{ K}^{-1}$  and  $C_{hmin} = 2.2 \text{ J m}^{-3} \text{ K}^{-1}$ . The impact of  $C_{hmin}$  on the retrieved values of  $\lambda_{sat}$  and  $q$  is presented in Figs. R2.3 and R2.4, respectively. The impact of  $C_{hmin}$  on the  $q$  pedotransfer function will be published in the final version of this work.

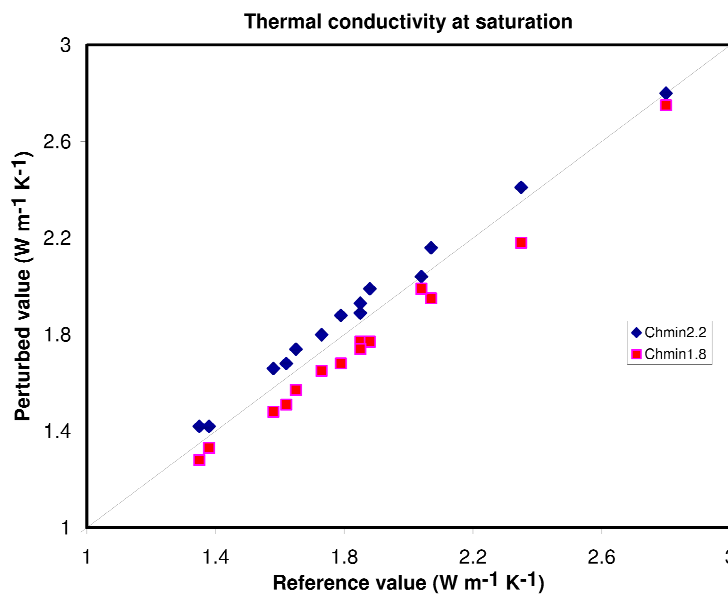


**Figure R2.3** - Impact on the retrieved  $\lambda_{sat}$  of using values of  $C_{hmin} = 1.8 \text{ J m}^{-3} \text{ K}^{-1}$  and  $C_{hmin} = 2.2 \text{ J m}^{-3} \text{ K}^{-1}$  instead of  $C_{hmin} = 2.0 \text{ J m}^{-3} \text{ K}^{-1}$ .

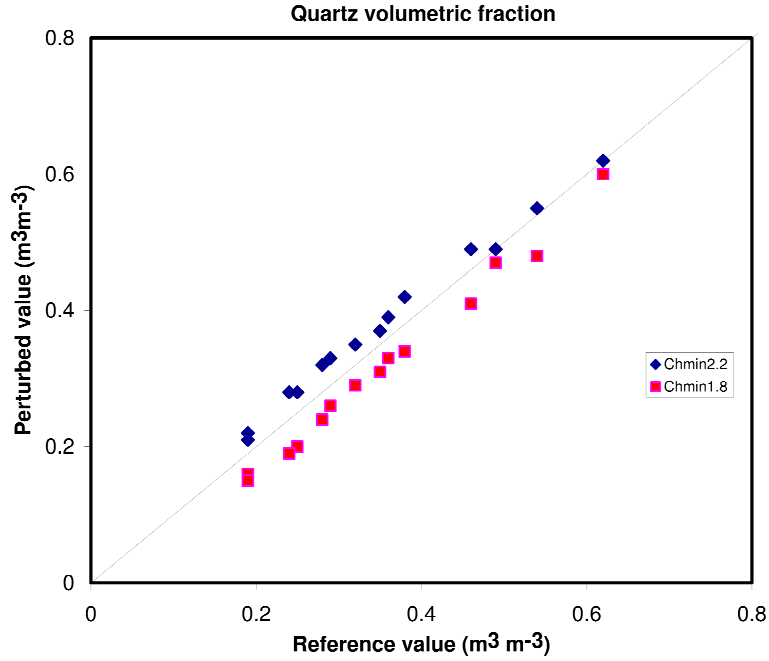


**Figure R2.4** - As in Fig. R2.3, except for volumetric fraction of quartz.

### CHANGES 2.3 (Sect. 4.1)

" In this study, the de Vries (1963) mixing model is applied to estimate soil volumetric heat capacity, and a fixed value of  $2.0 \text{ MJ m}^{-3} \text{ K}^{-1}$  is used for soil minerals (Eq. (6)). Soil-specific values for  $C_{hmin}$  may be more appropriate than using a constant standard value. For example, Tarara and Ham (1997) used a value of  $1.92 \text{ MJ m}^{-3} \text{ K}^{-1}$ . However, we did not measure this quantity and we were not able to find such values in the literature. We investigated the sensitivity of our results to these uncertainties, considering the following minimum and maximum  $C_{hmin}$  values:  $C_{hmin} = 1.92 \text{ MJ m}^{-3} \text{ K}^{-1}$  and  $C_{hmin} = 2.08 \text{ MJ m}^{-3} \text{ K}^{-1}$ . The impact of  $C_{hmin}$  on the retrieved values of  $\lambda_{sat}$  and  $f_q$  is presented in Fig. 9. On average, a change of  $+ (-) 0.08 \text{ MJ m}^{-3} \text{ K}^{-1}$  in  $C_{hmin}$  triggers a change in  $\lambda_{sat}$  and  $f_q$  of  $+ 1.7 \%$  ( $- 1.8 \%$ ) and  $+ 4.8 \%$  ( $- 7.0 \%$ ), respectively."

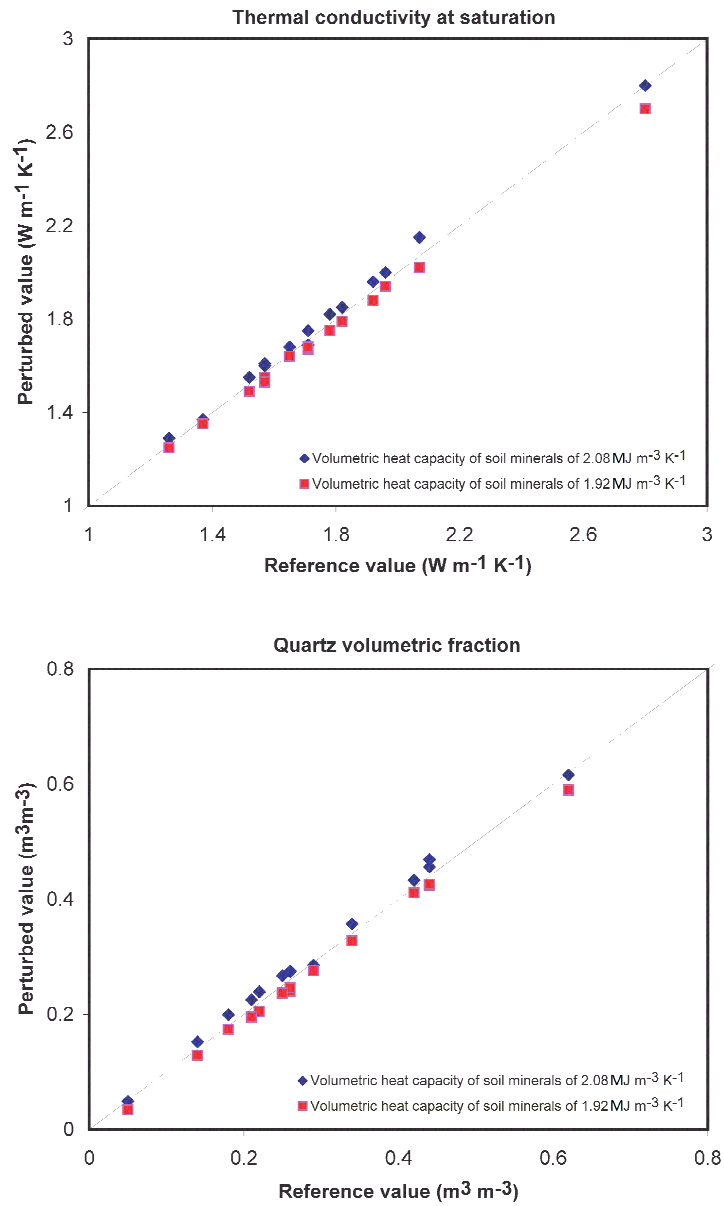


**Figure 9** - Impact of using values of  $C_{hmin} = 1.92 \text{ MJ m}^{-3} \text{ K}^{-1}$  and  $C_{hmin} = 2.08 \text{ MJ m}^{-3} \text{ K}^{-1}$  instead of  $C_{hmin} = 2.0 \text{ MJ m}^{-3} \text{ K}^{-1}$  on (top) the retrieved  $\lambda_{sat}$ , (bottom) the volumetric fraction of quartz.

**REFERENCES:**

de Vries, D.A.: Thermal properties of soils, in W.R. Van Wijk (ed.), *Physics of plant environment*, pp. 210–235, North-Holland Publ. Co., Amsterdam, 1963.

**Tarara, J.M., and J.M. Ham: Measuring soil water content in the laboratory and field with dual-probe heat-capacity sensors, *Agron. J.*, 89, 535–542, 1997.**

**2.4 [In addition, what were the volumetric fractions of grass roots in the 0-20 cm soil layer? Does the heat capacity of grass roots have a significant influence on the bulk soil heat capacity?]**

#### **RESPONSE 2.4**

The grasslands considered in this study are not intensively managed. They consist of set-aside fields cut once or twice a year. Calvet et al. (1999) gave an estimate of  $0.160 \text{ kg m}^{-2}$  for the root dry matter content of such soils for a site in southwestern France, with most roots contained in the 0.25m top soil layer. This represents a gravimetric fraction of organic matter  $\leq 0.0005 \text{ kg kg}^{-1}$ , i.e. less than 4% of the lowest  $m_{\text{SOM}}$  values observed in this study ( $0.013 \text{ kg kg}^{-1}$ ) or less than 5% of  $f_{\text{SOM}}$  values. We checked that increasing  $f_{\text{SOM}}$  values by 5% has negligible impact on heat capacity and on the  $\lambda$  retrievals.

#### **CHANGES 2.4**

**New Sect. 4.1: " The grasslands considered in this study are not intensively managed. They consist of set-aside fields cut once or twice a year. Calvet et al. (1999) gave an estimate of  $0.160 \text{ kg m}^{-2}$  for the root dry matter content of such soils for a site in southwestern France, with most roots contained in the 0.25m top soil layer. This represents a gravimetric fraction of organic matter  $\leq 0.0005 \text{ kg kg}^{-1}$ , i.e. less than 4% of the lowest  $m_{\text{SOM}}$  values observed in this study ( $0.013 \text{ kg kg}^{-1}$ ) or less than 5% of  $f_{\text{SOM}}$  values. We checked that increasing  $f_{\text{SOM}}$  values by 5% has negligible impact on heat capacity and on the  $\lambda$  retrievals".**

#### **REFERENCE:**

**Calvet, J.-C., Bessemoulin, P., Noilhan, J., Berne, C., Braud, I., Courault, D., Fritz, N., Gonzalez-Sosa, E., Goutorbe, J.-P., Haverkamp, R., Jaubert, G., Kergoat, L., Lachaud, G., Laurent, J.-P., Mordelet, P., Oliso, A., Péris, P., Roujean, J.-L., Thony, J.-L., Tosca,**

**C., Vauclin, M., Vignes, D.: MUREX: a land-surface field experiment to study the annual cycle of the energy and water budgets, *Ann. Geophys.*, 17, 838-854, 1999.**

2.5 [Third, no independent data or measurements were used to evaluate the estimates of soil thermal conductivity and quartz fraction. In Table 2, for example, the estimated thermal conductivity values for saturated soils ranged from 0.52 to 2.79 W m<sup>-1</sup> K<sup>-1</sup> for 15 soils, all were much lower than the published results of Lu et al. (2007) and Tarnawski et al. (2011). The authors may need to verify the results by compare the model estimates against thermal conductivity measurements with the line-source probe or the heat pulse technique.]

#### **RESPONSE 2.5**

It must be noted that in many studies (e.g. Lu et al., 2007)  $\lambda_{\text{sat}}$  estimates are derived from reassembled sieved soil samples excluding the gravels, while our data concern undisturbed soils.

In our revised analysis, we found  $\lambda_{\text{sat}}$  values ranging between 1.26 Wm<sup>-1</sup>K<sup>-1</sup> and 2.80 Wm<sup>-1</sup>K<sup>-1</sup>. These values are consistent with  $\lambda_{\text{sat}}$  values reported by other authors. Tarnawski et al. (2011) gave  $\lambda_{\text{sat}}$  values ranging between 2.5 Wm<sup>-1</sup>K<sup>-1</sup> and 3.5 Wm<sup>-1</sup>K<sup>-1</sup> for standard sands. Lu et al. (2007) gave  $\lambda_{\text{sat}}$  values ranging between 1.33 Wm<sup>-1</sup>K<sup>-1</sup> and 2.2 Wm<sup>-1</sup>K<sup>-1</sup>.

#### **CHANGES 2.5**

**New Sect. 4.3 (Applicability of the new  $\lambda_{\text{sat}}$  model to other soil types) uses the Lu et al. (2007) data as an independent benchmark.**

2.6 [Finally, I do not think the empirical equations (13) and (14), and related results and discussion, are related to and helpful for the purpose of this paper.]

#### **RESPONSE 2.6**

The empirical Eq. (13) for  $\theta_{\text{sat}}$  is used for the end-to-end simulation for the sensitivity study of Table 3, as such an equation has to be used in land surface models. Eq. (14) is equivalent to



Eq. (1). The impact of using Eq. (13) in the sensitivity study (current Sect. 4.1) will be shown and discussed. Note that we found and corrected a bug in the program we developed to perform this sensitivity analysis. In the revised manuscript, the sensitivity study will be performed with and without using this equation, and for several plausible pedotransfer functions.

### **CHANGES 2.6**

**Sect. 3.2: "Modelled values of  $\lambda_{\text{sat}}$  ( $\lambda_{\text{satMOD}}$ ) can be derived from  $f_{\text{qMOD}}$  using Eq. (10) together with  $\theta_{\text{sat}}$  observations. The  $\lambda_{\text{satMOD}}$   $r^2$ , RMSD, and mean bias scores are given in Table 5. Again, the best scores are obtained using the  $m_{\text{sand}}/m_{\text{SOM}}$  predictor of  $f_{\text{q}}$ , with  $r^2$ , RMSD, and mean bias values of 0.86, 0.14  $\text{Wm}^{-1}\text{K}^{-1}$ , and +0.01  $\text{Wm}^{-1}\text{K}^{-1}$ , respectively (Fig. 7)."**

**Sect. 3.3: "Figure 8 shows that using the  $\theta_{\text{sat}}$  observations instead of  $\theta_{\text{satMOD}}$  (Eqs. (13)) has little impact on  $\lambda_{\text{satMOD}}$  (Sect. 3.2)."**

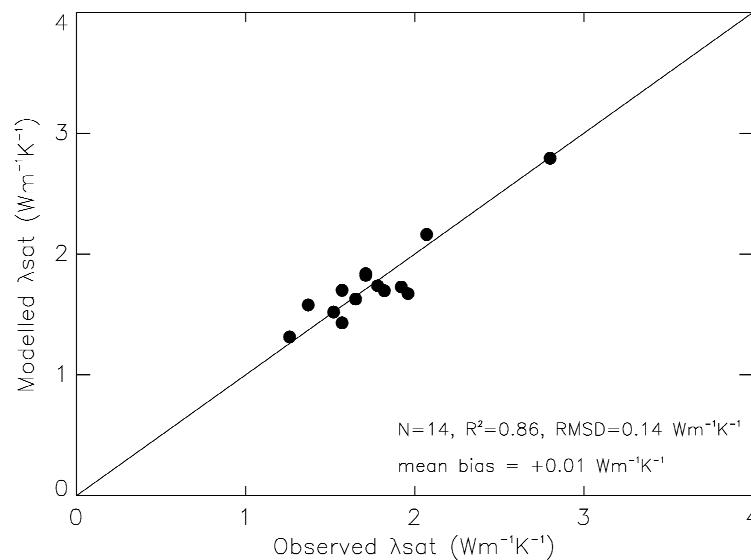


**Figure 7** –  $\lambda_{\text{satMOD}}$  values derived from the  $m_{\text{sand}} / m_{\text{SOM}}$  pedotransfer function for the volumetric quartz fractions, using observed  $\theta_{\text{sat}}$  values, vs.  $\lambda_{\text{sat}}$  retrievals.

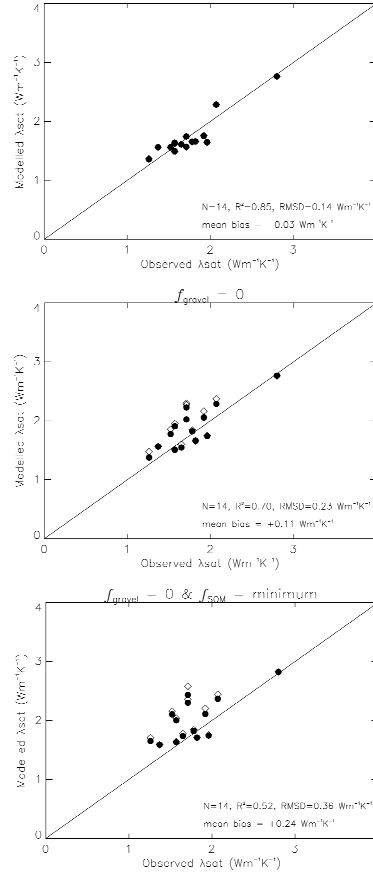


**Figure 8** –  $\lambda_{satMOD}$  values derived from the  $m_{sand}^*$  pedotransfer function for the volumetric quartz fractions, using or not  $\theta_{satMOD}$  (Eq. (13)) (dark dots and opened diamonds, respectively), vs.  $\lambda_{sat}$  retrievals: (top) full model, (middle)  $f_{SOM} = 0.013 \text{ m}^3\text{m}^{-3}$ , (bottom)  $f_{SOM} = 0.013 \text{ m}^3\text{m}^{-3}$  and  $f_{gravel} = 0 \text{ m}^3\text{m}^{-3}$ .

**Table 5** – Ability of the Eqs. (10)-(13) empirical model to estimate  $\lambda_{sat}$  values for 14 soils and impact of changes in gravel and SOM volumetric content:  $f_{gravel} = 0 \text{ m}^3\text{m}^{-3}$  and  $f_{SOM} = 0.013 \text{ m}^3\text{m}^{-3}$  (the smallest  $f_{SOM}$  value, observed for CBR).  $r^2$  values smaller than 0.60, RMSD values higher than  $0.20 \text{ Wm}^{-1}\text{K}^{-1}$ , and mean bias values higher (smaller) than  $+0.10$  ( $-0.10$ ) are in bold.

Model configuration	Predictor of $f_q$	$r^2$	RMSD ( $\text{Wm}^{-1}\text{K}^{-1}$ )	Mean bias ( $\text{Wm}^{-1}\text{K}^{-1}$ )
Model using $\theta_{sat}$ observations	$m_{sand} / m_{SOM}$	0.86	0.14	+0.01
	$m_{sand}^*$	0.83	0.15	-0.01
	$m_{sand}$	0.81	0.16	-0.03
	$1 - \theta_{sat} - f_{sand}$	0.82	0.16	-0.03
Full model using $\theta_{satMOD}$ (Eqs. (13))	$m_{sand} / m_{SOM}$	0.85	0.14	+0.03
	$m_{sand}^*$	0.85	0.14	-0.03
	$m_{sand}$	0.84	0.15	-0.03

	$1 - \theta_{\text{sat}} - f_{\text{sand}}$	0.82	0.16	-0.02
same with:	$m_{\text{sand}} / m_{\text{SOM}}$	<b>0.57</b>	<b>0.35</b>	<b>+0.20</b>
$f_{\text{SOM}} = 0.013 \text{ m}^3 \text{ m}^{-3}$	$m_{\text{sand}}^*$	0.83	0.15	+0.00
	$m_{\text{sand}}$	0.81	0.16	-0.02
	$1 - \theta_{\text{sat}} - f_{\text{sand}}$	0.83	0.15	-0.02
same with:	$m_{\text{sand}} / m_{\text{SOM}}$	0.87	0.19	<b>-0.12</b>
$f_{\text{gravel}} = 0 \text{ m}^3 \text{ m}^{-3}$	$m_{\text{sand}}^*$	0.70	<b>0.23</b>	<b>+0.11</b>
	$m_{\text{sand}}$	0.79	0.17	+0.04
	$1 - \theta_{\text{sat}} - f_{\text{sand}}$	0.81	0.17	+0.05
same with:	$m_{\text{sand}} / m_{\text{SOM}}$	0.63	<b>0.31</b>	<b>+0.16</b>
$f_{\text{SOM}} = 0.013 \text{ m}^3 \text{ m}^{-3}$	$m_{\text{sand}}^*$	<b>0.52</b>	<b>0.36</b>	<b>+0.24</b>
and $f_{\text{gravel}} = 0 \text{ m}^3 \text{ m}^{-3}$	$m_{\text{sand}}$	<b>0.59</b>	<b>0.29</b>	<b>+0.16</b>
	$1 - \theta_{\text{sat}} - f_{\text{sand}}$	0.70	<b>0.25</b>	<b>+0.16</b>

(\*) only  $m_{\text{sand}}$  values smaller than  $0.6 \text{ kg kg}^{-1}$  are used in the regression

2.7 [The current title does not fully represent the content of this paper. The title talks about the effects of gravels and organic matter on soil thermal conductivity values. In the text, on the other hand, the authors spent a lot effort on discussing the influences of quartz content on soil thermal conductivity. The title also addresses the grassland soils, but the detailed information about grass cover and roots was missing.]

## RESPONSE 2.7

Yes, in the revised version of the manuscript, the effects of gravels and organic matter on soil thermal conductivity values will be included in the result section. More information of vegetation characteristics will be given.

## CHANGES 2.7

Title: "gravels and organic matter" was replaced by "quartz".

Section 3: Sect. 4.1 was moved to Sect. 3.3.

New Sect. 4.1: " The grasslands considered in this study are not intensively managed. They consist of set-aside fields cut once or twice a year. Calvet et al. (1999) gave an estimate of  $0.160 \text{ kg m}^{-2}$  for the root dry matter content of such soils for a site in southwestern France, with most roots contained in the 0.25m top soil layer. This

represents a gravimetric fraction of organic matter  $\leq 0.0005 \text{ kg kg}^{-1}$ , i.e. less than 4% of the lowest  $m_{\text{SOM}}$  values observed in this study ( $0.013 \text{ kg kg}^{-1}$ ) or less than 5% of  $f_{\text{SOM}}$  values. We checked that increasing  $f_{\text{SOM}}$  values by 5% has negligible impact on heat capacity and on the  $\lambda$  retrievals".

2.8 [Page 739 Line 7-8: The authors stated that soil thermal conductivity was hard to obtain directly and in situ. This is not true today. Recent advances in line-source probe and heat pulse method have made it easy to monitor soil thermal conductivity in the field (e.g., Bristow, K.L., G.J. Kluitenberg, and R. Horton. 1994. Measurement of soil thermal properties with a dual-probe heat-pulse method. *Soil Sci. Soc. Am. J.* 58:1288–129; Zhang, X., J. Heitman, R. Horton and T. Ren. 2014. Measuring near-surface soil thermal properties with the heat-pulse method: correction of ambient temperature and soil–air interface effects. *Soil Sci. Soc. Am. J.* 78:1575–1583. The authors may also include the reference of Bristow (1998) who investigated the influences of quartz fraction on soil thermal conductivity.)

## RESPONSE 2.8

Yes, this sentence will be rephrased. Note however that such measurements are currently not made in operational meteorological networks. Using standard soil moisture and soil temperature observations is a way to investigate soil thermal properties over a large variety of soils, as the access to such data is facilitated by online databases (e.g. <https://ismn.geo.tuwien.ac.at/>).

## CHANGES 2.8

### Introduction:

"The construction and the verification of the  $\lambda$  models is not easy as  $\lambda$  is often measured in the lab on perturbed soil samples (Abu-Hamdeh et al., 2000; Lu et al., 2007). Although recent advances in line-source probe and heat pulse method have made it easier to monitor soil thermal conductivity in the field (Bristow et al., 1994; Zhang et al., 2014), such measurements are currently not made in operational meteorological networks."

**"The information on quartz fraction in a soil is usually unavailable as it can only be measured using X-ray diffraction or X-ray fluorescence techniques, which are difficult to implement (Schönenberger et al., 2012). This has a major effect on the accuracy of thermal conductivity models and their applications (Bristow, 1998)."**

**2.9 [Page 740 Line 21: Fig. 2 should be cited as Fig. 3 here. Page 741 Line 17: 'Figure 3' should be 'Figure 2'.]**

#### **RESPONSE 2.9**

Yes. This typo will be corrected.

**2.10 [Page 740 Line 23-26: How were gravel and SOM contents determined? Grass roots may also influence soil thermal conductivity and heat capacity in the shallow soil layers, but were ignored in the paper. Please give supporting evidence about this. In addition, what depth was bulk density measured? Did soil bulk density differ with depth?]**

#### **RESPONSE 2.10**

Soil texture, gravel and SOM fractions were measured by an independent laboratory we contracted (INRA-Arras) from samples we collected in situ.

We checked that grass roots should not significantly influence our results (see RESPONSE 2.4). One cannot exclude large root density values very close to the soil surface during the plant growth period, but the new data sorting procedure we implemented limits these soil heterogeneity effects (see RESPONSE 2.2).

Bulk density was measured at all depths (–0.05 m, –0.10 m, –0.20 m) using unperturbed oven-dried soil samples collected using metal cylinders of known volume. Most differences were observed from –0.05 m to –0.10 m, as soil density is lower close to the surface. The largest difference was observed for NBN ( $-284 \text{ kg m}^{-3}$  at –0.05 m with respect to –0.10 m, or –18%). For the 14 stations now presenting successful  $q$  retrieval, –0.05 m density relative differences with respect to density at –0.10 m range from  $\pm 3\%$  or less (MNT, SFL, LGC, CBR, LHS, SVN, PRD) to about –13% (SBR, BRN, PRG), and from –7% to –9% for CDM, LZC, MTM, and URG.

## **CHANGES 2.10**

**See Supplement 1 (Table S1.1) and Supplement 2.**

2.11 [Sect. 2.5: The estimated thermal conductivity values were used to retrieve quartz content data using the empirical thermal conductivity models. Leong et al. (2009) tried to use the Lu et al. (2007) model to inversely estimate quartz content in soil samples. In this work, the authors used the Yang et al. (2005) model. Please explain why the Yang et al. (2005) model was used, and how the quartz content estimates from the two models may differ.]

### **RESPONSE 2.11**

Yes, in the first version of this work, we used the Kersten number calculation used by Yang et al. (2005). Figure R2.5 shows the resulting  $K_e$  value, together the  $K_e$  value obtained using the Lu et al. (2007) model for fine and coarse soils. It can be seen that most differences between these models occur for  $S_d$  values  $< 0.4$ . Since we only use  $\lambda$  retrievals for  $S_d$  values  $> 0.4$ , the impact of the uncertainties in the determination of  $K_e$  is limited. However, using Lu et al. (2007) instead of Yang et al. (2005) tends to produce smaller values of  $\lambda_{sat}$  and  $q$  retrievals, as shown by Figs. R2.6 and R2.7. The impact of the Kersten number calculation will be discussed in the final version of this work.

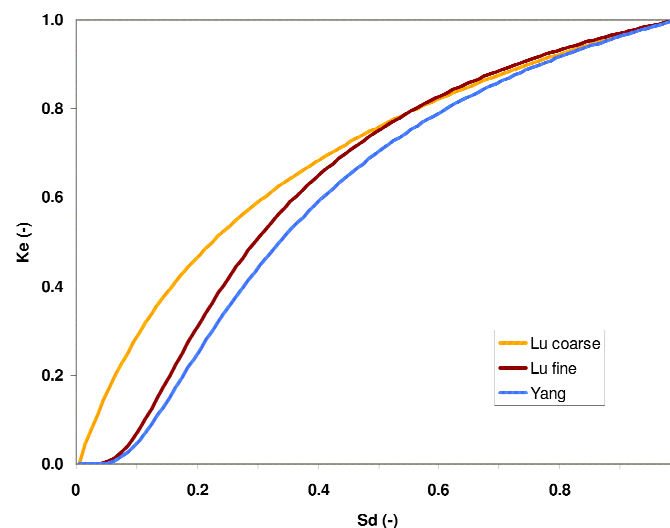


**Figure R2.5** - Kersten number vs. degree of saturation as modelled by Lu et al. (2007) for coarse and fine soils, and as modelled by Yang et al. (2005).

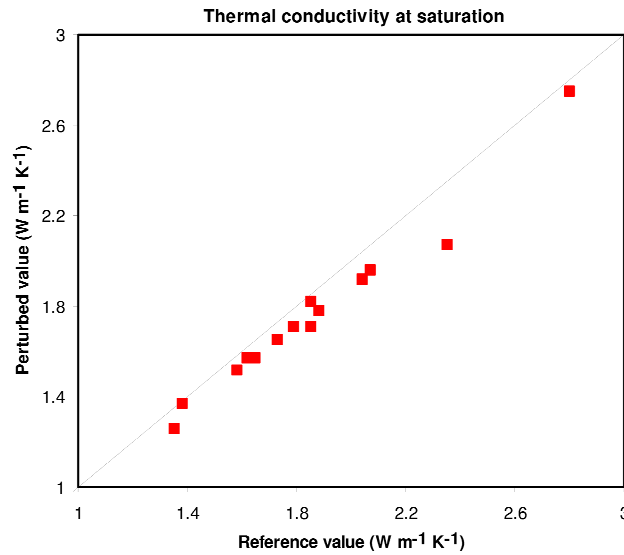


**Figure R2.6** -  $\lambda_{\text{sat}}$  retrievals using the Kersten number as modelled by Lu et al. (2007) vs. those using the Kersten number as modelled by Yang et al. (2005).

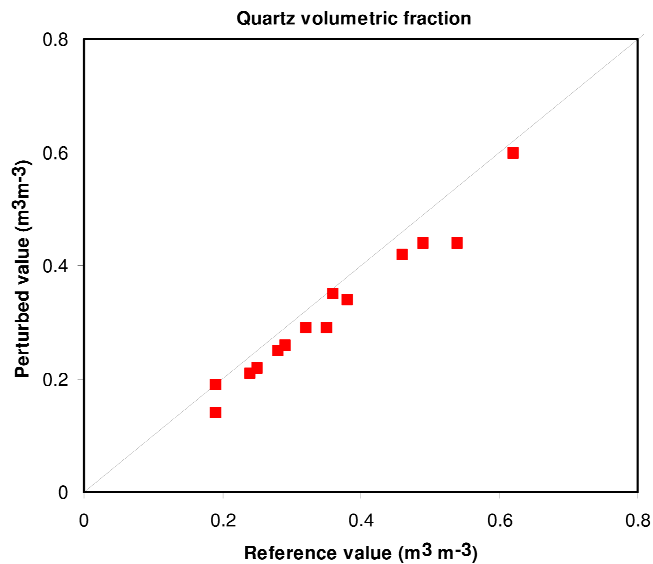


**Figure R2.7** - As in Fig. R2.6, except for  $q$  retrievals.

### CHANGES 2.11 (Sect. 2.5)

"In this study, the formula recommended by Lu et al. (2007) is used:

$$K_e = \exp\left\{\alpha\left(1 - S_d^{(\alpha-1.33)}\right)\right\},$$

with  $\alpha = 0.96$  for  $Mn_{\text{sand}} \geq 0.4 \text{ kg kg}^{-1}$ ,  $\alpha = 0.27$  for  $Mn_{\text{sand}} < 0.4 \text{ kg kg}^{-1}$ , and

$$S_d = \theta/\theta_{\text{sat}} \quad (9).$$

$Mn_{\text{sand}}$  represents the sand mass fraction of fine earth minerals (values are given in Supplement 1).

Following Peters-Lidard et al. (1998),  $\lambda_{\text{other}}$  is taken as  $2.0 \text{ Wm}^{-1}\text{K}^{-1}$  for soils with  $Mn_{\text{sand}} > 0.2 \text{ kg kg}^{-1}$ , and  $3.0 \text{ Wm}^{-1}\text{K}^{-1}$  otherwise. In this study,  $Mn_{\text{sand}} > 0.2 \text{ kg kg}^{-1}$  for all soils except for URG, PRG, and CDM."

2.12 [Sect. 2.6: More in-depth explanations are required to explain the calculation of quartz content.]

### **RESPONSE 2.12**

Yes, we will publish a Supplement to the final version of the paper explaining the various calculation steps.

### CHANGES 2.12 (Sect. 2.6)

"Only  $\lambda$  observations for  $S_d$  values higher than 0.4 are used because in dry conditions:, (1) conduction is not the only mechanism for heat exchange in soils, as the convective water vapour flux may become significant (Schelde et al., 1998, Parlange et al. 1998), (2) the  $K_e$  functions found in the literature display more variability, (3) the  $\lambda_{\text{sat}}$  retrievals are more sensitive to uncertainties in  $\lambda$  observations. The threshold value of  $S_d = 0.4$  results from a compromise between the need of limiting the influence of convection, of the shape of the  $K_e$  function on the retrieved values of  $\lambda_{\text{sat}}$ , and of using as many observations as possible in the retrieval process."



2.13 [Sect. 3.2: I am not sure how useful to develop the pedotransfer functions for estimating quartz content. It is apparent that all errors in the measurement (e.g., temperature, water content, bulk density, and gravel fraction) and calculations (thermal diffusivity and heat capacity) have been included in the results of quartz content. In addition, I had a hard time to figure out how quartz content was related to the fraction of soil organic matter (Eq. [12]).]

#### **RESPONSE 2.13**

In the revised version of the manuscript, we will improve the description and the assessment of the uncertainties affecting the obtained pedotransfer function(s).

#### **CHANGES 2.13**

**We improved the assessment of uncertainties on the pedotransfer function for quartz volumetric content:**

- **a variety of pedotransfer functions is now proposed, not only one**
- **a confidence interval for the coefficients of pedotransfer functions is given**
- **the impact of errors on the volumetric heat capacity of soil minerals is assessed**
- **the data from Lu et al. (2007) are used as an independent benchmark to verify the obtained pedotransfer functions.**

2.14 [Sect. 4.2: The authors suggested that the very low values of quartz content might be caused by (1) the natural heterogeneity of soil properties, (2) the living root biomass, and (3) stones that were not accounted for in the gravel fraction. All these factors lead to inaccurate estimates of soil thermal diffusivity and heat capacity. Therefore, I wonder if it is correct to include all the 21 stations in this work. On those soils with high fractions of gravel (and stones) and grass roots, it is impossible to obtain representative temperature and water content data at each depth, and it is inappropriate to apply the 1D heat transfer equation to estimate soil thermal diffusivity.]

#### **RESPONSE 2.14**

The difficulties we had can be explained by heterogeneities in soil properties, soil density in particular. An enhanced procedure was implemented in order to mitigate this effect (see RESPONSE 2.2). LHS, SVN, and PRD now present non-zero values of  $q$  and the NBN

observations are filtered out. We had no difficulty in measuring soil temperature and soil moisture, including at the BRN soil presenting the largest fraction of gravel (see Fig. R2.8). Note that the sensors we use are designed to work in such difficult conditions. The ThetaProbe and PT100 sensors have very strong rods, 0.06 m and 0.10 m long, respectively.

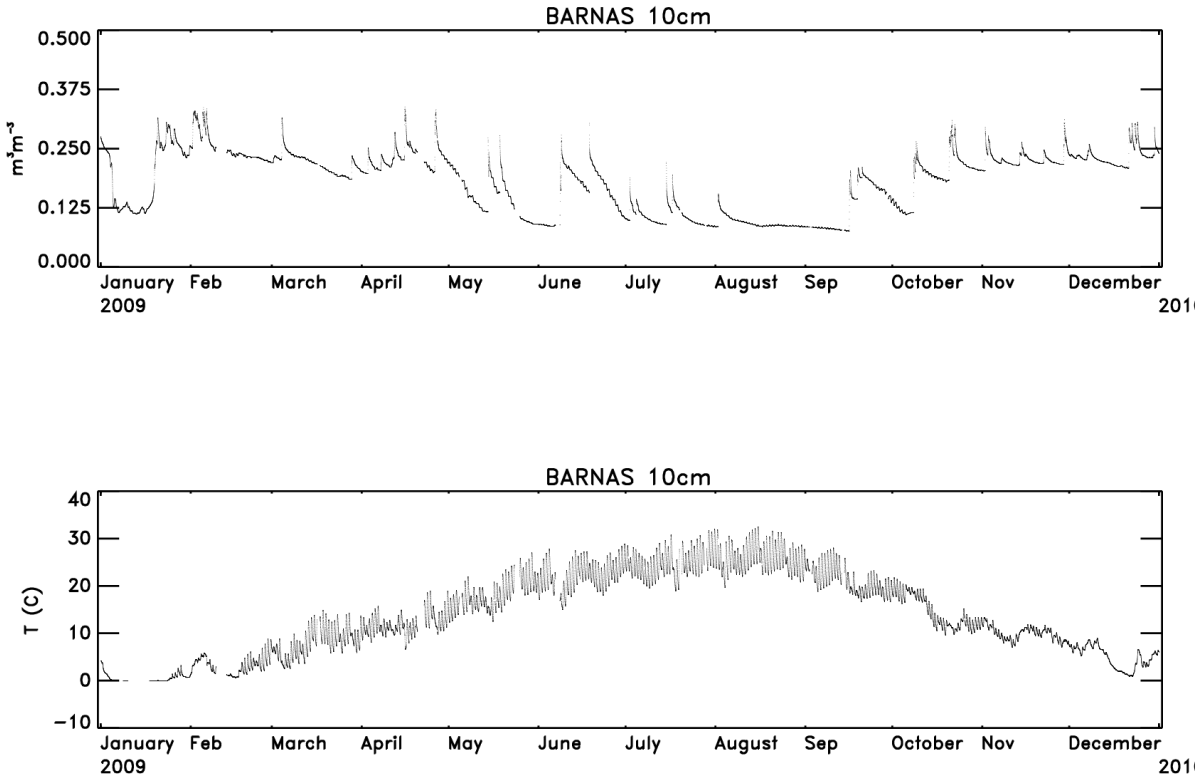


**Figure R2.8** - Soil temperature and soil moisture measured in 2009 at the BRN station at a depth of  $-0.10m$

## CHANGES 2.14 (Supplement 1)

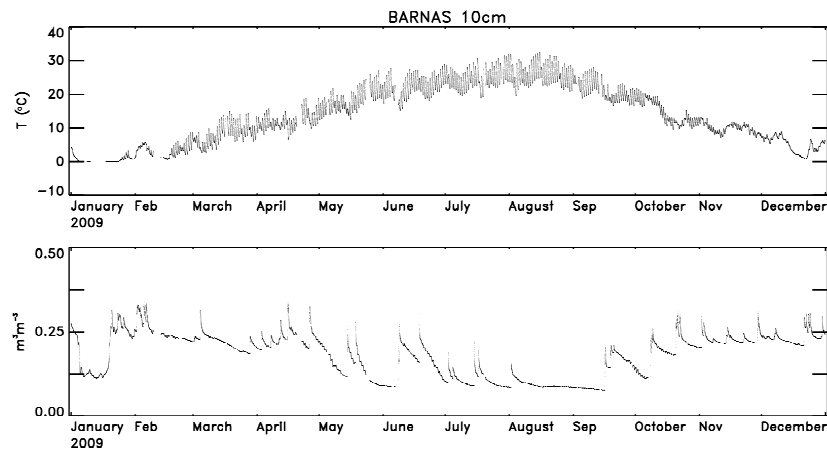


**Figure S1.2** - Soil temperature (top) and volumetric soil moisture (bottom) measured in 2009 at the Barnas station (BRN) at a depth of  $-0.10\text{m}$ .

2.15 [Most symbols in this paper are not properly defined.]

### **RESPONSE 2.15**

We tried to use symbols used in other works. It will be made clear that in this study,  $q$  ( $f_{\text{SOM}}$ ) represents the volumetric fraction of quartz (SOM) within the whole soil volume, while in many studies, it represents the volumetric fraction of quartz (SOM) within the volume of soil solids.

## CHANGES 2.15 (Sect. 2.5, Eq. (11))

**In order to clarify the definition of symbols, the volumetric fraction of quartz is now written as " $f_q$ " (instead of " $q$ "):**

$$f_q = Q \times (1 - \theta_{\text{sat}})$$

**with  $Q$  representing the fraction of quartz within soil solids.**

2.16 [Table 1: The soil texture should be mentioned together with the particle size distribution.]

### **RESPONSE 2.16**

A new table will be added, listing the particle size distribution observations.

**CHANGES 2.15**

**Supplement 1, Table S1.1.**

2.17 [Figure 2 and 3 do not match with their captions.]

**RESPONSE 2.17**

Yes. This typo will be corrected.

2.18 [Figure 4: How were the solid lines obtained? For the SBR site, why a large variation in thermal conductivity was observed in a narrow range of degree of saturation? How come a gravel soil (the PRD site) had very low thermal conductivity in the degree of saturation range of 0.4-0.5 range?]

**RESPONSE 2.18**

For several soils (SBR, SVN, LZC, PRD, LGC, BRN, and CBR), no  $\lambda$  retrieval or very few  $\lambda$  retrievals were obtained for  $S_d > 0.6$ . Since we did not use the data for  $S_d < 0.4$ , a narrow range of  $S_d$  is used for these soils. In the revised analysis (see RESPONSE 2.2), the lowest  $\lambda$  retrieval values are not considered as they result from heterogeneities in soil density.

**CHANGES 2.18**

**Sect. 2.6: "The threshold value of  $S_d = 0.4$  results from a compromise between the need of limiting the influence of convection, of the shape of the  $K_e$  function on the retrieved values of  $\lambda_{sat}$ , and of using as many observations as possible in the retrieval process."**

=====END=====

1                   **Impact of ~~gravels and organic matter~~quartz on the thermal**  
2                   **properties of grassland soils in southern France**  
3

4  
5                   Jean-Christophe Calvet, Nouredine Fritz,  
6                   Christine Berne, Bruno Piguët, William Maurel, and Catherine Meurey  
7  
8                   CNRM, ~~GAME~~ UMR 3589 (Météo-France, CNRS), Toulouse, France  
9

10                                   12 January 2016~~26 March 2015~~  
11  
12  
13  
14

15 **Abstract**

16  
17 The information on quartz fraction in soils is usually unavailable but has a major effect on  
18 the accuracy of soil thermal conductivity models and on their application in land surface  
19 models. This paper investigates the influence of quartz fraction, soil organic matter (SOM)  
20 and gravels on soil thermal conductivity. Field observations of soil temperature and water  
21 content from 21 weather stations in southern France, along with the information on soil  
22 texture and bulk density, are used to estimate soil thermal diffusivity and heat capacity, and  
23 then thermal conductivity. The quartz fraction is inversely estimated using an empirical  
24 thermal conductivity model. Several pedotransfer functions for estimating quartz content  
25 from soil texture information are analysed. It is found that the soil volumetric fraction of  
26 quartz ( $f_q$ ) is systematically better correlated to soil characteristics than the gravimetric  
27 fraction of quartz. More than 60 % of the variance of  $f_q$  can be explained using indicators  
28 based on the sand fraction. It is shown that SOM and (or) gravels may have a marked  
29 impact on thermal conductivity values depending on which predictor of  $f_q$  is used. For the  
30 grassland soils examined in this study, the ratio of sand to SOM fractions is the best  
31 predictor of  $f_q$ . An error propagation analysis and a comparison with independent data

32 from Lu et al. (2007) show that the gravimetric fraction of sand is a better predictor of  $f_q$   
33 when a larger variety of soil types is considered.

34 ~~Soil moisture is the main driver of temporal changes in values of the soil thermal~~  
35 ~~conductivity. The latter is a key variable in land surface models (LSMs) used in~~  
36 ~~hydrometeorology, for the simulation of the vertical profile of soil temperature in relation~~  
37 ~~to soil moisture. Shortcomings in soil thermal conductivity models tend to limit the impact~~  
38 ~~of improving the simulation of soil moisture in LSMs. Models of the thermal conductivity of~~  
39 ~~soils are affected by uncertainties, especially in the representation of the impact of soil~~  
40 ~~properties such as the volumetric fraction of quartz ( $q$ ), soil organic matter, and gravels. As~~  
41 ~~soil organic matter and gravels are often neglected in LSMs, the soil thermal conductivity~~  
42 ~~models used in most LSMs represent the mineral fine earth, only. Moreover, there is no~~  
43 ~~map of  $q$  and it is often assumed that this quantity is equal to the volumetric fraction of~~  
44 ~~sand. In this study,  $q$  values are derived by reverse modelling from the continuous soil~~  
45 ~~moisture and soil temperature sub-hourly observations of the Soil Moisture Observing~~  
46 ~~System—Meteorological Automatic Network Integrated Application (SMOSMANIA)~~  
47 ~~network at 21 grassland sites in southern France, from 2008 to 2015. The soil temperature~~  
48 ~~observations are used to retrieve the soil thermal diffusivity ( $D_h$ ) at a depth of 0.10 m in~~  
49 ~~unfrozen conditions, solving the thermal diffusion equation. The soil moisture and  $D_h$~~   
50 ~~values are then used together with the measured soil properties to retrieve soil thermal~~  
51 ~~conductivity ( $\lambda$ ) values. For ten sites, the obtained  $\lambda$  value at saturation ( $\lambda_{\text{sat}}$ ) cannot be~~  
52 ~~retrieved or is lower than the value corresponding to a null value of  $q$ , probably in relation~~  
53 ~~to a high density of grass roots at these sites or to the presence of stones. For the remaining~~  
54 ~~eleven sites,  $q$  is negatively correlated with the volumetric fraction of solids other than sand.~~

55 ~~The impact of neglecting gravels and organic matter on  $\lambda_{\text{sat}}$  is assessed. It is shown that~~

56 ~~these factors have a major impact on  $\lambda_{\text{sat}}$ .~~

57

58

59

60

61

## 61 1. Introduction

62  
63 Soil moisture is the main driver of temporal changes in values of the soil thermal conductivity.  
64 The latter is a key variable in land surface models (LSMs) used in hydrometeorology, for the  
65 simulation of the vertical profile of soil temperature in relation to soil moisture. Shortcomings in  
66 soil thermal conductivity models tend to limit the impact of improving the simulation of soil  
67 moisture in LSMs. Models of the thermal conductivity of soils are affected by uncertainties,  
68 especially in the representation of the impact of soil properties such as the volumetric fraction of  
69 quartz ( $f_q$ ), soil organic matter, and gravels. As soil organic matter and gravels are often neglected  
70 in LSMs, the soil thermal conductivity models used in most LSMs represent the mineral fine  
71 earth, only. Today,  $f_q$  estimates are not given in global digital soil maps and it is often assumed  
72 that this quantity is equal to the fraction of sand.

73 Soil thermal properties are characterized by two key variables: the soil volumetric heat capacity  
74 ( $C_h$ ), and the soil thermal conductivity ( $\lambda$ ), in  $\text{Jm}^{-3}\text{K}^{-1}$  and  $\text{Wm}^{-1}\text{K}^{-1}$ , respectively. Provided the  
75 volumetric fractions of moisture, minerals and organic matter are known,  $C_h$  can be calculated  
76 easily. On the other hand, the estimation of  $\lambda$  relies on empirical models and is affected by  
77 uncertainties (Peters-Lidard et al., 1998 ; Tarnawski et al., 2012). The construction and the  
78 verification of the  $\lambda$  models is not easy as  ~~$\lambda$  is difficult to measure directly in situ and~~ is often  
79 measured in the lab on perturbed soil samples (Abu-Hamdeh et al., 2000; Lu et al., 2007).  
80 Although recent advances in line-source probe and heat pulse methods have made it easier to  
81 monitor soil thermal conductivity in the field (Bristow et al., 1994; Zhang et al., 2014), such  
82 measurements are currently not made in operational meteorological networks. Moreover, for  
83 given soil moisture conditions,  $\lambda$  depends to a large extent on the fraction of soil minerals



84 presenting high thermal conductivities such as quartz, hematite, dolomite or pyrite (Côté and  
85 Conrad, 2005). At mid-latitudes, quartz is the main driver of  $\lambda$ . The information on quartz  
86 fraction in a soil fraction of quartz is usually unavailable generally unknown as it can only be  
87 measured using X-ray diffraction or X-ray fluorescence techniques, which are difficult to  
88 implement (Schönenberger et al., 2012). This has a major effect on the accuracy of thermal  
89 conductivity models and their applications (Bristow, 1998).

90 Today, most of the Land Surface Models (LSMs) used in meteorology and hydrometeorology  
91 simulate  $\lambda$  following the approach proposed by Peters-Lidard et al. (1998). This approach  
92 consists of an updated version of the Johansen (1975) model, and assumes that the volumetric  
93 gravimetric fraction of quartz ( $\varphi_Q$ ) is equal to the volumetric-gravimetric fraction of sand within  
94 mineral fine earth( $f_{\text{sand}}$ ). This is a strong assumption, as some sandy soils (e.g. calcareous sands)  
95 may contain little quartz, and as quartz may be found in the silt and clay fractions of the soil  
96 minerals. Moreover, soil organic matter (SOM) and gravels are often neglected in LSMs, and the  
97  $\lambda$  models used in most LSMs represent the mineral fine earth, only. Yang et al. (2005) and Chen  
98 et al. (2012) have shown the importance of accounting for SOM and gravels in  $\lambda$  models for  
99 organic top soil layers of grasslands of the Tibetan plateau.

100 In this study, an attempt is made to use routine automatic ~~soil moisture and~~ soil temperature sub-  
101 hourly measurements to retrieve instantaneous soil thermal diffusivity $\lambda$  values at 21 weather  
102 stations of the Soil Moisture Observing System – Meteorological Automatic Network Integrated  
103 Application (SMOSMANIA) network (Calvet et al., 2007) in southern France, at a depth of 0.10  
104 m. Using information on soil moisture, soil texture, soil gravel content, soil organic matter, and  
105 bulk density,  $\lambda$  values are derived from soil thermal diffusivity and heat capacity. The response of  
106  $\lambda$  to soil moisture is investigated and the feasibility of modelling the  $\lambda$  value at saturation ( $\lambda_{\text{sat}}$ )

107 with or without using SOM and gravel fraction observations is assessed using an empirical  
108 thermal conductivity model based on Lu et al. (2007). The volumetric fraction of quartz,  $f_q$   
109 values are retrieved by reverse modelling together with  $Q_s$ . Pedotransfer functions are further  
110 proposed for estimating quartz content from soil texture information.

111 The field data and the method to retrieve  $\lambda$  values are presented in Sect. 2. The  $\lambda$  and  $f_q$   
112 retrievals are presented in Sect. 3 together with a sensitivity analysis of  $\lambda_{\text{sat}}$  to SOM and gravel  
113 fractions. Finally, the results are discussed in Sect. 4, and the main conclusions are summarized  
114 in Sect. 5. Technical details are given in Supplements.

115

116

116 **2. Data and methods**

117

118

119 2.1. The SMOSMANIA data

120

121

122 The SMOSMANIA soil moisture network was developed by Calvet et al. (2007) in southern  
123 France in order to validate satellite-derived soil moisture products (Parrens et al., 2012), assess  
124 land surface models used in hydrological models (Draper et al., 2011) and in meteorological  
125 models (Albergel et al., 2010), and monitor the impact of climate change on water resources and  
126 droughts. The station network forms a transect between the Atlantic coast and the Mediterranean  
127 sea (Fig. 1). It consists of pre-existing automatic weather stations operated by Meteo-France,  
128 upgraded with four soil moisture probes at four depths: 0.05 m, 0.10 m, 0.20 m, and 0.30 m. In  
129 general, the stations are located on former cultivated fields and consist of grasslands. Soil  
130 properties were measured at each stations using soil samples collected during the installation of  
131 the probes. The 21 stations cover a very large range of soil texture characteristics (~~Fig. 2~~[see](#)  
132 [Supplement 1](#)). ~~At the same time, Fig. 2 shows that soil texture does not vary much with depth~~  
133 ~~(from 0.05 m to 0.20 m) at a given station.~~ Other properties such as the gravimetric fraction of the  
134 Soil Organic Matter (SOM) and of gravels were determined from the soil samples. In addition,  
135 the bulk dry density of the soil ( $\rho_d$ ) was measured using unperturbed oven-dried soil samples  
136 collected using metal cylinders of known volume (about  $7 \times 10^{-4} \text{ m}^3$ ).

137 Twelve SMOSMANIA stations were activated in 2006 in southwestern France. In 2008, nine  
138 more stations were installed along the Mediterranean coast, and the whole network (21 stations)  
139 was gradually equipped with temperature sensors at the same depths as soil moisture probes. The

140 soil moisture and soil temperature probes consisted of Thetaprobe ML2X and PT100 sensors,  
141 respectively.

142 The ThetaProbe sensors provide a voltage signal in units of V. In order to convert the voltage  
143 signal into volumetric soil moisture content ( $\text{m}^3 \text{ m}^{-3}$ ), site-specific calibration curves were  
144 developed using in situ gravimetric soil samples for all stations, and for all depths (Albergel et  
145 al., 2008). In this study, the calibration was revised in order to avoid spurious high soil moisture  
146 values during intense precipitation events. Logistics curves were used ([see Supplement 1](#)) instead  
147 of exponential curves in the previous version of the data set.

148 The soil temperature observations are recorded with a resolution of 0.1 °C.

149 The observations from the 48 soil moisture probes and from the 48 temperature probes are  
150 automatically recorded every 12 minutes. The data are available to the research community  
151 through the International Soil Moisture Network web site (<https://ismn.geo.tuwien.ac.at/>).

152 Figure [23](#) shows soil temperature time series at the Saint-Félix-de-Lauragais (SFL) station on 23  
153 February 2015. The impact of recording temperature with a resolution of 0.1 °C is clearly visible  
154 at all depths as this causes a levelling of the curves.

155 In this study, sub-hourly measurements of soil temperature and soil moisture at a depth of 0.10 m  
156 are used, together with soil temperature measurements at 0.05 m and 0.20 m, from 1 January  
157 2008 to [28-30 February-September](#) 2015.

158

## 159 2.2. Soil characteristics

160

161 The porosity values at a depth of 0.10 m are listed in Table 1 together with gravimetric and  
162 volumetric fractions of soil particle-size ranges (sand, clay, silt, gravel) and SOM. The porosity,

163 or soil volumetric moisture at saturation ( $\theta_{sat}$ ), is derived from the bulk dry density  $\rho_d$ , together  
 164 with soil texture and soil organic matter observations as:

$$165 \quad \theta_{sat} = 1 - \rho_d \left[ \frac{m_{sand} + m_{clay} + m_{silt} + m_{gravel}}{\rho_{min}} + \frac{m_{SOM}}{\rho_{SOM}} \right]$$

166 or

$$167 \quad \theta_{sat} = 1 - f_{sand} - f_{clay} - f_{silt} - f_{gravel} - f_{SOM} \quad (1)$$

168 where  $m_x$  ( $f_x$ ) represents the gravimetric (volumetric) fraction of the soil component  $x$ . The  $f_x$   
 169 values are derived from the measured gravimetric fractions, multiplied by the ratio of  $\rho_d$   
 170 observations to  $\rho_x$ , the density of each soil component  $x$ . Values of  $\rho_{SOM} = 1300 \text{ kg m}^{-3}$  and  $\rho_{min} =$   
 171  $2660 \text{ kg m}^{-3}$  are used for soil organic matter, and soil minerals, respectively.

172

173

174 2.3. Retrieval of soil thermal diffusivity

175

176 The soil thermal diffusivity ( $D_h$ ) is expressed in  $\text{m}^2\text{s}^{-1}$  and is defined as:

$$177 \quad D_h = \frac{\lambda}{C_h} \quad (2)$$

178 In this study, a simple numerical method is used to retrieve instantaneous values of  $D_h$  at a depth  
 179 of 0.10 m using three soil temperature observations at 0.05 m, 0.10 m and 0.20 m, performed  
 180 every 12 minutes, by solving the Fourier thermal diffusion equation. The latter can be written as:

$$181 \quad C_h \frac{\partial T}{\partial t} = \frac{\partial}{\partial z} \left( \lambda \frac{\partial T}{\partial z} \right) \quad (3).$$

182 In this study, given that soil properties are relatively homogeneous on the vertical (Sect. 2.1),  
 183 values of  $D_h$  can be derived from the Fourier one-dimensional law:

$$184 \quad \frac{\partial T}{\partial t} = D_h \frac{\partial^2 T}{\partial z^2} \quad (4).$$

185 However, large differences in soil bulk density, from the top soil layer to deeper soil layers were  
 186 observed for some soils (see Supplement 1). In order to limit this effect as much as possible, we  
 187 only used the soil temperature data presenting a relatively low vertical gradient close to the soil  
 188 surface, where most differences with deeper layers are found. This data sorting procedure is  
 189 described in Supplement 2.

190 Given that three soil temperatures  $T_i$  ( $i$  ranging from 1 to 3) are measured at depths  $z_1 = -0.05$  m,  
 191  $z_2 = -0.10$  m, and  $z_3 = -0.20$  m, the soil diffusivity  $D_{hi}$  at  $z_i = z_2 = -0.10$  m can be obtained by  
 192 solving the one-dimensional heat equation, using a finite difference method based on the implicit  
 193 Crank-Nicholson scheme. When three soil depths are considered,  $z_{i-1}$ ,  $z_i$ ,  $z_{i+1}$ , the change in soil  
 194 temperature  $T_i$  at depth  $z_i$ , from time  $t_{n-1}$  to time  $t_n$ , within the time interval  $\Delta t = t_n - t_{n-1}$  can be  
 195 written as:

$$196 \quad \frac{T_i^n - T_i^{n-1}}{\Delta t} = D_{hi} \left[ \frac{1}{2} \left( \frac{\gamma_{i+1}^n - \gamma_i^n}{\Delta z_m} \right) + \frac{1}{2} \left( \frac{\gamma_{i+1}^{n-1} - \gamma_i^{n-1}}{\Delta z_m} \right) \right] \quad \text{with}$$

$$197 \quad \gamma_i^n = \frac{T_i^n - T_{i-1}^n}{\Delta z_i}, \quad \Delta z_m = \frac{\Delta z_i + \Delta z_{i+1}}{2}, \quad \text{and} \quad \Delta z_i = z_i - z_{i-1} \quad (5).$$

198  
 199 In this study,  $\Delta z_i = -0.05$  m,  $\Delta z_{i+1} = -0.10$  m, and a value of  $\Delta t = 2880$  s (48 minutes) is used.  
 200 It is important to ensure that  $D_h$  retrievals are related to diffusion processes only and not to the  
 201 transport of heat by water infiltration or evaporation (Parlange et al., 1998 ; Schelde et al., 1998).

202 Therefore, only situations for which changes in soil moisture at all depths do not exceed 0.001  
203  $\text{m}^3\text{m}^{-3}$  within the  $\Delta t$  time lag are considered.

204

205 2.4. From soil diffusivity to soil thermal conductivity

206

207

208 The observed soil properties and volumetric soil moisture are used to calculate the soil  
209 volumetric heat capacity  $C_h$  at a depth of 0.10 m, using the de Vries (1963) mixing model. The  $C_h$   
210 values, in units of  $\text{Jm}^{-3}\text{K}^{-1}$ , are calculated as:

$$211 \quad C_h = \theta C_{h\text{water}} + f_{\min} C_{h\min} + f_{\text{SOM}} C_{h\text{SOM}} \quad (6)$$

212 where  $\theta$  and  $f_{\min}$  represent the volumetric soil moisture and the volumetric fraction of soil

213 minerals, respectively, and  $v$  values of  $4.2 \times 10^6 \text{ Jm}^{-3}\text{K}^{-1}$ ,  $2.0 \times 10^6 \text{ Jm}^{-3}\text{K}^{-1}$ , and  $2.5 \times 10^6 \text{ Jm}^{-3}\text{K}^{-1}$ , are

214 used for  $C_{h\text{water}}$ ,  $C_{h\min}$ ,  $C_{h\text{SOM}}$ , respectively.

215 The  $\lambda$  values at 0.10 m are then derived from the  $D_h$  and  $C_h$  estimates (Eq. (2)).

216

217 2.5. Soil thermal conductivity model

218

219 In dry conditions, soils present low thermal conductivity values ( $\lambda_{\text{dry}}$ ). Experimental evidence  
220 show that  $\lambda_{\text{dry}}$  is negatively correlated with porosity. For example, Lu et al. (2007) give:

$$221 \quad \lambda_{\text{dry}} = 0.51 - 0.56 \times \theta_{\text{sat}} \quad (\text{in } \text{Wm}^{-1}\text{K}^{-1}) \quad (7)$$

222 When soil pores are gradually filled with water,  $\lambda$  tends to increase towards a maximum value at  
223 saturation ( $\lambda_{\text{sat}}$ ). Between dry and saturation conditions,  $\lambda$  is expressed as:

$$224 \quad \lambda = \lambda_{\text{dry}} + K_e (\lambda_{\text{sat}} - \lambda_{\text{dry}}) \quad (8)$$

225 where,  $K_e$  is the Kersten number. The latter is related to the volumetric soil moisture,  $\theta$ , i.e. to the  
 226 degree of saturation ( $S_d$ ). In this study, the formula recommended by [Yang-Lu et al. \(20052007\)](#)  
 227 is used:

$$228 \quad K_e = \exp\left\{\alpha\left(1 - S_d^{(\alpha-1.33)}\right)\right\} K_e = \exp(k_T(1 - 1/S_d)),$$

229 with  $\alpha = 0.96$  for  $Mn_{sand} \geq 0.4 \text{ kg kg}^{-1}$ ,  $\alpha = 0.27$  for  $Mn_{sand} < 0.4 \text{ kg kg}^{-1}$ , and

$$230 \quad \text{with } k_T = 0.36 \text{ and } S_d = \theta/\theta_{sat}$$

231 \_\_\_\_\_ (9).

232  $Mn_{sand}$  represents the sand mass fraction of mineral fine earth (values are given in Supplement 1).

233 Following Peters-Lidard et al. (1998),  $\lambda_{other}$  is taken as  $2.0 \text{ Wm}^{-1}\text{K}^{-1}$  for soils with  $Mn_{sand} > 0.2$

234  $\text{kg kg}^{-1}$ , and  $3.0 \text{ Wm}^{-1}\text{K}^{-1}$  otherwise. In this study  $Mn_{sand} > 0.2 \text{ kg kg}^{-1}$  for all soils, except for

235 URG, PRG, and CDM.

236 The geometric mean equation for  $\lambda_{sat}$  proposed by Johansen (1975) for the mineral components

237 of the soil can be generalized to include the SOM thermal conductivity (Chen et al., 2012) as:

$$238 \quad \ln(\lambda_{sat}) = f_q \ln(\lambda_q) + f_{other} \ln(\lambda_{other}) + \theta_{sat} \ln(\lambda_{water}) + f_{SOM} \ln(\lambda_{SOM})$$

$$239 \quad \text{_____}$$

$$240 \quad \text{_____} \quad (10)$$

241 where  $f_q$  is the volumetric fraction of quartz, and  $\lambda_q = 7.7 \text{ Wm}^{-1}\text{K}^{-1}$ ,  $\lambda_{other} = 2.0 \text{ Wm}^{-1}\text{K}^{-1}$ ,  $\lambda_{water}$

242  $= 0.594 \text{ Wm}^{-1}\text{K}^{-1}$ ,  $\lambda_{SOM} = 0.25 \text{ Wm}^{-1}\text{K}^{-1}$  are the thermal conductivities of quartz, soil minerals

243 other than quartz, water and SOM, respectively. The volumetric fraction of soil minerals other

244 than quartz is defined as:

$$245 \quad f_{other} = 1 - f_q - \theta_{sat} - f_{SOM}$$



246 with  $f_q = Q \times (1 - \theta_{sat})$  \_\_\_\_\_ (11)

247

## 248 2.6. Reverse modelling

249

250 The  $\lambda_{sat}$  values are retrieved through reverse modelling using the  $\lambda$  model described above (Eqs.

251 (7)-(11)). The  $\lambda$  model is used to produce simulations of  $\lambda$  at the same soil moisture conditions as

252 those encountered for the  $\lambda$  values derived from observations in Sect. 2.4. For a given station, a

253 set of 401  ~~$\lambda$~~ -simulations is produced for  $\lambda_{sat}$  ranging from 0  $\text{Wm}^{-1}\text{K}^{-1}$  to 4  $\text{Wm}^{-1}\text{K}^{-1}$ , with a

254 resolution of 0.01  $\text{Wm}^{-1}\text{K}^{-1}$ . The  $\lambda_{sat}$  retrieval corresponds to the  $\lambda$  simulation presenting the

255 lowest root mean square difference (RMSD) value with respect to the  $\lambda$  observations. Only  $\lambda$

256 observations for  $S_d$  values higher than 0.4 are used, becauseas in dry conditions: (1) conduction is

257 not the only mechanism for heat exchange in soils, as the convective water vapour flux may

258 become significant (Schelde et al., 1998, Parlange et al. 1998), (2) the  $K_e$  functions found in the

259 literature display more variability, (3) the  $\lambda_{sat}$  retrievals are ~~very~~-more sensitive to uncertainties in

260  $\lambda$  observations-~~obtained in dry conditions~~. The threshold value of  $S_d = 0.4$  results from a

261 compromise between the need of limiting the influence of convection, of the shape of the  $K_e$

262 function on the retrieved values of  $\lambda_{sat}$ , and of using as many observations as possible in the

263 retrieval process. Moreover, the data filtering technique to limit the impact of soil

264 heterogeneities, described in Supplement 2, is used to select valid  $\lambda$  observations.

265 Finally, the  ~~$f_q$~~  value is derived from the retrieved  $\lambda_{sat}$  ~~by~~-solving Eq. (10), ~~provided at least~~

266 ~~twenty  $\lambda$  observations can be used. When negative values of  $q$  are obtained, a null value of  $q$  is~~

267 ~~imposed~~

268

269 2.7. Scores

270

271 Pedotransfer functions for quartz and  $\lambda_{\text{sat}}$  are evaluated using the following scores:

272 • the Pearson correlation coefficient ( $r$ ), and the squared correlation coefficient ( $r^2$ ) is used

273 to assess the fraction of explained variance,

274 • the RMSD,

275 • the Mean Absolute Error (MAE), i.e. the mean of absolute differences,

276 • the mean bias, i.e. the mean of differences.

277 In order to test the predictive and generalization power of the pedotransfer regression equations, a

278 simple bootstrapping resampling technique is used. It consists in calculating a new estimate of  $f_q$

279 for each soil using the pedotransfer function obtained without using this specific soil. Gathering

280 these new  $f_q$  estimates, one can calculate new scores with respect to the retrieved  $f_q$  values. Also,

281 this method provides a range of possible values of the coefficients of the pedotransfer function

282 and permits assessing the influence of a given  $f_q$  retrieval on the final result.

283

### 283 3. Results

284  
285

#### 286 3.1. $\lambda_{\text{sat}}$ and $f_{\text{q}}$ retrievals

287  
288

289 Retrievals of  $\lambda_{\text{sat}}$  and  $f_{\text{q}}$  could be obtained for 14 soils. Figure 34 shows retrieved and modelled  $\lambda$   
290 values vs. the observed degree of saturation of the soil, at a depth of 0.10 m, for contrasting  
291 retrieved values of  $\lambda_{\text{sat}}$ , from high to low  $\lambda_{\text{sat}}$  values (2.8079, 1.9645, 1.52, and 1.26070  
292  $\text{Wm}^{-1}\text{K}^{-1}$ ) at the SBR, MNT, MTM, and PRD stations, respectively.

293 All the obtained  $\lambda_{\text{sat}}$  and  $f_{\text{q}}$  retrievals are listed in Table 2, together with the  $\lambda$  RMSD values and  
294 the number of available-selected  $\lambda$  observations. For six-three stations-soils (CRD, PZN, MZN,  
295 and VLV, MJN, and BRZ), the reverse modelling technique described in Sect. 2.6 cannot could  
296 not be implemented-applied as not enough  $\lambda$  observations could be obtained for  $S_{\text{d}}$  values higher  
297 than 0.4. For four soils (NBN, PZN, BRZ, and MJN), all the  $\lambda$  retrievals were filtered out as the  
298 obtained values were influenced by heterogeneities in soil density (see Supplement 2). For the  
299 other 145 stationssoils,  $\lambda_{\text{sat}}$  and  $f_{\text{q}}$  retrievals awere obtained using a subset of 20  $\lambda$  retrievals per  
300 soil, at most, corresponding to the soil temperature data presenting the lowest vertical gradient  
301 close to the soil surface (Supplement 2). 62 to 1939  $\lambda$  observations. For the five stations (LHS,  
302 SVN, NBN, and PRD) presenting the lowest  $\lambda_{\text{sat}}$  retrievals, ranging between 0.52 and 1.11  
303  $\text{Wm}^{-1}\text{K}^{-1}$ , null values of  $q$  are obtained. The  $\lambda$  model (Eqs. (7)–(11)) is fully operative, with non-  
304 null values of  $q$ , for eleven stations: SBR, URG, PRG, CDM, MNT, SFL, MTM, LZC, LGC,  
305 BRN, CBR.

306

#### 307 3.2 A-pPedotransfer functions for quartz

308

309 The  $f_q$  retrievals can be used to assess the possibility to estimate  $f_q$  using other soil  
 310 characteristics, which can be easily measured. Another issue is whether volumetric or gravimetric  
 311 fraction of quartz should be used. Figure 4 presents the fraction of variance ( $r^2$ ) of  $Q$  and  $f_q$   
 312 explained by various indicators. A key result is that  $f_q$  is systematically better correlated to soil  
 313 characteristics than  $Q$ . More than 60 % of the variance of  $f_q$  can be explained using indicators  
 314 based on the sand fraction (either  $f_{sand}$  or  $m_{sand}$ ). The use of other soil mineral fractions does not  
 315 give good correlations, even when they are associated to the sand fraction as shown by Fig. 4. For  
 316 example, the  $f_{gravel}$  and  $f_{gravel}+f_{sand}$  indicators present low  $r^2$  values of 0.04 and 0.24, respectively.  
 317 The  $f_q$  values cannot be derived directly from the indicators as illustrated by Fig. 5: assuming  $f_q =$   
 318  $f_{sand}$  tends to markedly underestimate  $\lambda_{sat}$ . Therefore, more elaborate pedotransfer equations are  
 319 needed. They can be derived from the best indicators, using them as predictors of  $f_q$ . The  
 320 modelled  $f_q$  is written as:

321  
 322 ~~For the 11 stations with  $q > 0$ , a good correlation is found between  $q$  retrievals and  $f_{sand}$  ( $r^2 = 0.66$ ,~~  
 323 ~~F-test  $p$ -value = 0.0025, RMSD = 0.09 m<sup>3</sup> m<sup>-3</sup>). However, a better result is found considering the~~  
 324 ~~sum of the fractions of the other soil particles, and the modelled  $q$  values can be derived from the~~  
 325 ~~following pedotransfer function:~~

$$326 \quad f_{qMOD} = a_0 + a_1 \times P$$

$$327 \quad \text{and } f_{qMOD} \leq 1 - \theta_{sat} - f_{SOM} \text{ or } q_{MOD} = 0.70 - 1.075 \times (1 - \theta_{sat} - f_{sand})$$

$$328 \quad (12)$$

329 where  $P$  represents the predictor of  $f_q$  ( $r^2 = 0.78$ , F-test  $p$ -value = 0.0003, RMSD = 0.07 m<sup>3</sup> m<sup>-3</sup>).

330 The values of  $q_{MOD}$  vs.  $q$  are shown in Fig. 5.

331 The  $a_0$  and  $a_1$  coefficients are given in Table 3 for four pedotransfer functions based on the best  
332 predictors of  $f_q$ . The pedotransfer functions are illustrated in Fig. 6. The scores are displayed in  
333 Table 4. The bootstrapping indicates that the SBR sandy soil has the largest individual impact on  
334 the obtained regression coefficients. This is why the scores without SBR are also presented in  
335 Table 4.

336 For the  $m_{\text{sand}}$  predictor, a  $r^2$  value of 0.56 is obtained without SBR, against a value of 0.67 when  
337 all the 14 soils are considered. An alternative to this  $m_{\text{sand}}$  pedotransfer function consists in  
338 considering only  $m_{\text{sand}}$  values smaller than  $0.6 \text{ kg kg}^{-1}$  in the regression, thus excluding the SBR  
339 soil. The corresponding predictor is called  $m_{\text{sand}}^*$ . In this configuration, the sensitivity of  $f_q$  to  
340  $m_{\text{sand}}$  is much increased (with  $a_1 = 0.944$ , against  $a_1 = 0.572$  with SBR). For SBR,  $f_q$  is  
341 overestimated by the  $m_{\text{sand}}^*$  equation but this is corrected by the  $f_{q\text{MOD}}$  limitation of Eq. (12), and  
342 in the end a better  $r^2$  score is obtained when the 14 soils are considered ( $r^2 = 0.74$ ).

343 Values of  $r^2$  larger than 0.7 are obtained for two predictors of  $f_q$ :  $m_{\text{sand}}/m_{\text{SOM}}$  and  $m_{\text{sand}}^*$ . A value  
344 of  $r^2 = 0.65$  is obtained for  $1 - \theta_{\text{sat}} - f_{\text{sand}}$  (the fraction of soil solids other than sand). The  
345  $m_{\text{sand}}/m_{\text{SOM}}$  predictor presents the best  $r^2$  and RMSD scores in all the configurations (regression,  
346 bootstrap, and regression without SBR). Another characteristic of the  $m_{\text{sand}}/m_{\text{SOM}}$  pedotransfer  
347 function is that the confidence interval for the  $a_0$  and  $a_1$  coefficients derived from bootstrapping is  
348 narrower than for the other pedotransfer functions (Table 3), indicating a more robust relationship  
349 of  $f_q$  with  $m_{\text{sand}}/m_{\text{SOM}}$  than with other predictors.

350 Modelled values of  $\lambda_{\text{sat}}$  ( $\lambda_{\text{satMOD}}$ ) can be derived from  $f_{q\text{MOD}}g_{\text{MOD}}$  using Eq. (10) together with  $\theta_{\text{sat}}$   
351 observations. and The  $\lambda_{\text{satMOD}}$  following  $r^2$ , RMSD, and mean bias scores are obtained for  
352  $\lambda_{\text{satMOD}}$ , with respect to the  $\lambda_{\text{sat}}$  retrievals:  $0.87$ ,  $0.15 \text{ Wm}^{-1}\text{K}^{-1}$ , and  $0.01 \text{ Wm}^{-1}\text{K}^{-1}$ , respectively  
353 (Table 3) given in Table 5. Again, the best scores are obtained using the  $m_{\text{sand}}/m_{\text{SOM}}$  predictor of

354  $f_q$ , with  $r^2$ , RMSD, and mean bias values of 0.86, 0.14  $\text{Wm}^{-1}\text{K}^{-1}$ , and +0.01  $\text{Wm}^{-1}\text{K}^{-1}$ , respectively  
 355 (Fig. 7).

356 Finally, we investigated the possibility of estimating  $\theta_{\text{sat}}$  from the soil characteristics listed in  
 357 Table 1 and of deriving a statistical model for  $\theta_{\text{sat}}$  ( $\theta_{\text{satMOD}}$ ). We found the following statistical  
 358 relationship between  $\theta_{\text{satMOD}}$ ,  $m_{\text{clay}}$ ,  $m_{\text{silt}}$ , and  $m_{\text{SOM}}$ :

$$359 \quad \theta_{\text{satMOD}} = 0.456 - 0.0735 \frac{m_{\text{clay}}}{m_{\text{silt}}} + 2.238 m_{\text{SOM}} \quad (13)$$

360 ( $r^2 = 0.48$ , F-test  $p$ -value = 0.0027, RMSD=0.036  $\text{m}^3\text{m}^{-3}$ ).

361 Volumetric fractions of soil components need to be consistent with  $\theta_{\text{satMOD}}$  and can be calculated  
 362 using the modelled bulk density values,  $\rho_{\text{dMOD}}$ , derived from  $\theta_{\text{satMOD}}$  as using Eq. (1).

$$363 \quad \rho_{\text{dMOD}} = \frac{1 - \theta_{\text{satMOD}}}{\frac{m_{\text{sand}} + m_{\text{clay}} + m_{\text{silt}} + m_{\text{gravel}}}{\rho_{\text{min}}} + \frac{m_{\text{SOM}}}{\rho_{\text{SOM}}}} \quad (14)$$

364 Equations (10) to (14) constitute an empirical end-to-end model of  $\lambda_{\text{sat}}$ . Table 3-5 shows that  
 365 using  $\theta_{\text{satMOD}}$  (Eqs. (13)-(14)) instead of the  $\theta_{\text{sat}}$  observations has little impact on the  $\lambda_{\text{satMOD}}$   
 366 scores.

367

368

368 **4. Discussion**

369

370 ~~3.34.1. Impact of gravels and SOM on  $q$  and  $\lambda_{\text{sat}}$~~

371

372 Gravels and SOM are often neglected in soil thermal conductivity models used in LSMs.

373 ~~Moreover, it is often assumed that  $q$  is equal to  $f_{\text{sand}}$ .~~ The Eqs. (10)-(134) empirical model

374 obtained in Sect. 3.2 permits the assessment of the impact of  ~~$q$ ,  $f_{\text{gravel}}$  and  $f_{\text{SOM}}$~~  on  $\lambda_{\text{sat}}$ . Table ~~3-5~~

375 shows the impact on  $\lambda_{\text{satMOD}}$  scores of imposing ~~a null values to of  $f_{\text{gravel}}$  and a small value of  $f_{\text{SOM}}$~~

376 ~~to all the soils. and of assuming  $q = f_{\text{sand}}$ .~~ The combination of these assumptions is evaluated,

377 also.

378 ~~Imposing  $f_{\text{SOM}} = 0.013 \text{ m}^3 \text{ m}^{-3}$  (the smallest  $f_{\text{SOM}}$  value, observed for CBR) has a limited impact~~

379 ~~on the scores, except for the  $m_{\text{sand}}/m_{\text{SOM}}$  pedotransfer function. In this case,  $\lambda_{\text{sat}}$  is overestimated~~

380 ~~by  $+0.20 \text{ Wm}^{-1} \text{ K}^{-1}$ , and  $r^2$  drops to 0.57.~~

381 ~~Neglecting gravels ( $f_{\text{gravel}} = 0 \text{ m}^3 \text{ m}^{-3}$ ) also has a limited impact but triggers the underestimation~~

382 ~~(overestimation) of  $\lambda_{\text{sat}}$  for the  $m_{\text{sand}}/m_{\text{SOM}}$  ( $m_{\text{sand}}^*$ ) pedotransfer function, by  $-0.12 \text{ Wm}^{-1} \text{ K}^{-1}$~~

383 ~~( $+0.11 \text{ Wm}^{-1} \text{ K}^{-1}$ ).~~

384 ~~On the other hand, it appears that combining these assumptions has a marked impact on all the~~

385 ~~pedotransfer functions. Neglecting gravels ( $f_{\text{gravel}} = 0 \text{ m}^3 \text{ m}^{-3}$ ) and imposing  $f_{\text{SOM}} = 0.013 \text{ m}^3 \text{ m}^{-3}$~~

386 has a major impact on  $\lambda_{\text{sat}}$ : the modelled  $\lambda_{\text{sat}}$  is overestimated ~~by all the pedotransfer functions~~

387 ~~(with a mean bias of ranging from  $+0.165 \text{ Wm}^{-1} \text{ K}^{-1}$  to  $+0.24 \text{ Wm}^{-1} \text{ K}^{-1}$ ) and  $r^2 = 0.65$  is markedly~~

388 ~~smaller, especially for the  $m_{\text{sand}}$  and  $m_{\text{sand}}^*$  pedotransfer functions. while the full model is~~

389 ~~virtually unbiased and presents a  $r^2$  value of 0.87. These results are illustrated in Fig. 8 in the case~~

390 ~~of the  $m_{\text{sand}}^*$  pedotransfer function. Figure 8 also shows that using the  $\theta_{\text{sat}}$  observations instead of~~

391  $\theta_{\text{satMOD}}$  (Eq. (13)) has little impact on  $\lambda_{\text{satMOD}}$  (Sect. 3.2) but tends to enhance the impact of  
392 neglecting gravels. A similar result is found with the  $m_{\text{sand}}$  pedotransfer function (not shown).  
393 Neglecting SOM also triggers an overestimation of  $\lambda_{\text{sat}}$  ( $+0.12 \text{ Wm}^{-1}\text{K}^{-1}$ ) but has no impact on  $r^2$ .  
394 On the other hand, although neglecting SOM while accounting for gravels has no impact on  $r^2$ ,  
395 neglecting SOM tends to amplify the detrimental impact of neglecting gravels:  $r^2 = 0.51$  and the  
396 mean bias is equal to  $+0.41 \text{ Wm}^{-1}\text{K}^{-1}$ . Assuming  $q = f_{\text{sand}}$  tends to trigger an underestimation of  
397  $\lambda_{\text{sat}}$  ( $-0.22 \text{ Wm}^{-1}\text{K}^{-1}$ ), and to compensate for the bias caused by neglecting SOM. Combining Eq.  
398 (12) and Eq. (1), it appears that Eq. (12) boils down to  $q = 1.075 \times f_{\text{sand}}$  for  $\theta_{\text{sat}}$  values close to  
399  $0.35 \text{ m}^3 \text{ m}^{-3}$ . For higher  $\theta_{\text{sat}}$  values,  $q$  tends to be higher than  $1.075 \times f_{\text{sand}}$ . Since  $\theta_{\text{sat}}$  is higher than  
400  $0.35 \text{ m}^3 \text{ m}^{-3}$  at all the sites (Table1), the  $q = f_{\text{sand}}$  assumption tends to underestimate  $q$  and,  
401 subsequently,  $\lambda_{\text{sat}}$ .  
402 Table 3 shows that in the configuration representative of most soil thermal conductivity models  
403 currently used in LSMs (i.e. neglecting gravels and SOM while assuming  $q = f_{\text{sand}}$ ), only 61 % of  
404 the  $\lambda_{\text{sat}}$  variance is explained by the model ( $r^2 = 0.61$ ), and  $\lambda_{\text{sat}}$  is markedly overestimated (the  
405 mean bias is equal to  $+0.24 \text{ Wm}^{-1}\text{K}^{-1}$ ). The impact of this model configuration is illustrated in  
406 Fig. 6 (bottom), together with the impact of  $q = f_{\text{sand}}$  alone.  
407 Finally, the correlation of the retrieved values of  $q$  with the volumetric fraction of solids is  
408 analysed in Table 4. Using  $f_{\text{sand}}$  as a predictor of  $q$  gives a  $r^2$  value of 0.66, against 0.78 for Eq.  
409 (12). Gravels and silt have the largest impact on  $r^2$  ( $r^2 = 0.12$  and  $r^2 = 0.38$ , respectively).

410

## 411 4. Discussion

412

413 4.12. Sources of uncertainties in heat capacity estimates Null values of  $q$



414

415 ~~Null values of  $q$  are obtained for four stations: LHS, SVN, NBN, and PRD (Table 2 and Fig. 4).~~

416 ~~They correspond to the lowest values of the  $\lambda_{\text{sat}}$  retrievals, ranging from 0.52 to 1.11  $\text{Wm}^{-1}\text{K}^{-1}$ .~~

417 ~~Such values can be encountered for organic soils (e.g. Chen et al., 2012) or for volcanic ash soils~~

418 ~~(Farnawski et al., 2009) but are surprising for the soil types considered in this study.~~

419 ~~On the other hand, it must be noted that Eq. (12) predicts very low values of  $q$  for  $f_{\text{clay}} + f_{\text{silt}} +$~~

420  ~~$f_{\text{gravel}} + f_{\text{SOM}}$  close to  $0.65 \text{ m}^3 \text{ m}^{-3}$ . All the retrieved null values of  $q$  are obtained below this~~

421 ~~threshold (Fig. 4), from 0.43 to  $0.54 \text{ m}^3 \text{ m}^{-3}$ . Therefore, a possible marked underestimation of~~

422 ~~either  $f_{\text{clay}}, f_{\text{silt}}, f_{\text{gravel}}$ , or  $f_{\text{SOM}}$  may explain these discrepancies, or the overestimation of  $f_{\text{sand}}$  or  $\theta_{\text{sat}}$ .~~

423 In this study, the de Vries (1963) mixing model is applied to estimate soil volumetric heat

424 capacity, and a fixed value of  $2.0 \times 10^6 \text{ J m}^{-3} \text{ K}^{-1}$  is used for soil minerals (Eq. (6)). Soil-specific

425 values for  $C_{\text{hmin}}$  may be more appropriate than using a constant standard value. For example,

426 Tarara and Ham (1997) used a value of  $1.92 \times 10^6 \text{ J m}^{-3} \text{ K}^{-1}$ . However, we did not measure this

427 quantity and we were not able to find such values in the literature.

428 We investigated the sensitivity of our results to these uncertainties, considering the following

429 minimum and maximum  $C_{\text{hmin}}$  values:  $C_{\text{hmin}} = 1.92 \times 10^6 \text{ J m}^{-3} \text{ K}^{-1}$  and  $C_{\text{hmin}} = 2.08 \times 10^6 \text{ J m}^{-3}$

430  $\text{K}^{-1}$ . The impact of changes in  $C_{\text{hmin}}$  on the retrieved values of  $\lambda_{\text{sat}}$  and  $f_q$  is presented in Fig. 9. On

431 average, a change of  $+ (-) 0.08 \times 10^6 \text{ J m}^{-3} \text{ K}^{-1}$  in  $C_{\text{hmin}}$  triggers a change in  $\lambda_{\text{sat}}$  and  $f_q$  of  $+ 1.7 \%$

432  $(- 1.8 \%)$  and  $+ 4.8 \%$   $(- 7.0 \%)$ , respectively.

433 The impact of changes in  $C_{\text{hmin}}$  on the regression coefficients of the pedotransfer functions is

434 presented in Table 3 (last column). The impact is very small, except for the  $a_1$  coefficient of the

435  $m_{\text{sand}}^*$  pedotransfer function. However, even in this case, the impact of  $C_{\text{hmin}}$  on the  $a_1$  coefficient

436 is much lower than the confidence interval given by the bootstrapping, indicating that the

437 relatively small number of soils considered in this study (as in other studies, e.g. Lu et al. (2007))  
438 is a larger source of uncertainty.

439 Moreover, uncertainties in these  $f_{\text{clay}}$ ,  $f_{\text{silt}}$ ,  $f_{\text{gravel}}$ , or  $f_{\text{SOM}}$  fractions may be caused by (1) the  
440 natural heterogeneity of soil properties, (2) the living root biomass, (3) stones that ~~are~~ may not be  
441 accounted for in the gravel fraction.

442 In particular, during the installation of the probes, it was observed that stones are present at ~~the~~  
443 ~~four~~ some stations. Stones are not evenly distributed in the soil, and it is not possible to  
444 investigate whether the soil area where the temperature probes were inserted contains stones as it  
445 must be left unperturbed.

446 The grasslands considered in this study are not intensively managed. They consist of set-aside  
447 fields cut once or twice a year. Calvet et al. (1999) gave an estimate of  $0.160 \text{ kg m}^{-2}$  for the root  
448 dry matter content of such soils for a site in southwestern France, with most roots contained in  
449 the 0.25m top soil layer. This represents a gravimetric fraction of organic matter smaller than  
450  $0.0005 \text{ kg kg}^{-1}$ , i.e. less than 4% of the lowest  $m_{\text{SOM}}$  values observed in this study ( $0.013 \text{ kg kg}^{-1}$ )  
451 or less than 5% of  $f_{\text{SOM}}$  values. We checked that increasing  $f_{\text{SOM}}$  values by 5% has negligible  
452 impact on heat capacity and on the  $\lambda$  retrievals.

453

454

455

456 4.3. Applicability of the new  $\lambda_{\text{sat}}$  model to other soil types

457

458 The  $\lambda_{\text{sat}}$  values found in this study are consistent with values reported by other authors. In this  
459 study,  $\lambda_{\text{sat}}$  values ranging between  $1.26 \text{ Wm}^{-1}\text{K}^{-1}$  and  $2.80 \text{ Wm}^{-1}\text{K}^{-1}$  are found (Table 2).

460 Tarnawski et al. (2011) gave  $\lambda_{\text{sat}}$  values ranging between  $2.5 \text{ Wm}^{-1}\text{K}^{-1}$  and  $3.5 \text{ Wm}^{-1}\text{K}^{-1}$  for  
461 standard sands. Lu et al. (2007) gave  $\lambda_{\text{sat}}$  values ranging between  $1.33 \text{ Wm}^{-1}\text{K}^{-1}$  and  $2.2$   
462  $\text{Wm}^{-1}\text{K}^{-1}$ .

463 A key component of the  $\lambda_{\text{sat}}$  model is the pedotransfer function for quartz (Eq. (12)). The  $f_q$   
464 pedotransfer functions proposed in this study are based on basic soil characteristics. The current  
465 global soil digital maps provide information about SOM, gravels and bulk density (Nachtergaele  
466 et al., 2012). Therefore, using Eq. (1) and Eqs. (6)-(12) at large scale is possible, and porosity can  
467 be derived from Eq. (1).- On the other hand, the suggested  $f_q$  pedotransfer functions are obtained  
468 for temperate grassland soils containing a rather large amount of organic matter, and are valid for  
469  $m_{\text{sand}}/m_{\text{SOM}}$  ratio values lower than 40 (Table 2). These equations should be evaluated for other  
470 regions. In particular, hematite has to be considered together with quartz for tropical soils.  
471 Moreover, while the pedotransfer function we get for  $\theta_{\text{sat}}$  (Eq. (13)) is valid for the specific sites  
472 considered in this study and is used to conduct the sensitivity study of Sect. 3.3, Eq. (13) cannot  
473 be used to predict porosity in other regions.

474  
475 ~~A key component of the  $\lambda_{\text{sat}}$  model proposed in this study is the pedotransfer function for quartz~~  
476 ~~(Eq. (12)). This equation should be evaluated for other regions. In particular, hematite has to be~~  
477 ~~considered together with quartz for tropical soils. According to Eq. (12),  $q$  is close to 0.7 for~~  
478 ~~sandy soils and in such conditions, one should ensure that  $q \leq f_{\text{sand}}$ .~~

479 ~~While the pedotransfer function we get for  $\theta_{\text{sat}}$  (Eq. (13)) is valid for the specific sites considered~~  
480 ~~in this study and is used to conduct the sensitivity study of Sect. 4.1, Eq. (13) cannot be used to~~  
481 ~~predict porosity in other regions.~~

482 In order to assess the applicability of the pedotransfer function for quartz obtained in this study,  
483 we used the independent data from Lu et al. (2007) and Tarnawski et al. (2009), for ten Chinese  
484 soils (see Supplement 3 and Table S3.1). These soils consist of reassembled sieved soil samples  
485 and contain no gravel, while our data concern undisturbed soils. Moreover, most of these soils  
486 contain very little organic matter and the  $m_{\text{sand}}/m_{\text{SOM}}$  ratio can be much larger than the  $m_{\text{sand}}/m_{\text{SOM}}$   
487 values measured at our grassland sites. For the 14 French soils used to determine pedotransfer  
488 functions for quartz, the  $m_{\text{sand}}/m_{\text{SOM}}$  ratio ranges from 3.7 to 37.2 (Table 2). Only three soils of Lu  
489 et al. (2007) present such low values of  $m_{\text{sand}}/m_{\text{SOM}}$ . The other seven soils of Lu et al. (2007)  
490 present  $m_{\text{sand}}/m_{\text{SOM}}$  values ranging from 48 to 1328 (see Table S3.1).

491 We used  $\lambda_{\text{sat}}$  experimental values derived from Table 3 in Tarnawski et al. (2009) to calculate  $Q$   
492 and  $f_{\text{q}}$  for the ten Lu et al. (2007) soils. Figure 10 shows the statistical relationship between these  
493 quantities and  $m_{\text{sand}}$ . Very good correlations of  $Q$  and  $f_{\text{q}}$  with  $m_{\text{sand}}$  are observed, with  $r^2$  values of  
494 0.72 and 0.83, respectively. This is consistent with our finding that  $f_{\text{q}}$  is systematically better  
495 correlated to soil characteristics than  $Q$  (Sect. 3.2).

496 The pedotransfer functions derived from French soils tend to overestimate  $f_{\text{q}}$  for the Lu et al.  
497 (2007) soils, especially for the seven soils presenting  $m_{\text{sand}}/m_{\text{SOM}}$  values larger than 40. Note that  
498 Lu et al. (2007) obtained a similar result for coarse-textured soils with their model, which  
499 assumed  $Q = m_{\text{sand}}$ . For the three other soils, presenting  $m_{\text{sand}}/m_{\text{SOM}}$  values smaller than 40,  $f_{\text{q}}$   
500 MAE values are given in Table 4. The best MAE score ( $0.071 \text{ m}^3 \text{ m}^{-3}$ ) is obtained for the  $m_{\text{sand}}^*$   
501 predictor of  $f_{\text{q}}$ .

502 These results are illustrated by Fig. 11 for the  $m_{\text{sand}}$  predictor of  $f_{\text{q}}$ . Figure 11 also shows the  $f_{\text{q}}$   
503 and  $\lambda_{\text{sat}}$  estimates obtained using specific coefficients in Eq. (12), based on the seven Lu et al.  
504 (2007) soils presenting  $m_{\text{sand}}/m_{\text{SOM}}$  values larger than 40. These coefficients are given together

505 with the scores in Table 6. Table 6 also present these values for other predictors of  $f_q$ . It appears  
506 that  $m_{\text{sand}}$  gives the best scores. The contrasting coefficient values between Table 6 and Table 3  
507 (Chinese and French soils, respectively) illustrate the variability of the coefficients of  
508 pedotransfer functions from one soil category to another, and the  $m_{\text{sand}}/m_{\text{SOM}}$  ratio seems to be a  
509 good indicator of the validity of a given pedotransfer function.

510 On the other hand, the  $m_{\text{sand}}/m_{\text{SOM}}$  ratio is not a good predictor of  $f_q$  for the Lu et al. (2007) soils  
511 presenting  $m_{\text{sand}}/m_{\text{SOM}}$  values larger than 40, and  $r^2$  presents a small value of 0.40 (Table 6). This  
512 can be explained by the very large range of  $m_{\text{sand}}/m_{\text{SOM}}$  values for these soils (see Table S3.1).  
513 Using  $\ln(m_{\text{sand}}/m_{\text{SOM}})$  instead of  $m_{\text{sand}}/m_{\text{SOM}}$  is a way to obtain a predictor linearly correlated to  $f_q$ .  
514 This is shown by Fig. 12 for the ten Lu et al. (2007) soils: the correlation is increased to a large  
515 extent ( $r^2 = 0.60$ ).

516

#### 517 4.4. Can $m_{\text{sand}}$ -based $f_q$ pedotransfer functions be used across soil types ?

518 Given the results presented in Tables 3, 4, and 6, it can be concluded that  $m_{\text{sand}}$  is the best  
519 predictor of  $f_q$  across mineral soil types. The  $m_{\text{sand}}/m_{\text{SOM}}$  predictor is relevant for the mineral soils  
520 containing the largest amount of organic matter.

521 The results presented in this study suggest that the  $m_{\text{sand}}/m_{\text{SOM}}$  ratio can be used to differentiate  
522 temperate grassland soils containing a rather large amount of organic matter ( $3.7 < m_{\text{sand}}/m_{\text{SOM}} <$   
523 40) from soils containing less organic matter ( $m_{\text{sand}}/m_{\text{SOM}} > 40$ ). The  $m_{\text{sand}}$  predictor can be used  
524 in both cases, with the following  $a_0$  and  $a_1$  coefficient values in Eq. (12): 0.15 and 0.572 for  
525  $m_{\text{sand}}/m_{\text{SOM}}$  ranging between 3.7 and 40 (Table 3), and 0.04 and 0.386 for  $m_{\text{sand}}/m_{\text{SOM}} > 40$  (Table  
526 6), respectively.

527 Although the  $m_{\text{sand}}/m_{\text{SOM}}$  predictor gives the best  $r^2$  scores for the 14 grassland soils considered in  
 528 this study, it seems more difficult to apply this predictor to other soils, as shown by the high  
 529 MAE score (MAE =  $0.135 \text{ m}^3 \text{ m}^{-3}$ ) for the corresponding Lu et al. (2007) soils in Table 4.  
 530 Moreover, the scores are very sensitive to errors in the estimation of  $m_{\text{SOM}}$  as shown by Table 5.  
 531 Although the  $m_{\text{sand}}^*$  predictor gives slightly better scores than  $m_{\text{sand}}$  (Table 4), the  $a_1$  coefficient in  
 532 more sensitive to errors in  $C_{\text{hmin}}$  (Table 3), and the bootstrapping reveals large uncertainties in  $a_0$   
 533 and  $a_1$  values.

534

#### 535 4.54. Prospects for using soil temperature profiles

536

537 Using standard soil moisture and soil temperature observations is a way to investigate soil  
 538 thermal properties over a large variety of soils, as the access to such data is facilitated by online  
 539 databases (Dorigo et al., 2013).

540 A key-limitation of the data used in this study, however, is that soil temperature observations ( $T_i$ )  
 541 are recorded with a resolution of  $\Delta T_i = 0.1 \text{ }^\circ\text{C}$  only (see Sect. 2.1). This low resolution affects the  
 542 accuracy of the soil thermal diffusivity estimates. In order to limit the impact of this effect, a data  
 543 filtering technique is used (see Supplement 4) and  $D_h$  is retrieved with a precision of 18 %.

544 Since  $T_i$  is recorded with a resolution of

$$545 \quad \Delta T_i = \left| \frac{\partial(T_i^n - T_i^{n-1})}{\partial T_i} \right| = \left| \frac{\partial(T_{i+1}^n - T_i^n)}{\partial T_i} \right| = 0.1 \text{ }^\circ\text{C} \quad (15);$$

546 the retrieved  $D_h$  values are affected by uncertainties and the relative uncertainty of  $D_h$  can be  
 547 estimated as:

$$548 \quad \left| \frac{\partial D_{hi}}{D_{hi}} \right| = \Delta T_i \times \left\{ \frac{1}{\left| T_i^n - T_i^{n-1} \right| + \left| \gamma_{i+1}^n - \gamma_i^n \right| + \left| \gamma_{i+1}^{n-1} - \gamma_i^{n-1} \right|} + \frac{\Delta z_{i+1}^{-1} + \Delta z_i^{-1}}{\left| \gamma_{i+1}^n - \gamma_i^n \right| + \left| \gamma_{i+1}^{n-1} - \gamma_i^{n-1} \right|} \right\} \quad (16).$$

549 ~~Therefore,  $D_h$  retrievals are more accurate in conditions when soil temperature at  $z_i = 0.10$  m~~  
550 ~~changes rapidly and when differences in vertical gradients of soil temperature above and below  $z_i$~~   
551 ~~are more pronounced. In general, this occurs around noon (between 0900 LST and 1400 LST),~~  
552 ~~and at dusk to a lesser extent, between 1700 LST and 0000 LST. In this study, we have imposed~~  
553 ~~the following conditions for using the obtained  $D_h$  retrievals:~~

$$554 \quad \left| T_i^n - T_i^{n-1} \right| > 0.8^\circ\text{C}, \left| \gamma_{i+1}^n - \gamma_i^n \right| > 30\text{Km}^{-1}, \text{ and } \left| \gamma_{i+1}^{n-1} - \gamma_i^{n-1} \right| > 30\text{Km}^{-1} \quad (17).$$

555 ~~According to Eq. (7), this ensures that~~

$$556 \quad \left| \frac{\partial D_{hi}}{D_{hi}} \right| < 18\% \quad (18).$$

557 It can be noticed that if  $T_i$  data were recorded with a resolution of  $0.03^\circ\text{C}$  (which corresponds to  
558 the typical uncertainty of PT100 probes),  $D_h$  could be retrieved with a precision of about 5 % in  
559 the conditions of Eq. (S4.317). ~~Alternatively, Eq. (17) conditions could be relaxed in order to get~~  
560 ~~more values of  $\lambda$  estimates for  $S_d > 0.4$  (Sect. 2.6) and increase the number of usable stations.~~  
561 Therefore, one may recommend to revise the current practise of most observation networks  
562 consisting in recording soil temperature with a resolution of  $0.1^\circ\text{C}$  only. More precision in the  $\lambda$   
563 estimates would permit investigating other processes of heat transfer in the soil such as those  
564 related to water transport (Rutten, 2015).

565

566

567

567 **5. Conclusions**

568

569 An attempt was made to use routine soil temperature and soil moisture observations of a network  
570 of automatic weather stations to retrieve instantaneous values of the soil thermal conductivity at  
571 a depth of 0.10 m. The data from the SMOSMANIA network, in southern France, are used. First,  
572 the thermal diffusivity is derived from consecutive measurements of the soil temperature, ~~at a 48-~~  
573 ~~minute interval, at three depths (0.05, 0.10, and 0.20 m). The thermal diffusion equation is solved~~  
574 ~~using an implicit scheme. It is shown that, as the soil temperature records have a resolution of 0.1~~  
575 ~~°C, the thermal diffusivity can be obtained with a relative error of 18 %.~~ The  $\lambda$  values are then  
576 derived from the thermal diffusivity retrievals and from the volumetric heat capacity calculated  
577 using measured soil properties. The relationship between the  $\lambda$  estimates and the measured soil  
578 moisture at a depth of 0.10 m permits the retrieval of  $\lambda_{\text{sat}}$  for 145 stations. ~~The Lu et al. (2007) A~~  
579 ~~empirical classic~~  $\lambda$  model is then used to retrieve the quartz volumetric content by reverse  
580 modelling. ~~For four stations, low values of  $\lambda_{\text{sat}}$  and null values of  $q$  are obtained, probably in~~  
581 ~~relation to uncertainties in the gravel and stone fraction. For eleven stations, a number of~~  
582 pedotransfer functions is proposed for volumetric fraction of quartz, for the considered region in  
583 France. For the grassland soils examined in this study, the ratio of sand to SOM fractions is the  
584 best predictor of  $f_q$ . A sensitivity study shows that ~~gravels have a major impact on  $\lambda_{\text{sat}}$  and that~~  
585 omitting gravels and the SOM information has a major impact on  $\lambda_{\text{sat}}$  ~~tends to enhance this~~  
586 ~~impact. Eventually, an error propagation analysis and a comparison with independent  $\lambda_{\text{sat}}$  data~~  
587 ~~from Lu et al. (2007) show that the gravimetric fraction of sand within soil solids, including~~  
588 ~~gravels and SOM, is a good predictor of the volumetric fraction of quartz when a larger variety of~~  
589 ~~soil types is considered. This technique is easy to implement and is based on fully automatic in~~



590 ~~situ observations associated to a characterisation of soil properties in the lab. Therefore, this~~  
591 ~~study could be extended to other regions and biomes. However, using temperature records with a~~  
592 ~~resolution of 0.1 °C limits the applicability of the method. It is recommended to acquire~~  
593 ~~temperature measurements with a better resolution. More precision in the  $\lambda$  estimates would then~~  
594 ~~permit investigating other processes of heat transfer in the soil such as those related to water~~  
595 ~~transport (Rutten, 2015).~~

596

### 597 **Acknowledgements**

598 We thank Dr. Xinhua Xiao (NC State University Soil Physics, Raleigh, USA) and Dr. Tusheng  
599 Ren (China Agricultural University, Beijing, China) for their review of the manuscript and for  
600 their fruitful comments. We thank Dr. Aaron Boone (CNRM, Toulouse, France) for his helpful  
601 comments. We thank our Meteo-France colleagues for their support in collecting and archiving  
602 the SMOSMANIA data: Catherine Bienaimé, Marc Bailleul, Laurent Brunier, Anna Chaumont,  
603 Jacques Couzinier, Mathieu Créau, Philippe Gillodes, Sandrine Girres, Michel Gouverneur,  
604 Maryvonne Kerdoncuff, Matthieu Lacan, Pierre Lantuejoul, Dominique Paulais, Fabienne Simon,  
605 Dominique Simonpietri, Marie-Hélène Théron, Marie Yardin.

606

606 **References**

607

608 Abu-Hamdeh, N. H., and Reeder, R. C.: Soil thermal conductivity: effects of density, moisture,  
609 salt concentration, and organic matter, *Soil Sci. Soc. Am. J.*, 64, 1285–1290, 2000.

610 Albergel, C., Rüdiger, C., Pellarin, T., Calvet, J.-C., Fritz, N., Froissard, F., Suquia, D., Petitpa,  
611 A., Piguet, B., and Martin, E.: From near-surface to root-zone soil moisture using an  
612 exponential filter: an assessment of the method based on in-situ observations and model  
613 simulations, *Hydrol. Earth Syst. Sci.*, 12, 1323–1337, 2008.

614 Albergel, C., Calvet, J.-C., de Rosnay, P., Balsamo, G., Wagner, W., Hasenauer, S., Naeimi, V.,  
615 Martin, E., Bazile, E., Bouyssel, F., and Mahfouf, J.-F.: Cross-evaluation of modelled and  
616 remotely sensed surface soil moisture with in situ data in southwestern France, *Hydrol. Earth  
617 Syst. Sci.*, 14, 2177–2191, doi:10.5194/hess-14-2177-2010, 2010.

618 Bristow, K. L., Kluitenberg, G. J., and Horton R.: Measurement of soil thermal properties with a  
619 dual-probe heat-pulse technique, *Soil Sci. Soc. Am. J.*, 58, 1288–1294,  
620 doi:10.2136/sssaj1994.03615995005800050002x, 1994.

621 Bristow, K. L.: Measurement of thermal properties and water content of unsaturated sandy soil  
622 using dual-probe heat-pulse probes, *Agr. Forest Meteorol.*, 89, 75-84, 1998.

623 Calvet, J.-C., Bessemoulin, P., Noilhan, J., Berne, C., Braud, I., Courault, D., Fritz, N., Gonzalez-  
624 Sosa, E., Goutorbe, J.-P., Haverkamp, R., Jaubert, G., Kergoat, L., Lachaud, G., Laurent, J.-  
625 P., Mordelet, P., Olioso, A., Péris, P., Roujean, J.-L., Thony, J.-L., Tosca, C., Vauclin, M.,  
626 Vignes, D.: MUREX: a land-surface field experiment to study the annual cycle of the energy  
627 and water budgets, *Ann. Geophys.*, 17, 838-854, 1999.

628 Calvet, J.-C., Fritz, N., Froissard, F., Suquia, D., Petitpa, A., and Piguet, B.: In situ soil moisture  
629 observations for the CAL/VAL of SMOS: the SMOSMANIA network, *International*

630 Geoscience and Remote Sensing Symposium, IGARSS, Barcelona, Spain, 23–28 July 2007,  
631 1196–1199, doi:10.1109/IGARSS.2007.4423019, 2007.

632 Chen, Y. Y., Yang, K., Tang, W., Qin, J., and Zhao, L.: Parameterizing soil organic carbon's  
633 impacts on soil porosity and thermal parameters for Eastern Tibet grasslands, *Sci. China*  
634 *Earth Sci.*, 55 (6), 1001–1011, doi:10.1007/s11430-012-4433-0, 2012.

635 Côté, J. and Konrad, J.-M.: A generalized thermal conductivity model for soils and construction  
636 materials, *Can. Geotech. J.*, 42, 443:458, doi:10.1139/T04-106, 2005.

637 de Vries, D. A.: Thermal properties of soils, in W.R. Van Wijk (ed.), *Physics of plant*  
638 *environment*, pp. 210–235, North-Holland Publ. Co., Amsterdam, 1963.

639 Dorigo, W. A., Wagner, W., Hohensinn, R., Hahn, S., Paulik, C., Xaver, A., Gruber, A., Drusch,  
640 M, Mecklenburg, S., van Oevelen, P., Robock, A., and Jackson, T.: *The International Soil*  
641 *Moisture Network: a data hosting facility for global in situ soil moisture measurements,*  
642 *Hydrol. Earth Syst. Sci.*, 15, 1675–1698, doi:10.5194/hess-15-1675-2011, 2011.

643 Draper, C., Mahfouf, J.-F., Calvet, J.-C., Martin, E., and Wagner, W.: Assimilation of ASCAT  
644 near-surface soil moisture into the SIM hydrological model over France, *Hydrol. Earth Syst.*  
645 *Sci.*, 15, 3829–3841, doi:10.5194/hess-15-3829-2011, 2011.

646 Johansen, O.: Thermal conductivity of soils. Ph.D. thesis, University of Trondheim, 236 pp.,  
647 †Available from Universitetsbiblioteket i Trondheim, Høgskoleringen 1, 7034 Trondheim,  
648 Norway, a translation is available ~~on~~at:  
649 <http://www.dtic.mil/dtic/tr/fulltext/u2/a044002.pdf>~~http://www.dtic.mil/cgi-~~  
650 ~~bin/GetTRDoc?AD=ADA044002~~ (last access January 2016), 1975.

651 Lu, S., Ren, T., Gong, Y., and Horton, R.: An improved model for predicting soil thermal  
652 conductivity from water content at room temperature, *Soil Sci. Soc. Am. J.*, 71, 8-14,  
653 doi:10.2136/sssaj2006.0041, 2007.

654 Nachtergaele, F., van Velthuize, H., Verelst, L., Wiberg, D., Batjes, N., Dijkshoorn, K., van  
655 Engelen, V., Fischer, G., Jones, A., Montanarella, L., Petri, M., Prieler, S., Teixeira, E., and  
656 Shi, X.: Harmonized World Soil Database, Version 1.2, FAO/IIASA/ISRIC/ISS-CAS/JRC,  
657 FAO, Rome, Italy and IIASA, Laxenburg, Austria, available at:  
658 [http://webarchive.iiasa.ac.at/Research/LUC/External-World-soil-  
659 database/HWSD\\_Documentation.pdf](http://webarchive.iiasa.ac.at/Research/LUC/External-World-soil-<br/>659 database/HWSD_Documentation.pdf) (last access January 2016), 2012.

660 Parlange, M. B., Cahill, A. T., Nielsen, D. R., Hopmans, J. W., and Wendroth, O.: Review of  
661 heat and water movement in field soils, *Soil Till. Res.*, 47, 5-10, 1998.

662 Parrens, M., Zakharova, E., Lafont, S., Calvet, J.-C., Kerr, Y., Wagner, W., and Wigneron, J.-P.:  
663 Comparing soil moisture retrievals from SMOS and ASCAT over France, *Hydrol. Earth Syst.*  
664 *Sci.*, 16, 423–440, doi:10.5194/hess-16-423-2012, 2012.

665 Peters-Lidard, C.D., Blackburn, E., Liang, X., and Wood, E.F.: The effect of soil thermal  
666 conductivity parameterization on surface energy fluxes and temperatures, *J. Atmos. Sci.*, 55,  
667 1209–1224, 1998.

668 Rutten, M. M.: Moisture in the topsoil: From large-scale observations to small-scale process  
669 understanding, PhD Thesis, Delft university of Technology, doi:10.4233/uuid:89e13a16-  
670 b456-4692-92f0-7a40ada82451, available at:  
671 <http://repository.tudelft.nl/view/ir/uuid:89e13a16-b456-4692-92f0-7a40ada82451/> (last  
672 access: January 2016), 2015.

673 ~~available from: [http://repository.tudelft.nl/view/ir/uuid%3A89e13a16-b456-4692-92f0-](http://repository.tudelft.nl/view/ir/uuid%3A89e13a16-b456-4692-92f0-7a40ada82451/)~~  
674 ~~[7a40ada82451/](http://repository.tudelft.nl/view/ir/uuid%3A89e13a16-b456-4692-92f0-7a40ada82451/), 2015.~~

675 Schelde, K., Thomsen, A., Heidmann, T., Schjonning, P., and Jansson, P.-E.: Diurnal fluctuations  
676 of water and heat flows in a bare soil, *Water Resour. Res.*, 34, 11, 2919-2929, 1998.

677 Schönerberger, J., Momose, T., Wagner, B., Leong, W. H., and Tarnawski, V. R.: Canadian field  
678 soils I. Mineral composition by XRD/XRF measurements, *Int. J. Thermophys.*, 33, 342–362,  
679 doi:10.1007/s10765-011-1142-4, 2012.

680 [Tarara, J.M., and J.M. Ham: Measuring soil water content in the laboratory and field with dual-](#)  
681 [probe heat-capacity sensors, \*Agron. J.\*, 89, 535–542, 1997.](#)

682 Tarnawski, V. R., McCombie, M. L., Leong, W. H., Wagner, B., Momose, T., and  
683 Schönerberger J.: Canadian field soils II. Modeling of quartz occurrence, *Int. J.*  
684 *Thermophys.*, 33, 843–863, doi:10.1007/s10765-012-1184-2, 2012.

685 Tarnawski, V. R., Momose, T., and Leong, W. H.: Assessing the impact of quartz content on the  
686 prediction of soil thermal conductivity, *Géotechnique*, 59, 4, 331–338, doi:  
687 10.1680/geot.2009.59.4.331, 2009.

688 Yang, K., Koike, T., Ye, B., and Bastidas, L.: Inverse analysis of the role of soil vertical  
689 heterogeneity in controlling surface soil state and energy partition, *J. Geophys. Res.*, 110,  
690 D08101, 15 pp., doi:10.1029/2004JD005500, 2005.

691 [Zhang, X., Heitman, J., Horton, R., and Ren, T.: Measuring near-surface soil thermal properties](#)  
692 [with the heat-pulse method: correction of ambient temperature and soil–air interface effects,](#)  
693 [\*Soil Sci. Soc. Am. J.\*, 78, 1575–1583, doi:10.2136/sssaj2014.01.0014, 2014.](#)

694

694 **Table 1** – Soil characteristics at 10 cm for the 21 stations of the SMOSMANIA network.  
695 Porosity values are derived from Eq. (1). Solid fraction values higher than 0.3 are in bold. The  
696 stations are listed from West to East (from top to bottom).  $\rho_d$ ,  $\theta_{sat}$ ,  $f$ , and  $m$ , stand for soil bulk  
697 density, porosity, volumetric fractions, and gravimetric fractions, respectively.  
698

<b>Station</b> <b>Soil</b>	$\rho_d$ (kg m <sup>-3</sup> )	$\theta_{sat}$ (m <sup>3</sup> m <sup>-3</sup> )	$f_{sand}$ (m <sup>3</sup> m <sup>-3</sup> )	$f_{clay}$ (m <sup>3</sup> m <sup>-3</sup> )	$f_{silt}$ (m <sup>3</sup> m <sup>-3</sup> )	$f_{gravel}$ (m <sup>3</sup> m <sup>-3</sup> )	$f_{SOM}$ (m <sup>3</sup> m <sup>-3</sup> )	$m_{sand}$ (kg kg <sup>-1</sup> )	$m_{clay}$ (kg kg <sup>-1</sup> )	$m_{silt}$ (kg kg <sup>-1</sup> )	$m_{gravel}$ (kg kg <sup>-1</sup> )	$m_{SOM}$ (kg kg <sup>-1</sup> )
SBR	1680	0.352	<b>0.576</b>	0.026	0.013	0.002	0.032	<b>0.911</b>	0.041	0.020	0.003	0.024
URG	1365	0.474	0.076	0.078	<b>0.341</b>	0.005	0.025	0.149	0.153	<b>0.665</b>	0.009	0.024
CRD	1435	0.438	<b>0.457</b>	0.027	0.033	0.000	0.045	<b>0.848</b>	0.051	0.060	0.000	0.041
PRG	1476	0.431	0.051	0.138	0.138	0.214	0.028	0.092	0.250	0.248	<b>0.385</b>	0.025
CDM	1522	0.413	0.073	0.241	0.231	0.012	0.030	0.128	<b>0.422</b>	<b>0.404</b>	0.020	0.026
LHS	1500	0.416	0.102	0.202	0.189	0.051	0.039	0.181	<b>0.359</b>	<b>0.335</b>	0.091	0.034
SVN	1453	0.445	0.127	0.073	0.176	0.162	0.017	0.233	0.133	<b>0.322</b>	0.296	0.015
MNT	1444	0.447	0.135	0.066	0.230	0.102	0.020	0.248	0.121	<b>0.424</b>	0.188	0.018
SFL	1533	0.413	0.127	0.071	0.118	0.250	0.021	0.221	0.123	0.205	<b>0.434</b>	0.018
MTM	1540	0.405	0.110	0.081	0.076	0.297	0.032	0.189	0.140	0.131	<b>0.512</b>	0.027
LZC	1498	0.429	0.129	0.066	0.068	0.292	0.015	0.229	0.117	0.121	<b>0.519</b>	0.013
NBN	1545	0.401	0.063	0.135	0.075	0.290	0.035	0.109	0.232	0.130	<b>0.499</b>	0.030
PZN	1311	0.495	0.222	0.074	0.131	0.054	0.023	<b>0.450</b>	0.151	0.266	0.111	0.023
PRD	1317	0.494	0.038	0.052	0.069	<b>0.326</b>	0.021	0.076	0.105	0.139	<b>0.659</b>	0.021
LGC	1496	0.428	0.253	0.044	0.042	0.214	0.019	<b>0.451</b>	0.078	0.074	<b>0.380</b>	0.017
MZN	1104	0.560	0.212	0.037	0.045	0.097	0.049	<b>0.510</b>	0.089	0.109	0.234	0.057
VLV	1274	0.506	0.294	0.054	0.086	0.031	0.029	<b>0.614</b>	0.112	0.179	0.064	0.030
BRN	1630	0.379	0.105	0.009	0.016	<b>0.474</b>	0.016	0.171	0.015	0.027	<b>0.774</b>	0.013
MJN	1276	0.506	0.064	0.029	0.056	<b>0.317</b>	0.028	0.133	0.060	0.118	<b>0.661</b>	0.029
BRZ	1280	0.508	0.097	0.074	0.109	0.190	0.020	0.202	0.154	0.228	<b>0.396</b>	0.021
CBR	1310	0.501	0.120	0.057	0.068	0.241	0.013	0.243	0.116	0.139	<b>0.489</b>	0.013

699  
700

700 **Table 2** – Thermal properties of 14 grassland soils in southern France:  $\lambda_{\text{sat}}$ ,  $f_q$  and  $Q$  retrievals  
 701 using the  $\lambda$  model (Eqs. (7)-(9) and Eq. (10), respectively) for degree of saturation values higher  
 702 than 0.4, together with the minimized RMSD between the simulated and observed  $\lambda$  values, and  
 703 the number of used  $\lambda$  observations ( $n$ ). The soils are sorted from the largest to the smallest ratio  
 704 of  $m_{\text{sand}}$  to  $m_{\text{SOM}}$ .  
 705

Soil	$\lambda_{\text{sat}}$ ( $\text{Wm}^{-1}\text{K}^{-1}$ )	RMSD ( $\text{Wm}^{-1}\text{K}^{-1}$ )	$n$	$f_q$ ( $\text{m}^3\text{m}^{-3}$ )	$Q$ ( $\text{kg kg}^{-1}$ )	$\frac{m_{\text{sand}}}{m_{\text{SOM}}}$
SBR	2.80	0.255	6	0.62	0.96	37.2
LGC	2.07	0.311	20	0.44	0.77	26.6
CBR	1.92	0.156	20	0.44	0.88	18.4
LZC	1.71	0.107	20	0.29	0.51	17.3
SVN	1.78	0.163	20	0.34	0.61	15.4
MNT	1.96	0.058	20	0.42	0.76	13.8
BRN	1.71	0.131	20	0.25	0.40	13.5
SFL	1.57	0.134	20	0.22	0.37	12.5
MTM	1.52	0.095	20	0.21	0.35	7.0
URG	1.37	0.066	20	0.05	0.10	6.2
LHS	1.57	0.136	20	0.26	0.45	5.3
CDM	1.82	0.086	20	0.26	0.44	5.0
PRG	1.65	0.086	20	0.18	0.32	3.7
PRD	1.26	0.176	20	0.14	0.28	3.7

706  
 707  
 708  ~~$\lambda_{\text{sat}}$  and  $q$  retrievals using the  $\lambda$  model (Eqs. (7)-(9) and Eq. (10), respectively) for degree of~~  
 709 ~~saturation values higher than 0.4, together with the minimized RMSD between the simulated and~~  
 710 ~~observed  $\lambda$  values, and the number of used  $\lambda$  observations ( $n$ ). The four stations with  $q = 0$  are in~~  
 711 ~~bold.~~  
 712

Station	Station full name	$\lambda_{\text{sat}}$ ( $\text{Wm}^{-1}\text{K}^{-1}$ )	$q$ ( $\text{m}^3\text{m}^{-3}$ )	RMSD ( $\text{Wm}^{-1}\text{K}^{-1}$ )	$n$
SBR	SABRES	2.79	0.61	0.233	118
URG	URGONS	1.28	0.13	0.102	62
CRD	CREON D'ARMAGNAC	-	-	-	0
PRG	PEYRUSSE GRANDE	1.59	0.26	0.105	94
CDM	CONDOM	1.36	0.13	0.263	132
<b>LHS</b>	<b>LAHAS</b>	<b>1.03</b>	<b>0.00</b>	<b>0.405</b>	<b>116</b>
<b>SVN</b>	<b>SAVENES</b>	<b>1.11</b>	<b>0.00</b>	<b>0.276</b>	<b>997</b>
MNT	MONTAUT	1.45	0.38	0.103	207
SFL	SAINT FELIX DE LAURAGAIS	1.40	0.14	0.183	1078

<b>MTM</b>	<b>MOUTHOUMET</b>	<b>1.45</b>	<b>0.18</b>	<b>0.137</b>	<b>1939</b>
<b>LZC</b>	<b>LEZIGNAN-CORBIERES</b>	<b>1.49</b>	<b>0.19</b>	<b>0.166</b>	<b>557</b>
<b>NBN</b>	<b>NARBONNE</b>	<b>0.52</b>	<b>0.00</b>	<b>0.101</b>	<b>100</b>
<b>PZN</b>	<b>PEZENAS</b>	<b>-</b>	<b>-</b>	<b>-</b>	<b>0</b>
<b>PRD</b>	<b>PRADES-LE-LEZ</b>	<b>0.70</b>	<b>0.00</b>	<b>0.165</b>	<b>490</b>
<b>LGC</b>	<b>LA-GRAND-COMBE</b>	<b>1.80</b>	<b>0.34</b>	<b>0.368</b>	<b>305</b>
<b>MZN</b>	<b>MAZAN-L'ABBAYE</b>	<b>-</b>	<b>-</b>	<b>-</b>	<b>0</b>
<b>VLV</b>	<b>VILLEVIEILLE</b>	<b>-</b>	<b>-</b>	<b>-</b>	<b>0</b>
<b>BRN</b>	<b>BARNAS</b>	<b>1.35</b>	<b>0.07</b>	<b>0.335</b>	<b>469</b>
<b>MJN</b>	<b>MEJANNES-LE-CLAP</b>	<b>-</b>	<b>-</b>	<b>-</b>	<b>0</b>
<b>BRZ</b>	<b>BERZEME</b>	<b>-</b>	<b>-</b>	<b>-</b>	<b>0</b>
<b>CBR</b>	<b>CABRIERES-D'AVIGNON</b>	<b>1.72</b>	<b>0.36</b>	<b>0.241</b>	<b>85</b>

713  
714  
715  
716  
717



717 **Table 3—**  
 718 Ability of the Eqs. (10)–(13) empirical model to estimate  $\lambda_{\text{sat}}$  values at the 11 stations presenting  
 719 non-null  $q$  values and impact of changes in the model, in order of decreasing  $r^2$  score (from top to  
 720 bottom). Results for all 15 stations (including null  $q$  values) are between brackets.  
 721

Model configuration	$r^2$	RMSD ( $\text{Wm}^{-1}\text{K}^{-1}$ )	Mean bias ( $\text{Wm}^{-1}\text{K}^{-1}$ )
Full model using $\theta_{\text{sat}}$ observations	0.87 (0.03)	0.15 (1.08)	-0.01 (+0.62)
Full model using $\theta_{\text{satMOD}}$ (Eqs. (13)–(14))	0.88 (0.01)	0.14 (1.02)	-0.03 (+0.62)
— same with: $f_{\text{SOM}} = 0$	-0.87 (0.00)	-0.23 (1.18)	+0.12 (+0.78)
— same with: $f_{\text{SOM}} = 0$ and $q = f_{\text{sand}}$	-0.86 (0.02)	-0.22 (1.06)	+0.00 (+0.64)
— same with: $q = f_{\text{sand}}$	0.86 (0.12)	-0.26 (0.82)	-0.22 (+0.37)
— same with: $f_{\text{gravel}} = 0$ and $q = f_{\text{sand}}$	-0.77 (0.17)	-0.25 (0.81)	-0.15 (+0.39)
— same with: $f_{\text{gravel}} = 0$	0.65 (0.07)	-0.29 (1.06)	+0.15 (+0.73)
— same with: $f_{\text{gravel}} = 0, f_{\text{SOM}} = 0$ and $q = f_{\text{sand}}$	0.61 (0.04)	-0.42 (1.17)	+0.24 (+0.83)
— same with: $f_{\text{gravel}} = 0$ and $f_{\text{SOM}} = 0$	0.51 (0.01)	-0.56 (1.34)	+0.41 (+1.01)

722  
 723  
 724

724 **Table 4** — Coefficient of determination and RMSD of the regression equation of  $q$  vs. diverse  
 725 volumetric fractions of soil solids, for 11 SMOSMANIA stations. First line corresponds to the  
 726 pedotransfer function for quartz proposed in this study (Eq. (12)).  
 727

Predictor of $q$	$r^2$	RMSD ( $\text{m}^3 \text{m}^{-3}$ )
$f_{\text{clay}} + f_{\text{silt}} + f_{\text{gravel}} + f_{\text{SOM}}$	0.78	0.07
$f_{\text{clay}} + f_{\text{silt}} + f_{\text{gravel}}$	0.78	0.07
$f_{\text{silt}} + f_{\text{gravel}} + f_{\text{SOM}}$	0.67	0.09
$f_{\text{sand}}$	0.66	0.09
$f_{\text{clay}} + f_{\text{gravel}} + f_{\text{SOM}}$	0.38	0.12
$f_{\text{clay}} + f_{\text{silt}} + f_{\text{SOM}}$	0.12	0.14

728  
 729 **Table 3** – Coefficients of four pedotransfer functions of  $f_q$  for 14 soils of this study, together  
 730 with indicators of the coefficient uncertainty, derived by bootstrapping and by perturbing the  
 731 volumetric heat capacity of soil minerals ( $C_{\text{hmin}}$ ). The best predictor is in bold.

Predictor of $f_q$	Coefficients for 14 soils		Confidence interval from bootstrapping		Impact of a change of $\pm 0.08 \times 10^6 \text{ J m}^{-3} \text{ K}^{-1}$ in $C_{\text{hmin}}$	
	$a_0$	$a_1$	$a_0$	$a_1$	$a_0$	$a_1$
$m_{\text{sand}} / m_{\text{SOM}}$	0.12	0.0134	[0.10,0.14]	[0.012,0.014]	[0.11,0.13]	[0.013,0.013]
$m_{\text{sand}}^*$	0.08	0.944	[0.00,0.11]	[0.85,1.40]	[0.07,0.09]	[0.919,0.966]
<b><math>m_{\text{sand}}</math></b>	<b>0.15</b>	<b>0.572</b>	<b>[0.08,0.17]</b>	<b>[0.54,0.94]</b>	<b>[0.14,0.17]</b>	<b>[0.55,0.56]</b>
$1 - \theta_{\text{sat}} - f_{\text{sand}}$	0.73	-1.020	[0.71,0.89]	[-1.38, -0.99]	[0.70,0.73]	[-1.00, -0.99]

732 (\*) only  $m_{\text{sand}}$  values smaller than  $0.6 \text{ kg kg}^{-1}$  are used in the regression

733

733 **Table 4** – Scores of four pedotransfer functions of  $f_q$  for 14 soils of this study, together with the  
 734 scores obtained by bootstrapping, without the sandy SBR soil. The MAE score of these  
 735 pedotransfer functions for three Chinese soils of Lu et al. (2007) for which  $m_{\text{sand}}/m_{\text{SOM}} < 40$  is  
 736 given. The best predictor and the best scores are in bold.

<u>Predictor of <math>f_q</math></u>	<u>Regression scores</u>			<u>Bootstrap scores</u>			<u>Scores without SBR</u> (and MAE for 3 Lu soils)		
	<u><math>r^2</math></u>	<u>RMSD</u> ( $\text{m}^3 \text{m}^{-3}$ )	<u>MAE</u> ( $\text{m}^3 \text{m}^{-3}$ )	<u><math>r^2</math></u>	<u>RMSD</u> ( $\text{m}^3 \text{m}^{-3}$ )	<u>MAE</u> ( $\text{m}^3 \text{m}^{-3}$ )	<u><math>r^2</math></u>	<u>RMSD</u> ( $\text{m}^3 \text{m}^{-3}$ )	<u>MAE</u> ( $\text{m}^3 \text{m}^{-3}$ )
<u><math>m_{\text{sand}}/m_{\text{SOM}}</math></u>	<b>0.77</b>	<b>0.067</b>	0.053	<b>0.72</b>	<b>0.074</b>	<b>0.059</b>	<b>0.62</b>	<b>0.070</b>	0.057 (0.135)
<u><math>m_{\text{sand}}^*</math></u>	0.74	0.072	<b>0.052</b>	0.67	0.126	0.100	0.56	0.075	<b>0.056</b> (0.071)
<u><math>m_{\text{sand}}</math></u>	0.67	0.081	0.060	0.56	0.121	0.084	0.56	0.075	<b>0.056</b> (0.086)
<u><math>1 - \theta_{\text{sat}} - f_{\text{sand}}</math></u>	0.65	0.084	0.064	0.56	0.102	0.079	0.45	0.084	0.061 (0.158)

737 (\*) only  $m_{\text{sand}}$  values smaller than  $0.6 \text{ kg kg}^{-1}$  are used in the regression

738  
 739  
 740  
 741  
 742  
 743

743 **Table 5** – Ability of the Eqs. (10)-(13) empirical model to estimate  $\lambda_{\text{sat}}$  values for 14 soils and  
 744 impact of changes in gravel and SOM volumetric content:  $f_{\text{gravel}} = 0 \text{ m}^3\text{m}^{-3}$  and  $f_{\text{SOM}} = 0.013$   
 745  $\text{m}^3\text{m}^{-3}$  (the smallest  $f_{\text{SOM}}$  value, observed for CBR).  $r^2$  values smaller than 0.60, RMSD values  
 746 higher than  $0.20 \text{ Wm}^{-1}\text{K}^{-1}$ , and mean bias values higher (smaller) than  $+0.10$  ( $-0.10$ ) are in bold.

Model configuration	Predictor of $f_q$	$r^2$	RMSD ( $\text{Wm}^{-1}\text{K}^{-1}$ )	Mean bias ( $\text{Wm}^{-1}\text{K}^{-1}$ )
<u>Model using <math>\theta_{\text{sat}}</math> observations</u>	$m_{\text{sand}}/m_{\text{SOM}}$	0.86	0.14	+0.01
	$m_{\text{sand}}^*$	0.83	0.15	-0.01
	$m_{\text{sand}}$	0.81	0.16	-0.03
	$1 - \theta_{\text{sat}} - f_{\text{sand}}$	0.82	0.16	-0.03
<u>Full model using <math>\theta_{\text{satMOD}}</math> (Eqs. (13))</u>	$m_{\text{sand}}/m_{\text{SOM}}$	0.85	0.14	+0.03
	$m_{\text{sand}}^*$	0.85	0.14	-0.03
	$m_{\text{sand}}$	0.84	0.15	-0.03
	$1 - \theta_{\text{sat}} - f_{\text{sand}}$	0.82	0.16	-0.02
<u>same with:</u> <u><math>f_{\text{SOM}} = 0.013 \text{ m}^3\text{m}^{-3}</math></u>	$m_{\text{sand}}/m_{\text{SOM}}$	<b>0.57</b>	<b>0.35</b>	<b>+0.20</b>
	$m_{\text{sand}}^*$	0.83	0.15	+0.00
	$m_{\text{sand}}$	0.81	0.16	-0.02
	$1 - \theta_{\text{sat}} - f_{\text{sand}}$	0.83	0.15	-0.02
<u>same with:</u> <u><math>f_{\text{gravel}} = 0 \text{ m}^3\text{m}^{-3}</math></u>	$m_{\text{sand}}/m_{\text{SOM}}$	0.87	0.19	<b>-0.12</b>
	$m_{\text{sand}}^*$	0.70	<b>0.23</b>	<b>+0.11</b>
	$m_{\text{sand}}$	0.79	0.17	+0.04
	$1 - \theta_{\text{sat}} - f_{\text{sand}}$	0.81	0.17	+0.05
<u>same with:</u> <u><math>f_{\text{SOM}} = 0.013 \text{ m}^3\text{m}^{-3}</math></u> <u>and <math>f_{\text{gravel}} = 0 \text{ m}^3\text{m}^{-3}</math></u>	$m_{\text{sand}}/m_{\text{SOM}}$	0.63	<b>0.31</b>	<b>+0.16</b>
	$m_{\text{sand}}^*$	<b>0.52</b>	<b>0.36</b>	<b>+0.24</b>
	$m_{\text{sand}}$	<b>0.59</b>	<b>0.29</b>	<b>+0.16</b>
	$1 - \theta_{\text{sat}} - f_{\text{sand}}$	0.70	<b>0.25</b>	<b>+0.16</b>

(\*) only  $m_{\text{sand}}$  values smaller than  $0.6 \text{ kg kg}^{-1}$  are used in the regression

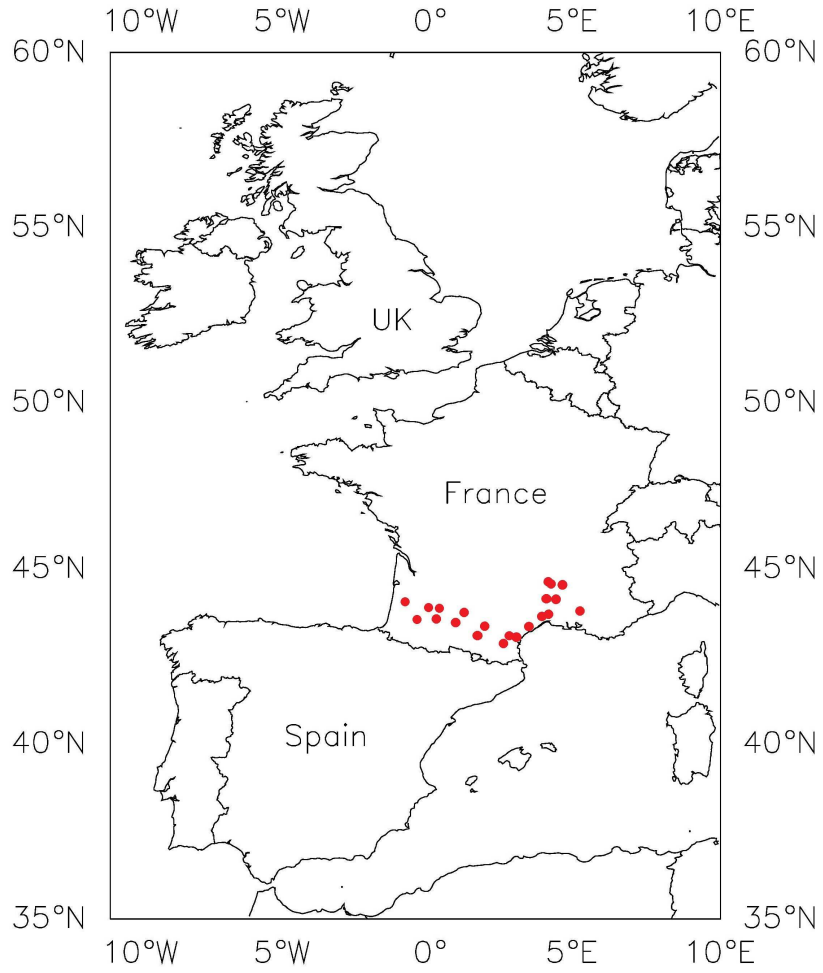
747  
748  
749  
750

750 **Table 6** – Pedotransfer functions of  $f_q$  for 7 soils of Lu et al. (2007) with  $m_{\text{sand}}/m_{\text{SOM}} > 40$ . The  
 751 best predictor and the best scores are in bold.

<u>Predictor of <math>f_q</math></u>	<u>Regression scores</u> <u>for 7 Lu soils with</u> <u><math>m_{\text{sand}}/m_{\text{SOM}} &gt; 40</math></u>			<u>Coefficients</u>	
	<u><math>r^2</math></u> <u>(p-value)</u>	<u>RMSD</u> <u>(<math>\text{m}^3\text{m}^{-3}</math>)</u>	<u>MAE</u> <u>(<math>\text{m}^3\text{m}^{-3}</math>)</u>	<u><math>a_0</math></u>	<u><math>a_1</math></u>
<u><math>m_{\text{sand}}/m_{\text{SOM}}</math></u>	<u>0.40</u> <u>(0.13)</u>	<u>0.089</u>	<u>0.075</u>	<u>0.20</u>	<u>0.000148</u>
<u><math>m_{\text{sand}}^*</math></u>	<u>0.82</u> <u>(0.005)</u>	<u>0.073</u>	<u>0.054</u>	<u>0.07</u>	<u>0.425</u>
<u><math>m_{\text{sand}}</math></u>	<b><u>0.82</u></b> <b><u>(0.005)</u></b>	<b><u>0.048</u></b>	<b><u>0.042</u></b>	<u>0.04</u>	<u>0.386</u>
<u><math>1 - \theta_{\text{sat}} - f_{\text{sand}}</math></u>	<u>0.81</u> <u>(0.006)</u>	<u>0.050</u>	<u>0.043</u>	<u>0.44</u>	<u>-0.814</u>

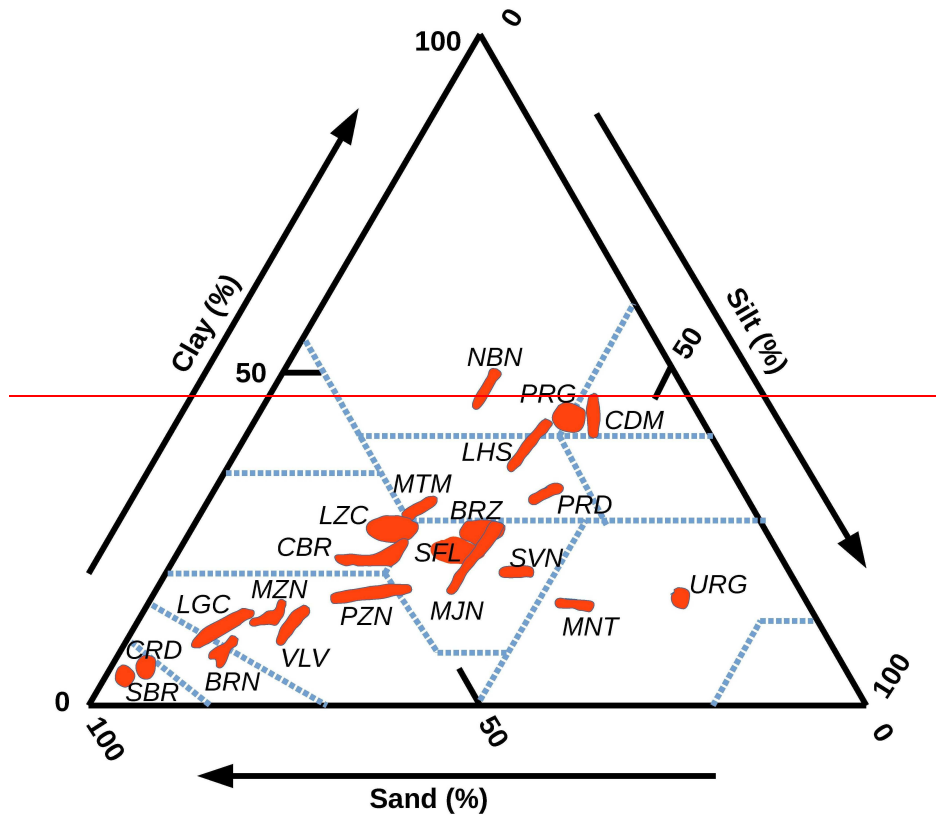
(\*) only  $m_{\text{sand}}$  values smaller than  $0.6 \text{ kg kg}^{-1}$  are used in the regression

752  
 753  
 754  
 755



756  
757  
758  
759  
760  
761  
762  
763  
764  
765  
766  
767

**Fig. 1** – Location of the 21 SMOSMANIA stations in southern France.

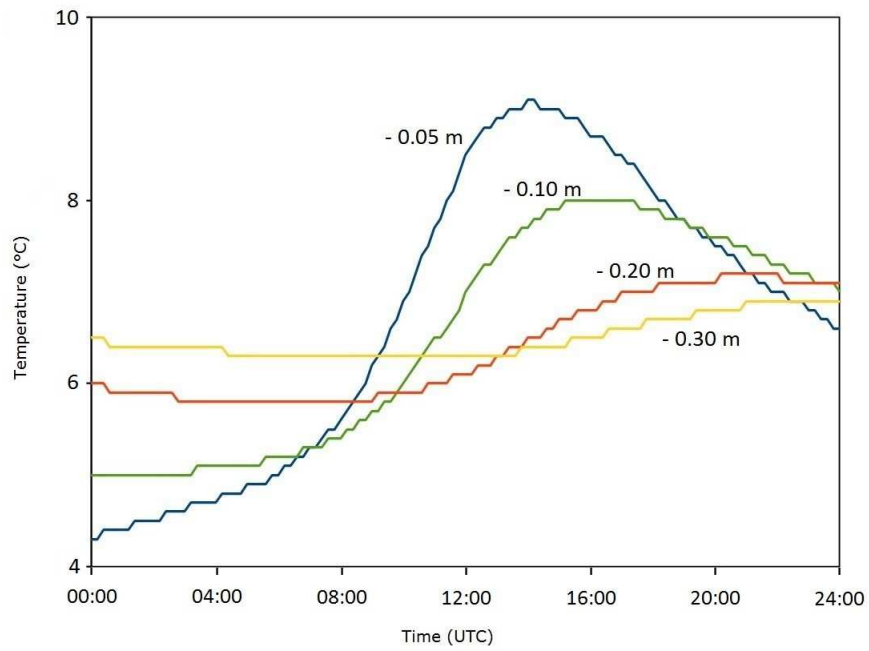


768  
 769  
 770  
 771  
 772  
 773  
 774  
 775  
 776  
 777  
 778  
 779  
 780  
 781  
 782

**Fig. 2** — Soil characteristics of the 21 SMOSMANIA stations at a depth of 10cm: mineral fine earth gravimetric fractions of clay, silt and sand. For a given station, the red mark covers the fraction values measured at 0.05, 0.10 and 0.20 m. Full station names are given in Table 2. The dashed blue lines correspond to the USDA textural soil classification.

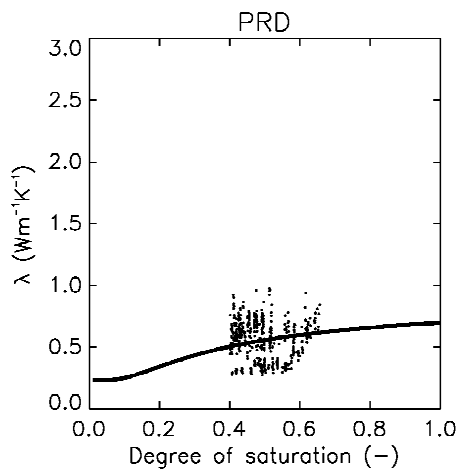
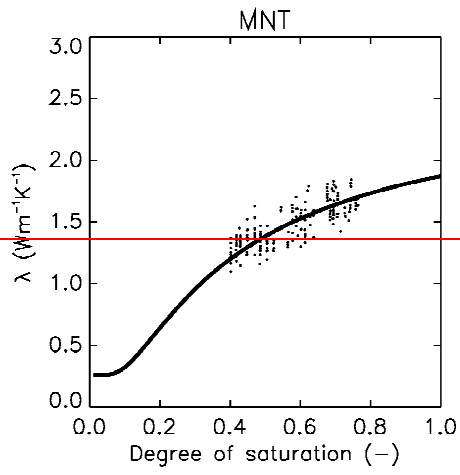
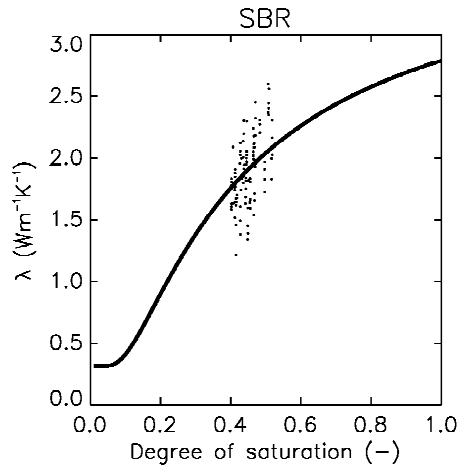


783  
784  
785  
786  
787

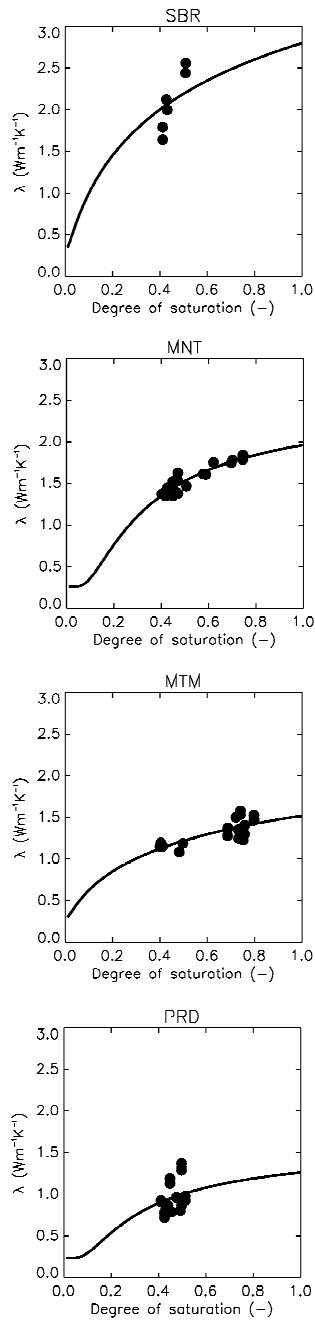


788  
789  
790  
791  
792  
793  
794  
795  
796  
797

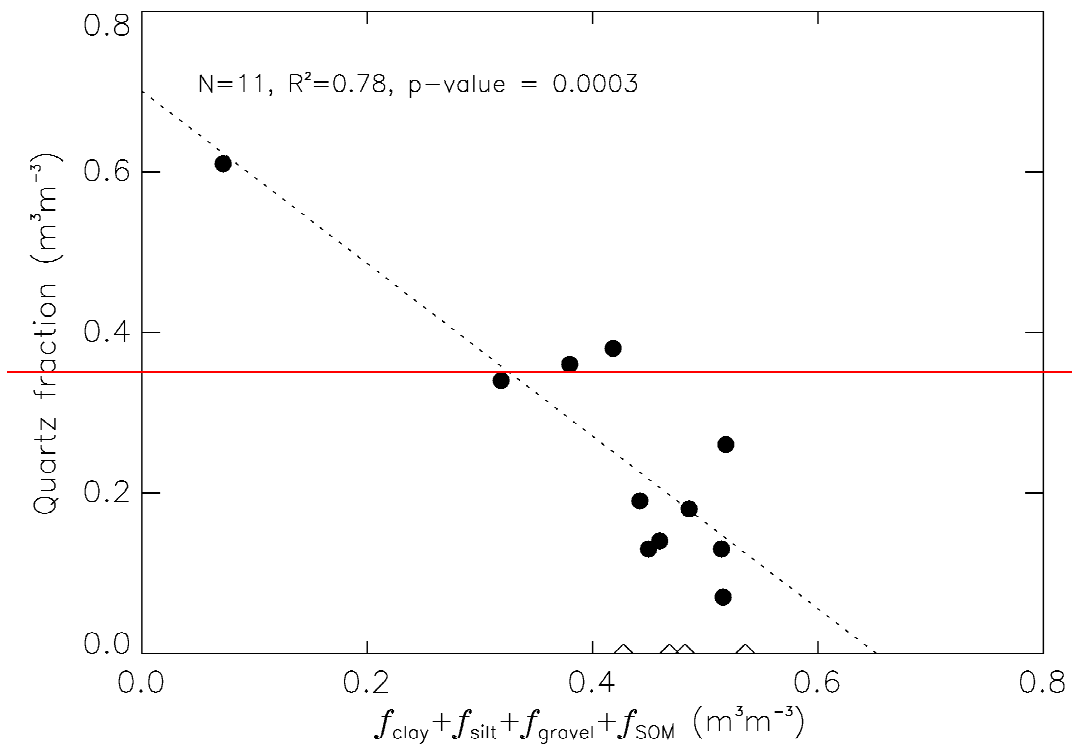
**Fig. 23** – Soil temperature measured at the Saint-Félix-de-Lauragais (SFL) station on 23 February 2015, at depths of 0.05, 0.10, 0.20, and 0.30 m. Levelling is due to the low resolution of the temperature records (0.1°C).



798  
799



800  
 801 **Fig. 34** – Retrieved  $\lambda$  values (dark dots) vs. the observed degree of saturation of the soil, at a  
 802 depth of 0.10 m, for (from top to bottom) Sabres (SBR), Montaut (MNT), Mouthoumet (MTM),  
 803 and Prades-le-Lez (PRD), together with simulated  $\lambda$  values from dry to wet conditions (dark  
 804 lines).  
 805  
 806

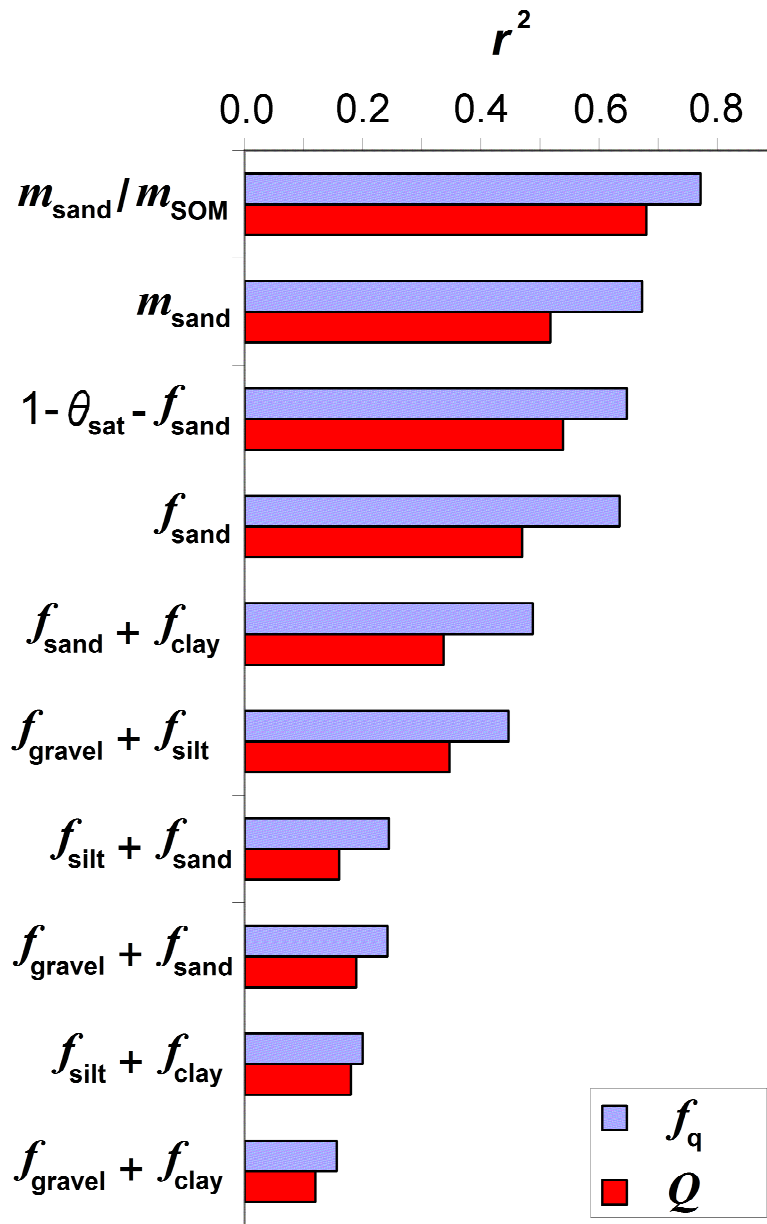


806  
807  
808  
809  
810  
811  
812  
813  
814

**Fig. 5** — Non-null and null  $q$  retrievals (dark dots and opened diamonds, respectively) vs. the sum of clay, silt, gravel and SOM volumetric fractions (empirical Equation (12)).

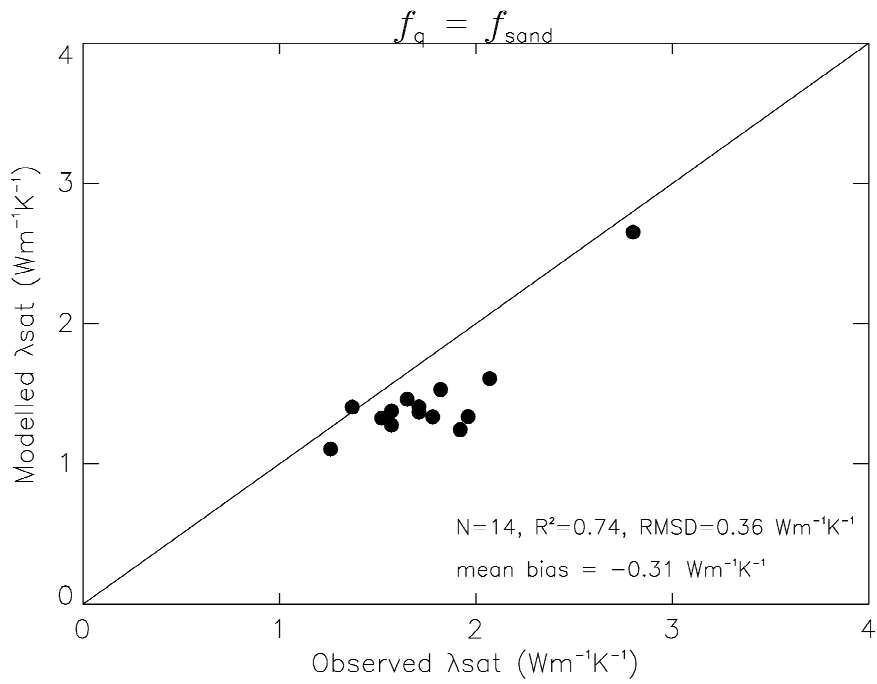
814  
815

|



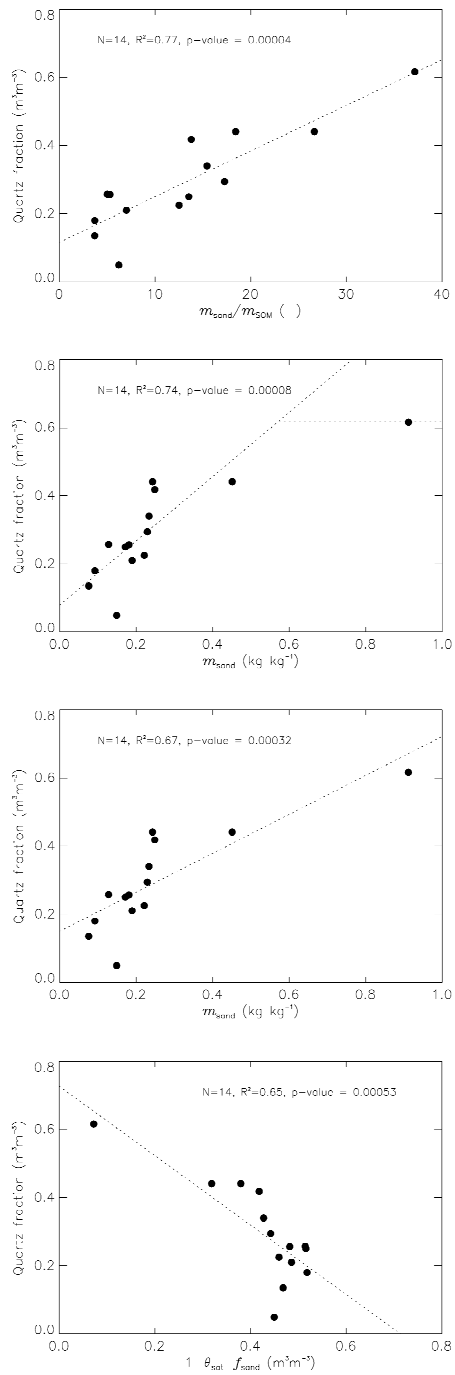
815  
816  
817  
818

**Fig. 4** – Fraction of variance ( $r^2$ ) of gravimetric and volumetric fraction of quartz ( $Q$  and  $f_q$ , red and blue bars, respectively) explained by various predictors.



819  
820  
821  
822

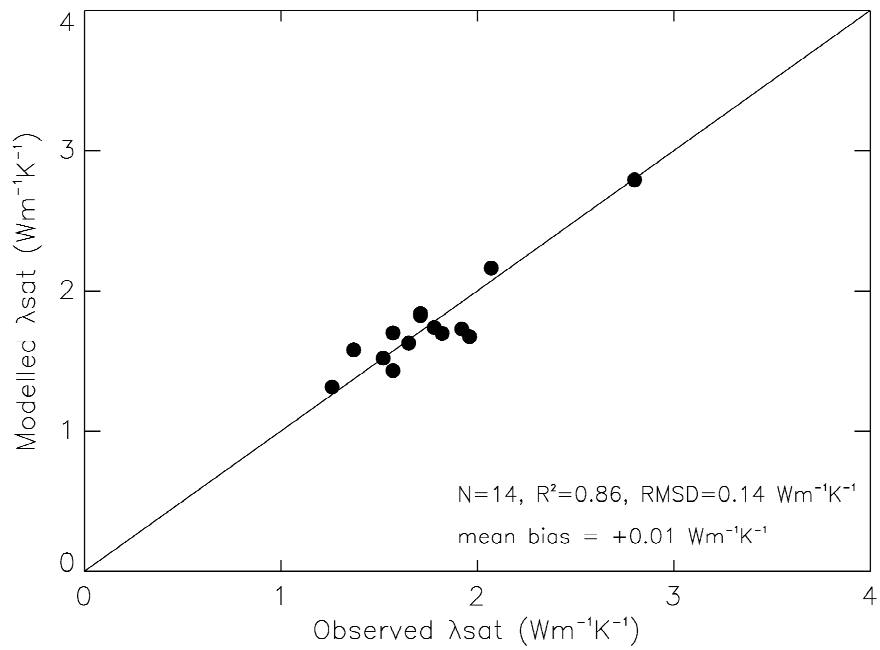
**Fig. 5** –  $\lambda_{satMOD}$  values derived from volumetric quartz fractions  $f_q$  assumed equal to  $f_{sand}$ , using observed  $\theta_{sat}$  values, vs.  $\lambda_{sat}$  retrievals.



822  
 823  
 824  
 825  
 826

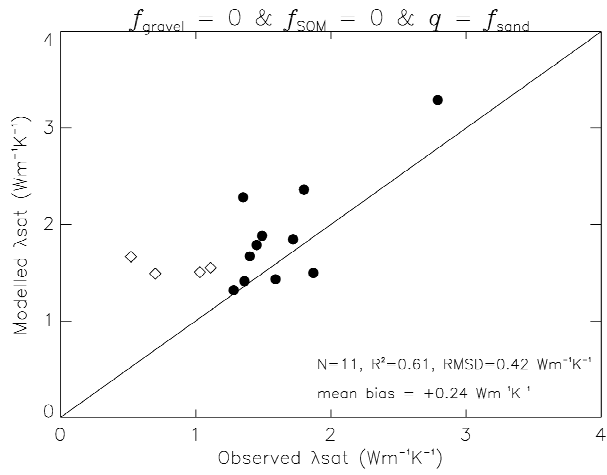
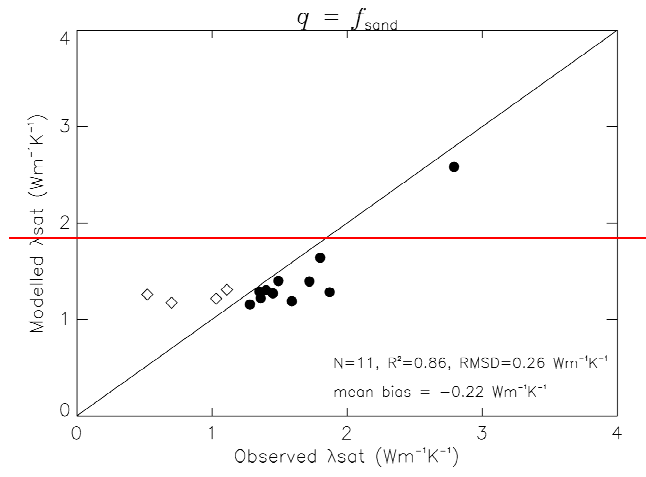
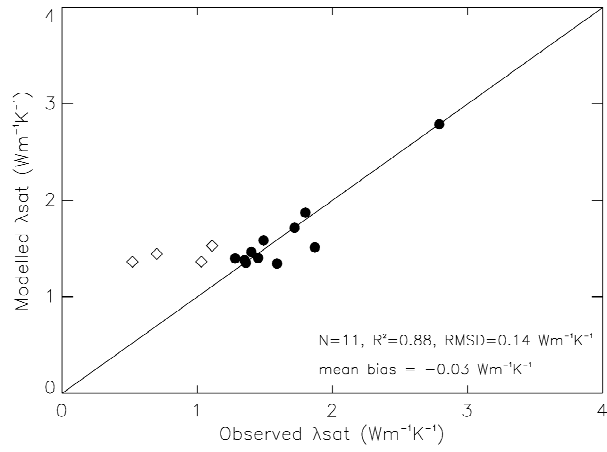
**Fig. 6 – Pedotransfer functions for quartz:  $f_q$  retrievals (dark dots) vs. the four predictors of  $f_q$  given in Table 3. The modelled  $f_q$  values are represented by the dashed lines.**

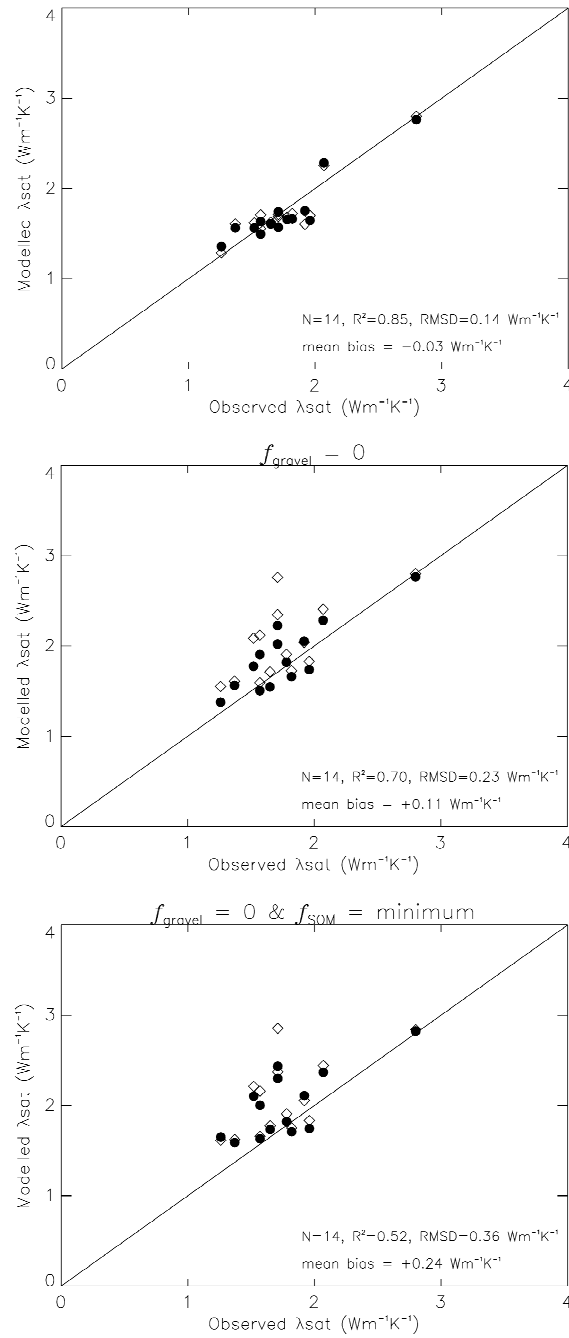




826  
 827  
 828  
 829

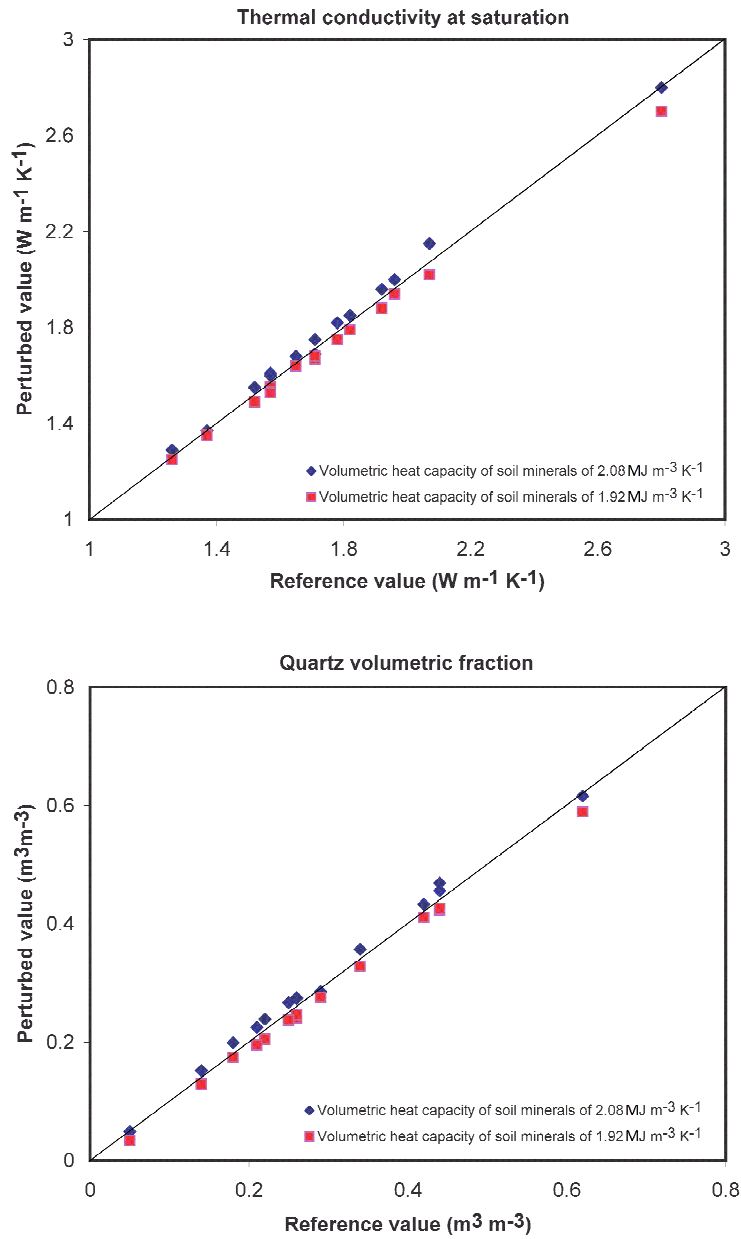
**Fig. 7** –  $\lambda_{\text{satMOD}}$  values derived from the  $m_{\text{sand}} / m_{\text{SOM}}$  pedotransfer function for the volumetric quartz fractions, using observed  $\theta_{\text{sat}}$  values, vs.  $\lambda_{\text{sat}}$  retrievals.





831  
 832 **Fig. 86** –  $\lambda_{satMOD}$  values derived from the  $m_{sand}^*$  pedotransfer function for the volumetric quartz  
 833 fractions, using  $\theta_{satMOD}$  (Eqs. (13)) or the observed  $\theta_{sat}$  (dark dots and opened diamonds,  
 834 respectively), vs.  $\lambda_{sat}$  retrievals: (top) full model, (middle)  $f_{SOM} = 0.013 m^3 m^{-3}$ , (bottom)  $f_{SOM} =$   
 835  $0.013 m^3 m^{-3}$  and  $f_{gravel} = 0 m^3 m^{-3}$ . Scores are given for the  $\theta_{satMOD}$  configuration.  
 836  ~~$\lambda_{satMOD}$  vs.  $\lambda_{sat}$  retrievals for non null and null  $q$  retrievals (dark dots and opened diamonds,~~  
 837 ~~respectively): (top) full model using  $\theta_{satMOD}$  (Eqs. (13)-(14)), (middle) replacing Eq. (12) by  $q =$~~   
 838  ~~$f_{sand}$ , (bottom) replacing Eq. (12) by  $q = f_{sand}$  and assuming  $f_{gravel} = 0$  and  $f_{SOM} = 0$  (Table 3).~~  
 839

840



841

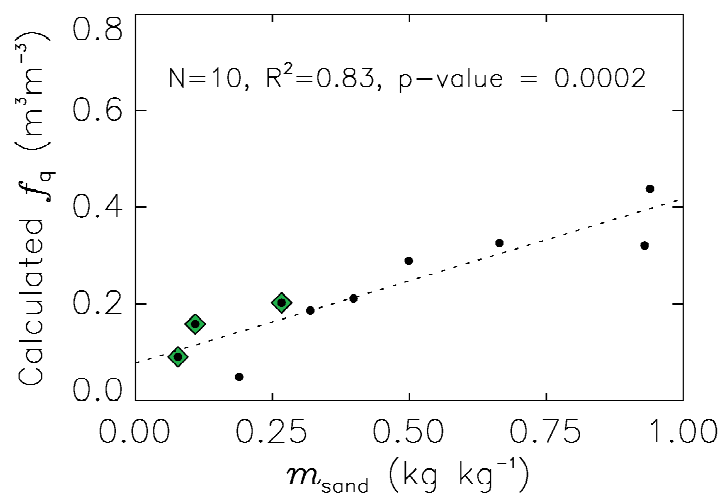
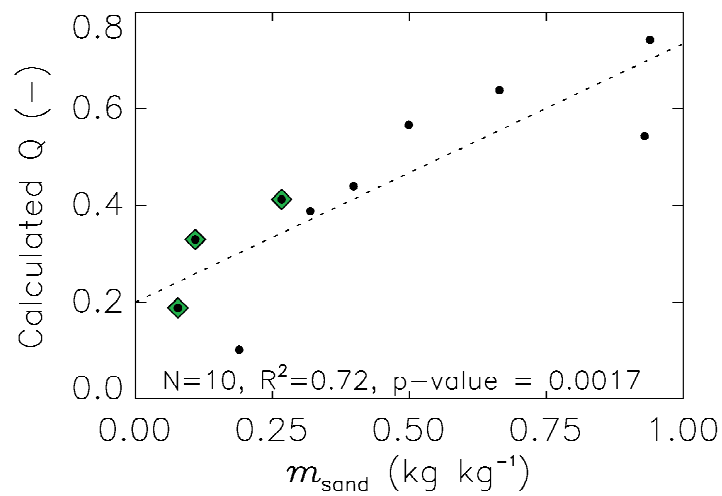
842

843

844

845

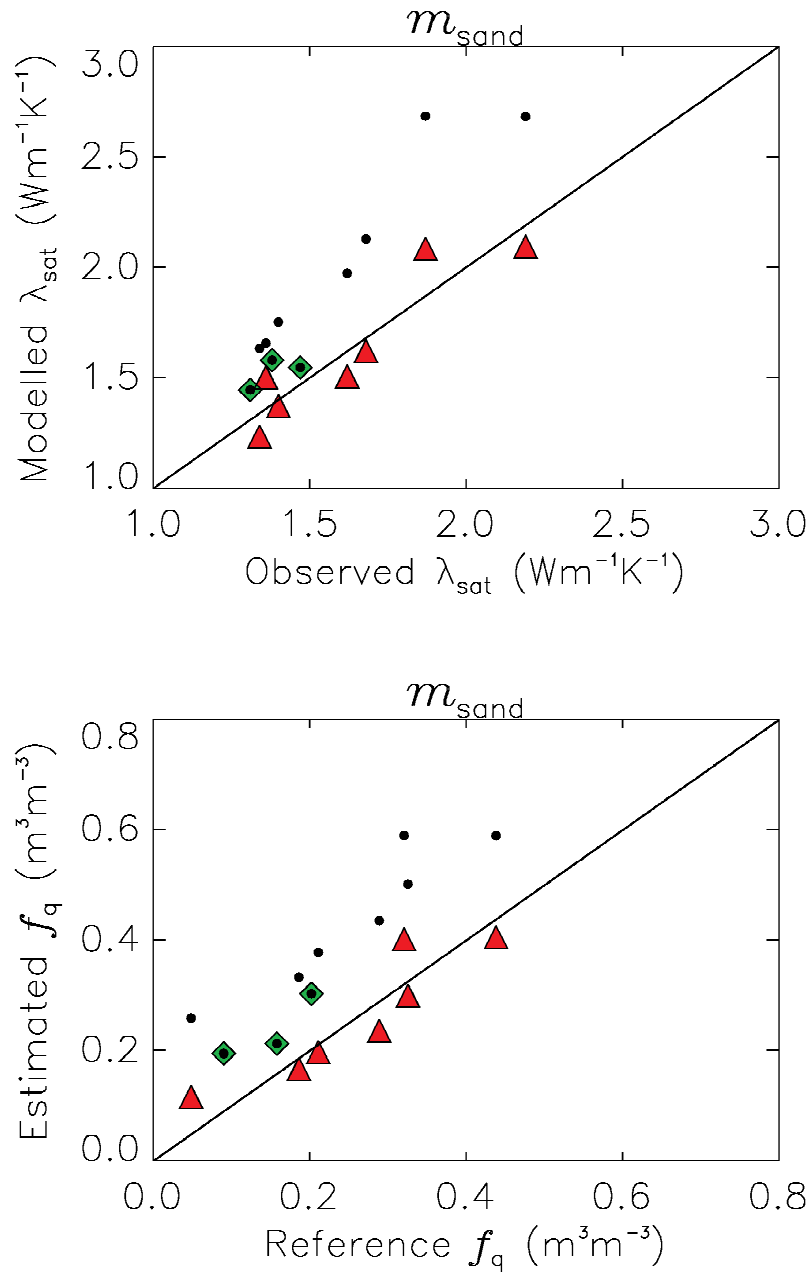
**Fig. 9 – Impact of using values of  $C_{hmin} = 1.92 \text{ MJ m}^{-3} \text{ K}^{-1}$  and  $C_{hmin} = 2.08 \text{ MJ m}^{-3} \text{ K}^{-1}$  instead of  $C_{hmin} = 2.0 \text{ MJ m}^{-3} \text{ K}^{-1}$  on (top) the retrieved  $\lambda_{sat}$ , (bottom) the volumetric fraction of quartz.**



846  
847  
848  
849  
850  
851  
852  
853  
854

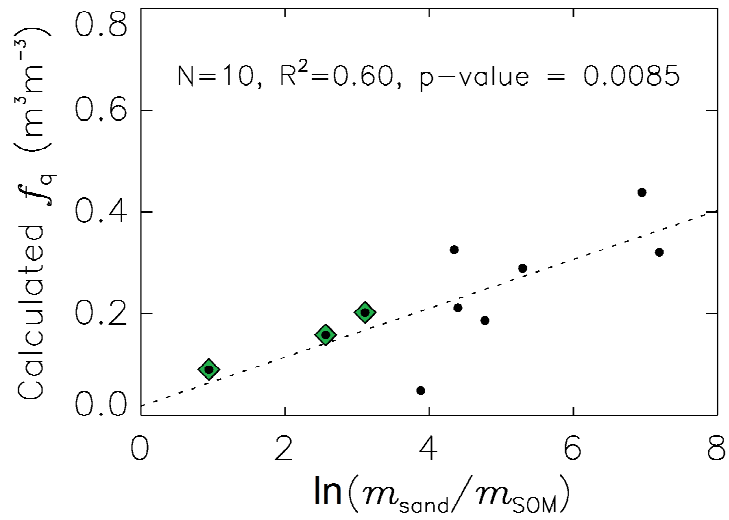
---

**Fig. 10** – Gravimetric and volumetric fraction of quartz (top and bottom, respectively) derived from the  $\lambda_{\text{sat}}$  observations of Lu et al. (2007) for 10 soils given by Tarnawski et al. (2009), vs. the gravimetric fraction of sand  $m_{\text{sand}}$ . The three soils for which  $m_{\text{sand}}/m_{\text{SOM}} < 40$  are indicated by green diamonds. The dashed lines represent the regression equations based on all soils:  $Q = 0.20 + 0.54 m_{\text{sand}}$  and  $f_q = 0.08 + 0.34 m_{\text{sand}}$ .



854  
 855  
 856  
 857  
 858  
 859  
 860  
 861  
 862  
 863

**Fig. 11** – Estimated  $\lambda_{\text{sat}}$  and volumetric fraction of quartz  $f_q$  (top and bottom, respectively) vs. values derived from the  $\lambda_{\text{sat}}$  observations of Lu et al. (2007) given by Tarnawski et al. (2009) for 10 Chinese soils, using the gravimetric fraction of sand  $m_{\text{sand}}$  as a predictor of  $f_q$ . Dark dots correspond to the estimations obtained using the  $m_{\text{sand}}$  pedotransfer function for southern France and the three soils for which  $m_{\text{sand}}/m_{\text{SOM}} < 40$  are indicated by green diamonds. Red triangles correspond to the estimations obtained using the  $m_{\text{sand}}$  pedotransfer function for the seven soils for which  $m_{\text{sand}}/m_{\text{SOM}} > 40$ .



864  
865  
866  
867  
868  
869  
870  
871

**Fig. 12** – Volumetric fraction of quartz derived from the  $\lambda_{\text{sat}}$  observations of Lu et al. (2007) given by Tarnawski et al. (2009), vs. the logarithm of the  $m_{\text{sand}}/m_{\text{SOM}}$  ratio. The three soils for which  $m_{\text{sand}}/m_{\text{SOM}} < 40$  are indicated by green diamonds. The dashed line represents the regression equation:  $f_q = 0.02 + 0.048 \ln(m_{\text{sand}}/m_{\text{SOM}})$ .